Alma Mater Studiorum – Università di Bologna

DOTTORATO DI RICERCA IN
SCIENZE E TECNOLOGIE AGROAMBIENTALI

Settore Concorsuale di afferenza: Agronomia e sistemi colturali erbacei ed ortofloricoli - 07/B1
Settore Scientifico disciplinare: Agronomia e Coltivazioni erbacee - AGR02

Ciclo XXIV

"NEW WATER USE EFFICIENCY STRATEGIES TO COPE WITH CLIMATE CHANGE"

Dr. Elisa Guerra

Coordinatore Dottorato:
Prof. Giovanni Dinelli

Relatore:
Prof. Paola Rossi Pisa

Co-relatori:
Dr. Francesca Ventura
Dr. Richard L. Snyder

Esame finale anno 2013

"Nascere uomo su questa terra è un incarico sacro. Abbiamo una responsabilità sacra, dovuta a questo dono eccezionale che ci è stato fatto, ben al di sopra del dono meraviglioso che è la vita delle piante, dei pesci, dei boschi, degli uccelli e di tutte le creature che vivono sulla terra. Noi siamo in grado di prenderci cura di loro".

Shenandoah

ABSTRACT

Crop water requirements are important elements for food production, especially in arid and semiarid regions. These regions are experience increasing population growth and less water for agriculture, which amplifies the need for more efficient irrigation. Improved water use efficiency is needed to produce more food while conserving water as a limited natural resource.

Evaporation (E) from bare soil and Transpiration (T) from plants is considered a critical part of the global water cycle and, in recent decades, climate change could lead to increased E and T. Because energy is required to break hydrogen bonds and vaporize water, water and energy balances are closely connected. The soil water balance is also linked with water vapour losses to evapotranspiration (ET) that are dependent mainly on energy balance at the Earth's surface.

This work addresses the role of evapotranspiration for water use efficiency by developing a mathematical model that improves the accuracy of crop evapotranspiration calculation; accounting for the effects of weather conditions, e.g., wind speed and humidity, on crop coefficients, which relates crop evapotranspiration to reference evapotranspiration.

The ability to partition ET into Evaporation and Transpiration components will help irrigation managers to find ways to improve water use efficiency by decreasing the ratio of evaporation to transpiration. The developed crop coefficient model will improve both irrigation scheduling and water resources planning in response to future climate change, which can improve world food production and water use efficiency in agriculture.

RIASSUNTO

I fabbisogni idrici delle colture sono caratteristiche determinanti per la scelta delle specie vegetali, soprattutto nelle zone dove il clima è arido o semi-arido. Queste aree stanno registrando un aumento del tasso di crescita della popolazione, fenomeno che amplifica la necessità di un'irrigazione sempre più efficiente. Un migliore utilizzo dell'acqua a scopi irrigui è, infatti, elemento necessario alla produzione di maggiori quantità di derrate alimentari, favorendo nello stesso tempo la conservazione dell'acqua come risorsa naturale limitata.

L'evaporazione da suolo nudo (E) e la traspirazione dalle piante (T) sono considerati passaggi cruciali all'interno del ciclo globale dell'acqua, che risulta accelerato in questi ultimi decenni, e i possibili effetti del cambiamento climatico potrebbero portare ad un aumento della (E) e della (T). Il ciclio dell'acqua e dell'energia sono strettamente collegati tra loro, dal momento che è necessaria energia per rompere i legami idrogeno. Il bilancio idrico del suolo è anche collegato alla perdita di vapore acqueo mediate il processo di evapotraspirazione (ET), che dipende principalmente dal bilancio energetico dello strato superficiale della Terra.

Per affrontare il tema dell'uso sostenibile dell'acqua in agricoltura questo studio si è focalizzato sullo sviluppo di un modello matematico, attraverso una dettagliata ricerca bibliografica dei calori dei coefficienti colturali presenti in letteratura, per elaborare poi un nuovo programma che ottimizza il calcolo dell'evapotraspirazione colturale, in grado di poter essere applicato in aree caratterizzate da climi diversi, che tenga conto degli effetti meteorologici diversi, quali ad esempio la velocità del vento e l'umidità sui coefficienti colturali. La suddivisione dell'ET nelle due componenti, evaporazione e traspirazione, aiuterà coloro che si occupano di gestione irrigua a migliorare l'efficienza dell'uso dell'acqua, diminuendo il rapporto di evaporazione per traspirazione. Questo modello potrà contribuire a migliorare la pianificazione dell'irrigazione per affrontare i futuri cambiamenti climatici, i possibili effetti sulla produzione agro-alimentare e le mutate disponibilità di risorse idriche destinabili a scopo irriguo.

TABLE OF CONTENTS

CHAPTER 1 – INTRODUCTION

1. AGRICULTURE AND CLIMATE CHANGE

World's science and policy agenda on global change are dominated by greenhouse warming. According to Vörösmarty et al. (2000), impacts of this climate change on water supply are fundamental concerns.

In many parts of the world, agriculture and food production depend on water supply. In arid and semi-arid climates, where water holding-capacity of the soil is low and precipitation is not adequate during the growing season, irrigation is practiced to avoid drought causing yield losses (Jagtap and Jones, 1989). Global food production has kept pace with population growth in recent decades; yet nearly 800 million people remain undernourished, and the population shift from rural to urban environments will certainly increase the pressures and problems associated with food security. A growing population needs more food and thus more water (FAO, 2003). Moreover, agriculture is highly sensitive to climate variability and weather extremes. Climate change and the increased frequency of weather extremes experienced in recent decades, increased linkages between energy and agricultural market due to growing demand for bio-fuels, and increased financing for food and agricultural commodities all suggest that price volatility is here to stay (FAO, 2011).

Some atmospheric characteristics, such as temperature, rainfall, concentration of carbon dioxide and ground level ozone, have already changed. The scientific community expects such trends to continue and this could mean that, while food production may benefit from a warmer climate, the increased potential for droughts, floods and heat waves will pose challenges for farmers. Additionally, the enduring changes in climate, the scarce water supply and the low soil moisture could make it less feasible to continue crop production in certain regions (Roderick and Farquhar, 2002). The impacts of changes in current climate have been deeply analysed. According to several studies, nearly all European Regions will be affected by future climate changes, though not at the same magnitude and effect (Parry et al., 1999; Rotmans et al., 1994; Beniston et al., 1998; Parry et al., 2000; Kundzewicz et al., 2001; EEA, 2006; Barnett and Adger, 2007; Alcamo et al., 2007; Rossi et al., 2007, EEA, 2008; CEC, 2009; Chatzidaki and Ventura, 2010).

Agriculture, including livestock husbandry, managed fisheries (aquaculture) and forestry, is the major land and water user across the globe. Agricultural production is driven by consumer

demand, and changes in consumer preferences have a key role on influencing water needed for food production. Therefore, water is a critical factor for production of a wide range of agricultural systems; including cereals, oils, fish and livestock (Figure 1; FAO World Bank, 2001).

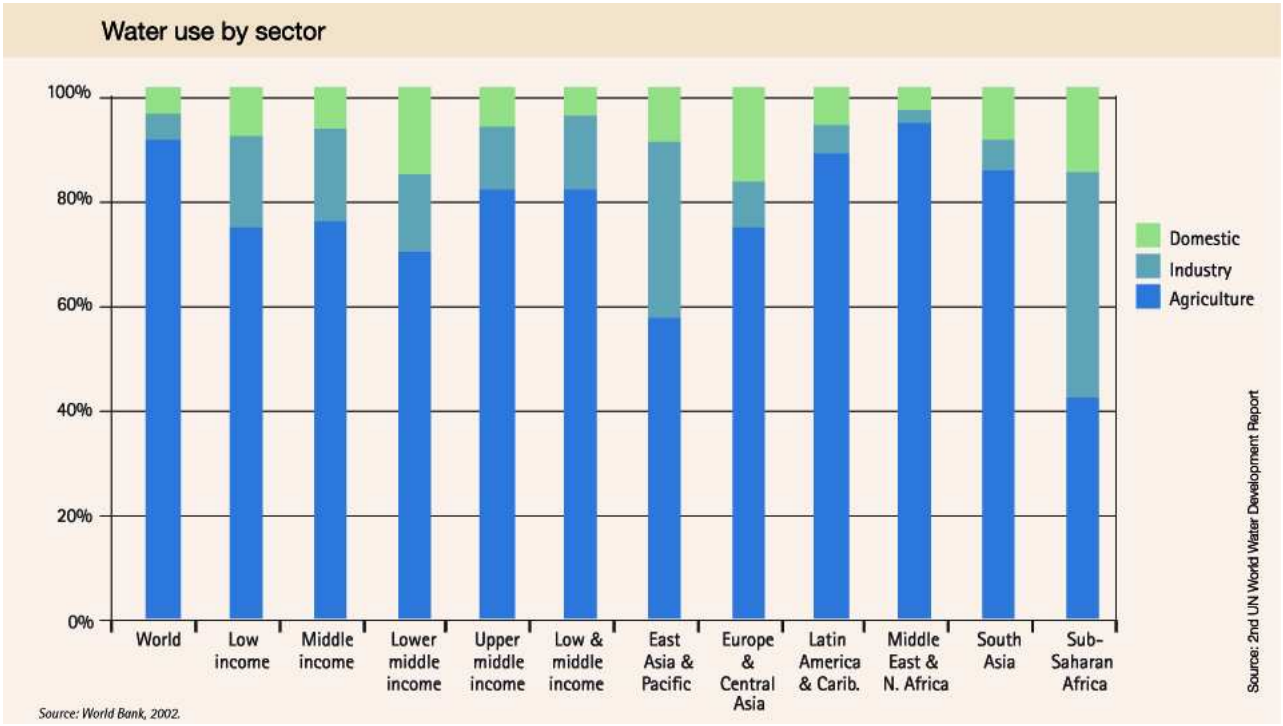

Figure 1. Water use by sector. Globally, the agricultural sector consumes about 70% of the accessible freshwater – more than twice that of industry (23%), and dwarfing municipal use (8%). (www.panda.org; World Agriculture and the Environment: A Commodity-by-Commodity Guide to Impacts and Practices Island Press).

Crops require water of adequate quality, in appropriate quantity and at the right time, to sustain their vegetative growth and development. Most of the water plants absorb performs the function of raising dissolved nutrients from the soil to the aerial organs where it vaporizes and cools the plants as it is released to the atmosphere by transpiration. Depending on local climatic conditions, crops have specific water requirements that depend on available energy to vaporize the water, plant physiology and morphology, and root and soil characteristics.

Table 1 gives examples of water required per unit and per year for major food products, including livestock, which consume the most water. An indicative figure for producing one kilogram of wheat is about 1000 litres of water that is returned to the atmosphere, paddy rice may require twice this amount. Meat production requires 6 to 20 times more water than cereals depending on the feed/meat conversion factor.

The amount of water involved in food production is significant. Most of it is provided directly by rainfall with only about 18% provided by irrigation (Villani et al., 2011). Uptake of water from rivers, lakes and aquifers provides about 40% of the water for irrigation with the rest coming from ground water. Evapotranspiration and deep percolation, i.e., infiltration below the crop root zone, comprise the main water losses.

Rainfed (non-irrigated) agriculture corresponds to about the 60% of production in developing countries. It depends entirely on rainfall stored in the soil profile, and it is possible only in regions where rainfall distribution ensures continuing availability of soil moisture during the critical crops growing periods. In rainfed agriculture, land management can have a significant impact on crop yields: an appropriate land preparation leads surface runoff to infiltrate close to the root zone, improving the soil moisture conservation. Rainwater harvesting can help in retaining water in situ, not only providing more water for the crops, but also enriching groundwater recharge and reducing soil erosion. For example, conservation tillage, a practice of conservation agriculture, has been proven to be effective in improving soil moisture conservation.

Table 1. Water requirement equivalent of main food products (FAO, 1997a)

Product	Unit	Equivalent water in m^3 per unit
Cattle	head	4000
Sheep and goats	head	500
Fresh beef	kg	15
Fresh lamb	kg	10
Fresh poultry	kg	6
Cereals	kg	1.5
Citrus fruits	kg	1
Palm oil	kg	2
Pulses, roots and tubers	kg	1

Where rainfall is subject to large seasonal and interannual variation, the potentials to improve rainfed production is limited. Because of the high risk of yield loss from dry spells and droughts, farmers are loath to invest in inputs such as plant nutrients, high-yielding seeds and pest management. In semi-arid regions, the objective of resource-poor farmers is to have sufficient production to ensure nutrition of the household through to the next harvest. This aim may be reached by using robust, drought-resistant varieties that are associated with low yields. Genetic engineering in fact has not yet delivered high-yield drought-resistant varieties.

1.1 ROLE OF IRRIGATION IN FOOD PRODUCTION

In irrigated agriculture, crops receive water partly or totally through human intervention. Irrigation water is taken from a water source, which can be river, lake or aquifer, and delivered to the field through an appropriate conveyance infrastructure. In order to satisfy their water requirements, irrigated crops can benefit from both irrigation water and from natural rainfall. Irrigation water provides an important management tool and allows farmers to grow high-yield seed varieties and to apply appropriate plant nutrition amounts, pest control and other inputs, which creates conditions for increasing yield. Figure 2 illustrates the typical yield response of a cereal crop to water availability and the synergy between irrigation, crop variety and inputs. Irrigation is crucial to the world's food supplies. For example, irrigated land makes up about one-fifth of the total arable area in developing countries but produces two-fifths of all crops and close to three-fifths of cereal production. The developed countries account for a quarter of the world's irrigated area (67 million ha). Their annual growth of irrigated area reached peak of 3% in 1970s and dropped to 0.2% in the 1990s (FAO, World Bank, 1998). The population of these countries is growing slowly and therefore a very slow growth in their demand and production of agricultural commodities is foreseen. The increasing interest on irrigation development is expected to grow especially in the developing countries group, where the demographic growth is higher. Because of the increasing competition from the higher valued industrial and domestic sector, the result is a decreasing amount of the overall available water for irrigation (Figure 3).

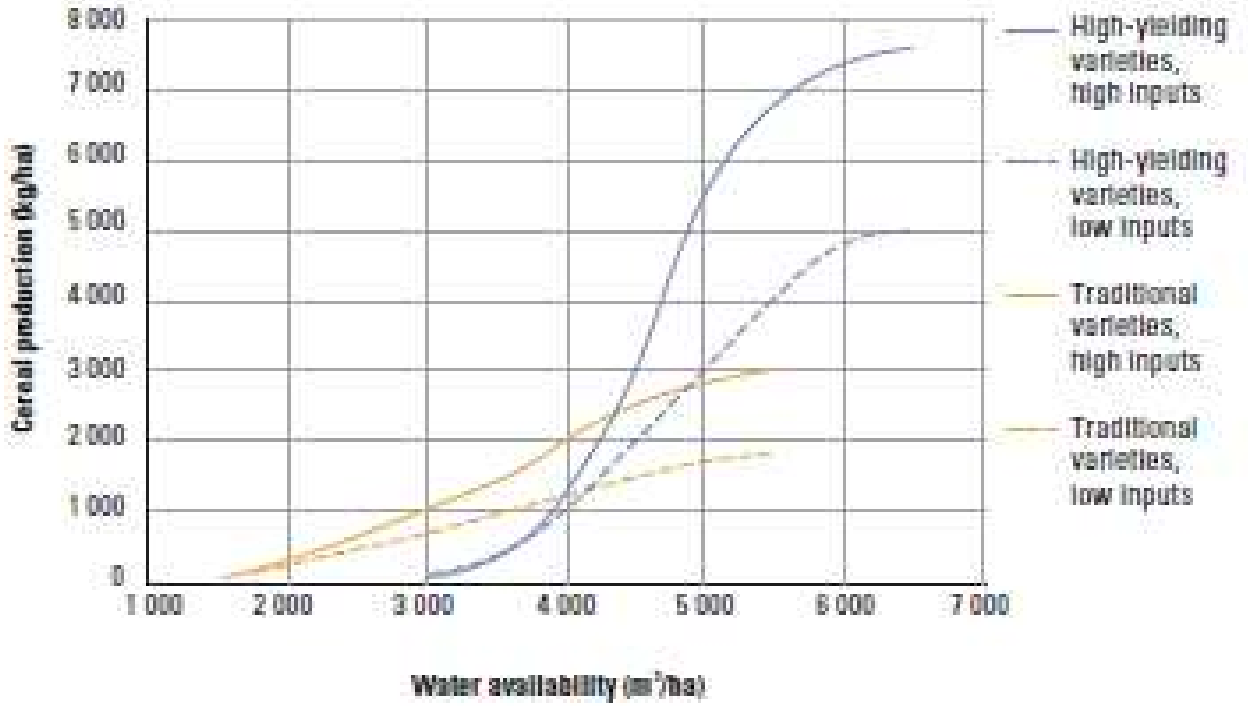

Figure 2. Typical response to water for cereal crops. The graph shows the yield response of crops to water availability: high yielding varieties produce more than rainfed varieties only when provided with adequate amount of water. Source: Smith et al., 2001.

Figure 4 shows a worldwide map of irrigated land as percentage of arable land. A high proportion of irrigated land is usually found in countries and regions with an arid or semi-arid climate. However, low proportions of irrigated land in sub-Saharan Africa point also to underdeveloped irrigation infrastructure. Data projections of irrigated land compared to irrigation potential in developing countries are shown in Figure 5.

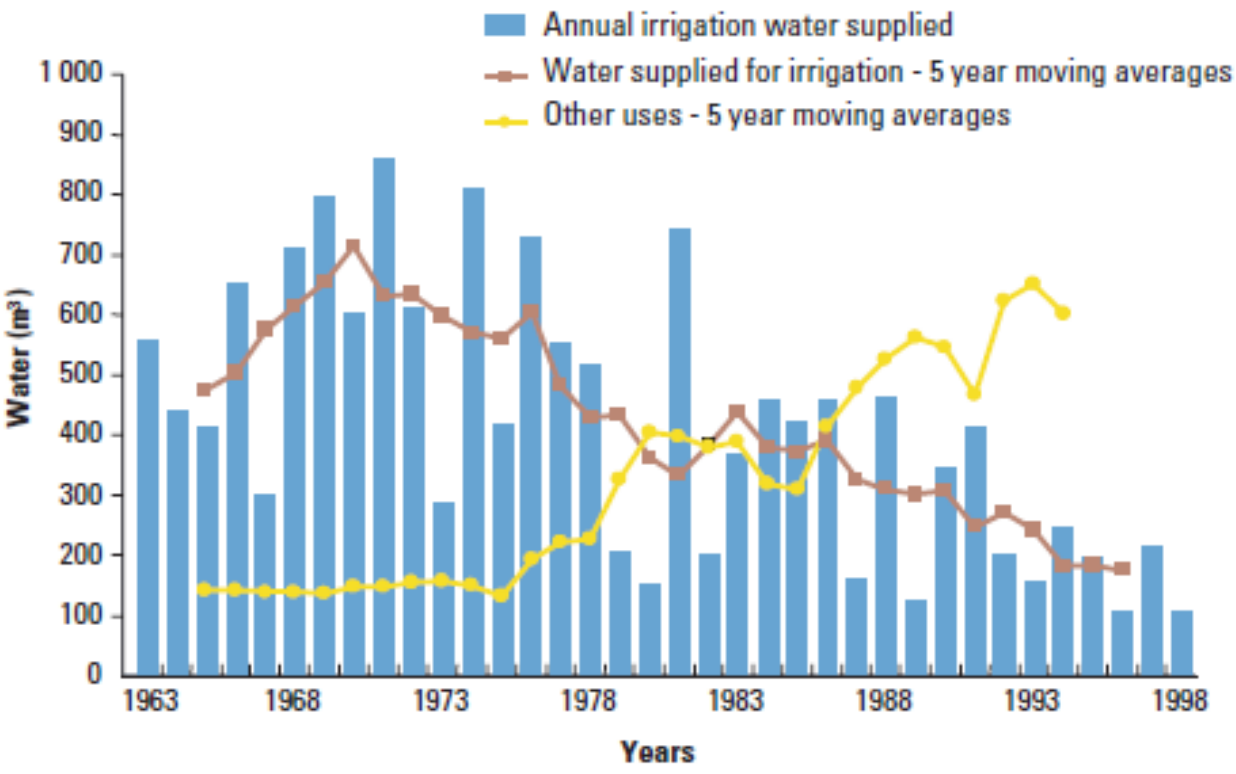

Figure 3. Competing uses of water in the Zhanghe irrigation district, China. This figure illustrates that increasing competition and demand from the industrial and domestic sectors result in the decrease of irrigation's share of water use (http://www.fao.org/docrep/006/Y4683E/y4683e07.htm).

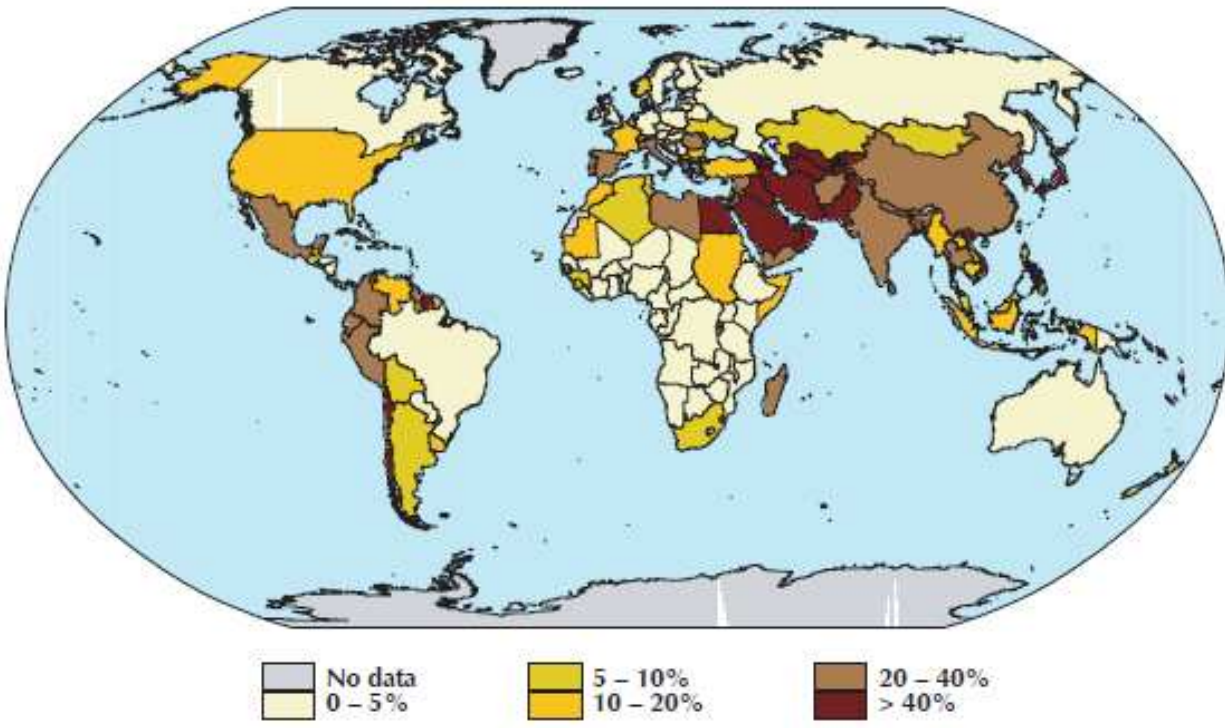

Figure 4. Area equipped for irrigation as percentage of cultivated land by country (1998). (Source: FAOSTAT, 2002).

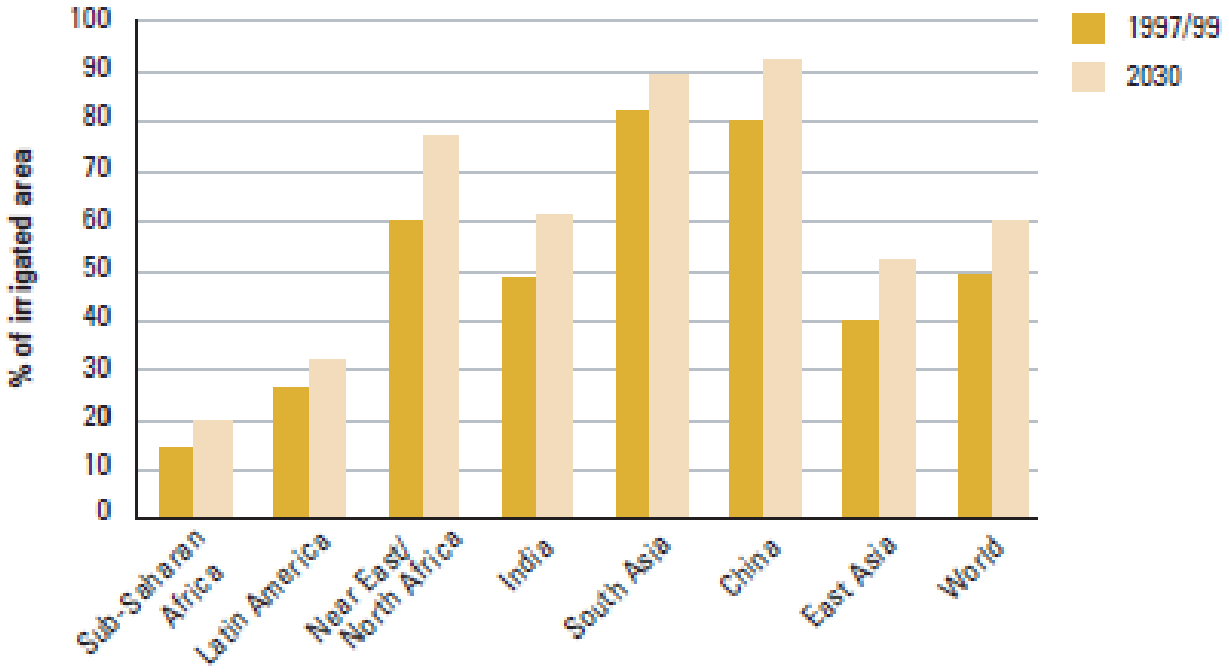

Figure 5. Irrigated area as proportion of irrigation potential in developing countries. A vast share of the irrigation potential is already being used in Asia and in the Near East but there remains a large potential still untapped in sub-Saharan Africa and Latin America. (Source: FAO, 2002).

The irrigation potential (Figure 5) already takes into account the availability of water. The graph shows that a sizeable part of potential irrigation is already used in the Near East/North Africa region, where water is the limiting factor, and in Asia, where land is often the limiting factor, whereas a large potential is still unused in sub-Saharan Africa and Latin America. FAO forecasts point out that the world competition for irrigation water in crop production is expected to increase in the coming decades. In particular, the area equipped for irrigation in developing countries is expected to expand by 20 percent of the arable land (40 million ha) by 2030. This means that 60% of the arable land with irrigation potential (402 million ha) will be in use by 2030. Because of the projected lower growth rate of food demand, increasing scarcity of suitable areas for irrigation, lack of water resources in some countries, and the rising costs of irrigation investments, the 2030 projections for increase in irrigated land is less than half the increase over the preceding 36 years.

1.2 WATER AS NATURAL LIMITED RESOURCE

Global food production has kept pace with population growth in recent decades. According to the Food and Agricultural Organization of the United Nation (FAO, 2003) nearly 800 million people remain undernourished, and the population shift from rural to urban environments. Causing increasing pressures ad problems associated with food and water security. To meet projected human growth in human population and per capita food demand, historical increases in agricultural production must continue, eventually doubling actual production (Tubiello et al., 2007). This implies a new conception of the natural resource water as limited. In fact, according to Pereira et al. (2002), water is becoming scarce not only in areas considered arid and drought, but also in region where rainfall is plentiful. The concept of water scarcity concerns the quantity of resource available and the quality of the water, since degraded water becomes an unavailable resource for more compelling requirements.

The priority for agriculture in water scarce regions is the sustainable use of water as a natural resource, environmental consideration, appropriate technology, economic viability and social acceptability of development issues. On the other hand, some countries are often experience regional and inter-regional conflicts, inter-sectorial competition, imbalance between availability and demand and degradation of surface and groundwater quality. Since irrigated agriculture is strictly dependent on water availability, innovations are required to enhance irrigation practices and management in irrigated regions.

Water scarcity results from several causes, e.g., temperature and precipitation distribution as well as nature and human pressures (Pereira, 1990; Vlachos and James, 1983). Xeric regimes are listed in Table 2, and they can be defined as:

Aridity – a permanent imbalance in water availability produced by nature and consisting in a low annual average precipitation rate, having a high spatial and temporal variability, resulting in a overall soil moisture and low carrying capacity of the ecosystem.

Drought – a temporary imbalance of water availability, always produced by nature, resulting in a persistent lower-than-average precipitation, of uncertain frequency, duration and severity, the occurrence of which is difficult to predict. The effect is a reduction of water resource availability and carrying capacity of the ecosystem. It corresponds both to a natural accident of almost unpredictable occurrence but of recognisable recurrence and to the failure of the precipitation regime; causing the disruption of the water supply to the natural and agricultural ecosystem as well as to human activities.

Desertification – a human caused permanent imbalance in water availability resulting from a combination of soil damage, inappropriate land use, mining of groundwater, increased flash flooding, loss of riparian ecosystems and deterioration of the carrying capacity of the ecosystem. It is often associated with soil erosion and salinity.

Table 2. Xeric regimes causing water scarcity (Source: Pereira et al., 2002)

Duration	Nature produced	Man-induced
Permanent	Aridity	Desertification
Temporary	Drought	Water shortage

The International Water Management Institute (IWMI) investigated the current and future water demand and supply situation of 118 countries over the period 1990-2025. The study was based on 4 groups of countries arranged in decreasing order of water scarcity. China and India were considered separately. The 2025 projections for the domestic sector withdrawals were based on a standard of basic needs of 20 m^3 per capita (Gleick, 1996) for countries below that level. Per capita withdrawals for irrigation are much larger than the per capita withdrawals for the other sectors, and they are projected to decrease over the 1990 to 2025 period. Figure 6 summarizes the result obtained for the 118 countries. Group 1 includes absolute water scarcity countries,

which are considered to be in a state of absolute water scarcity by 2025. These countries do not have sufficient annual water resources to meet reasonable per capita water needs for their rapidly expanding populations. They will almost certainly have to reduce the amount of water used in agriculture and transfer it to the other sectors, importing more food instead. Many of these countries will also have to increase their dependency on expensive and energy-consuming desalinization plants to meet domestic and industrial needs.

Because of the presence of important regional differences, the IWMI study listed China and India separately from the other countries. That study showed that around one-third of the population of both China and India live in regions that should be classified in the Absolute Water Scarcity Group. Group 2 refers to Economic Water Scarcity, where the regions have sufficient potential water resources to meet projected 2025 requirements, but many of these countries need to embark on massive water development programmes to utilize these resources. Thus, they face varying degrees of economic scarcity in 2025. These countries have been placed in the three subgroups, where countries in subgroup 1 have to more than double the amount of developed water supplies by 2025 to meet reasonable needs. These countries are mainly in sub-Saharan Africa, and it will be difficult to find the financial and other resources to rapidly achieve the water development. Countries of subgroup 2 also need to increase water development by between 25% and 100%. However, many of these countries in Latin America, North Africa and East Asia have more resources to achieve the objective. Finally, there are a large number of countries in subgroup 3 that have only modest requirements for additional water development and increased irrigation efficiency. Most of these countries are in North America and Europe. Behind these rather dry figures and groupings lie dramatic tragedies of water scarcity ranging from the need to carry heavy pots of water several kilometres everyday to meet household needs through the destitution of farmers who lose their land because of lack of sufficient irrigation water to flush salts from the soil, to the loss of wetlands and estuaries because upstream water depletion. Water scarcity leads to declining water quality and pollution and has an especially adverse impact on poor people.

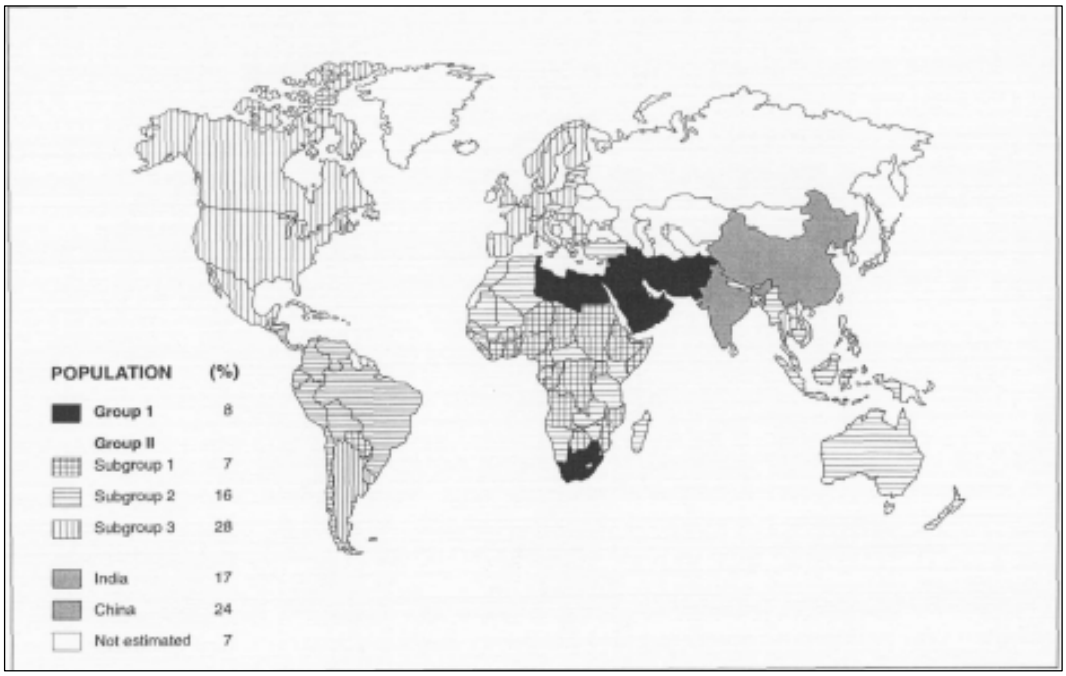

Figure 6. International Water Management Institute indicator of relative water scarcity. Note: percentages for India, China and the 4 groups are based on the total population of the Countries studied. Percentage of 'not estimated' category is based on the world population (Source: Seckler et al., 1999).

1.3 CLIMATE CHANGE IMPACTS ON AGRICULTURE

Widespread water scarcity in different parts of the world is expected to be further aggravated by numerous emerging threats. Those threats include climate change and attendant changing demand for water (Haileslassie et al., 2011). For example, as Figure 7 represents, rising global temperatures, as a result of climate change, might lead to an intensification of the hydrological cycle, resulting in drier season and wetter rainy seasons. This means that in some place, they expect more rain. So, temperatures will change, but not ecessarly increase everyhere.

The water cycle is a delicate balance of precipitation, evaporation, and surface and ground water transfer. Warmer temperatures are supposed to increase the rate of evaporation of water into the atmosphere, increasing the atmosphere water content. Increased evaporation may cause some areas to dry and on other areas an excess of precipitation rates.

As changes in rainfall amount during storms are occurring, the water cycle is already changing. In particular, the amount of rain falling during the most intense (1%) storms increased by almost 20%, over the past 50 years. Rising temperatures are also contributing to a melting of snow and glaciers, modifying the stream-flow timing in rivers that have their source in mountainous areas. Higher winter temperatures will likely lead to more precipitation as rain rather than snow (http://nca2009.globalchange.gov/projected-changes-water-cycle).

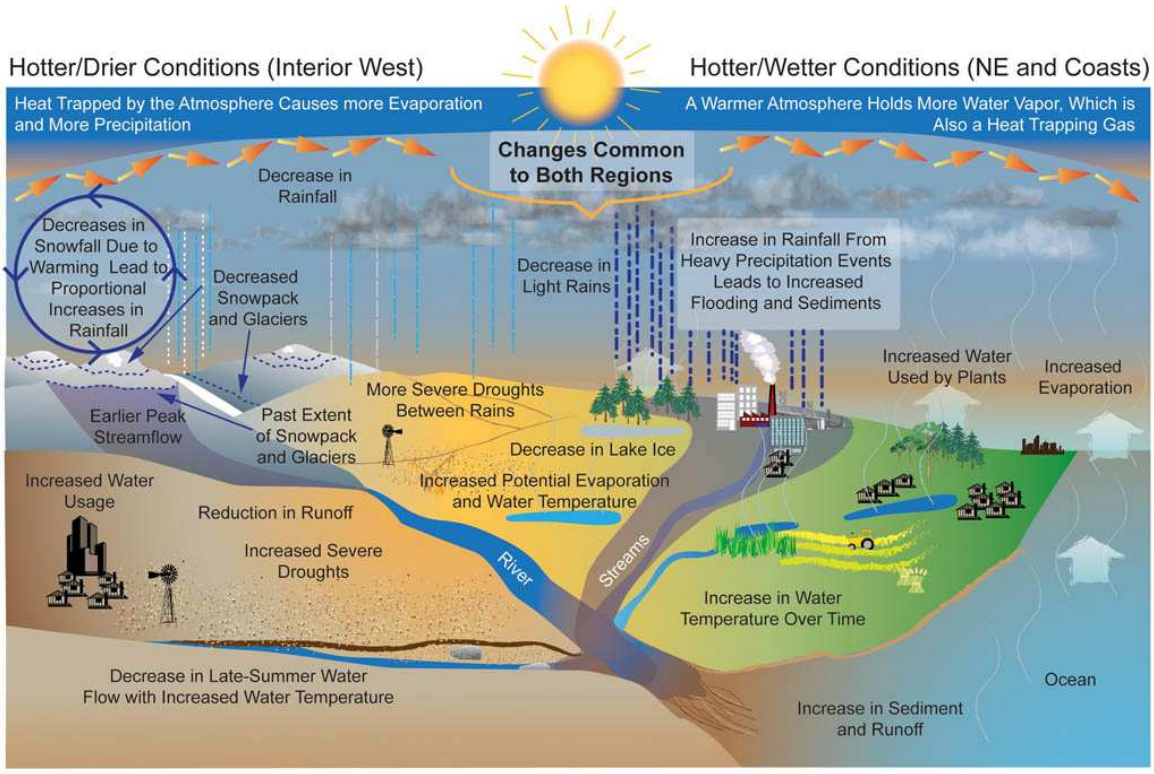

Figure 7. Projected changes in the water cycle. The water cycle exhibits many changes as the Earth warms. Wet and dry areas respond differently (Source: http://nca2009.globalchange.gov/projected-changes-water-cycle).

Climate change may also contribute to land degradation and desertification, which occurs in arid, semi-arid and sub-humid climates. Climate change refers, in fact, to any significant change in measures of climate (e.g., radiation, temperature, humidity, precipitation, and wind) lasting for an extended period (decades or longer), (www.epa.gov). They may result from:

1) natural factors, e.g., changes in the sun intensity or slow changes in the Earth's orbit around the Sun;

2) natural processes within the climate system (e.g. changes in ocean circulation);

3) human activities that change the atmosphere's composition (e.g. through burning fossil fuels) and the land surface (e.g. deforestation, reforestation, urbanization, desertification, etc.).

According to Chaouche et al. (2010), not only temperature but other factors can affect plant water demand, e.g., relative humidity and atmospheric CO_2 concentrations. There are some values that prove that independently from the cause, some climate variations exist and these are the variations per decade reported by Roderick and Farquhar (2002) in the last 50 years:

The mean temperature increased of + 0.15℃

The maximum temperature increased of + 0.1℃

The minimum temperature increased of + 0.2℃

As the average global temperature increases, humidity is expected to increase. Roderick and Farquar reported no change in the vapour pressure deficit in the last half century, because both the temperature and the humidity are rising. The explanation of this fact could be found in the increased cloud coverage and/or aerosols dampen the diurnal cycle by reducing the net loss of long-wave irradiance from the surface at night. Figure 8 shows the average daily solar radiation at the surface (in watts per square meter per day). In terms of climate change impact on solar radiation, crops in some areas will probably benefit from an increasing solar radiation while others will probably experience negative effects due to reduced radiation. Changes in radiation could lead to severe drought periods, which may cause a decreasing crop production or an increasing amount of irrigation water use, that provoke higher costs.

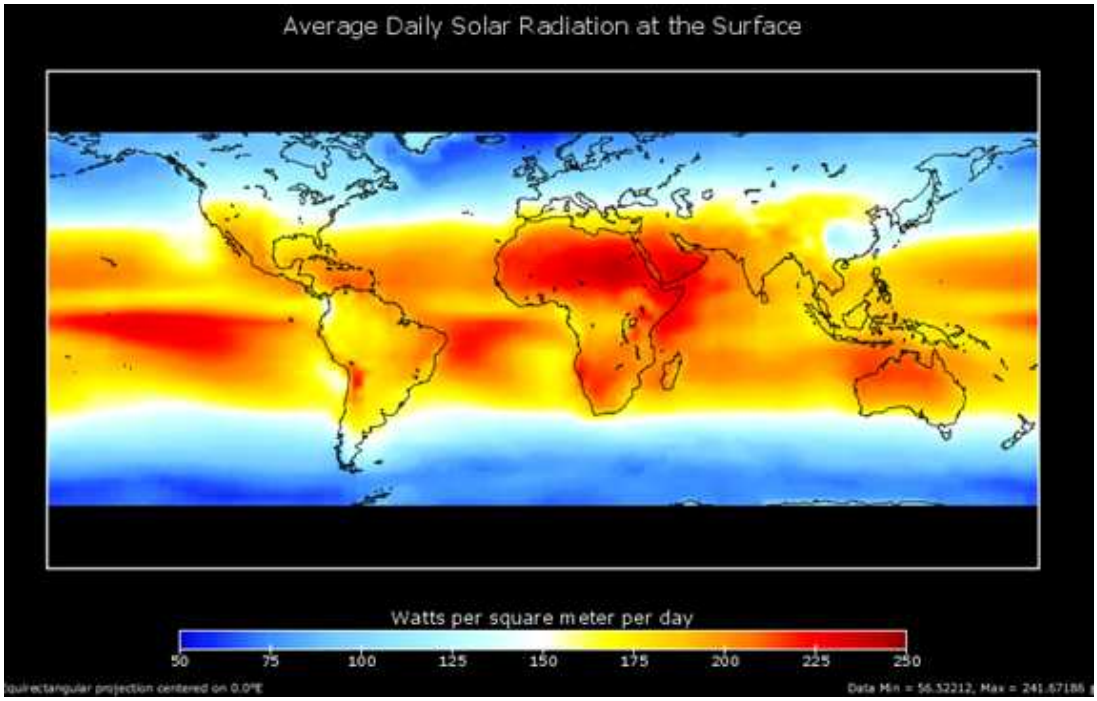

Figure 8 Averaged daily solar radiation at the surface in watts per square meter per day (Roderick and Farquhar, 2002).

There are a number of additional uncertainties in climate change impact studies. For example, the socio-economic drivers that influence greenhouse gas emissions provide the context in

which the impacts of climate change occur and adaptation takes place. The CO_2 emissions determine the levels of carbon dioxide concentration that influence plant photosynthesis and water use. The response to climate change is often closely tied to the prevailing soil and climatic conditions in particular in agriculture, may offset negative impacts or increase benefits compared with assuming unchanged management (Alexandrov et al., 2002; Olesen et al., 2007). All of these issues will add to the uncertainties in projected impacts of climate change.

2. WATER AND ENERGY BUDGETS

2.1. THE ENERGY BALANCE

Net Radiation

Net radiation, i.e., the net balance of solar and terrestrial radiation, provides the energy to do work in the Earth system (Figure 9). Technically, a surface is a plane separating two different media, in other words, the site where energy and mass exchange and conversion take place. The principal plane of climatic activity in a system is defined as the “active surface”. This plane corresponds to the level where the majority of the radiant energy is absorbed, reflected or emitted. The plane is where precipitations are intercepted and air mass are dragged (Oke, 1978). The approximation of the principal plane to a flat surface is necessary for climatic purposes, even if every surface is characterized by a roughness level. These physical phenomena happening at this level correspond to energy fluxes. The principal uses of the supplied energy is in the phase change of water to latent heat (LE), changing the temperature of the air through convection of sensible heat (H), surface conduction into the soil and other solids mainly as ground heat flux (G) and for metabolic processes (M). These terms, corresponding to energy flux density, are quantitatively related by Eq. (1), which is the general energy balance equation:

$$Rn - LE - H - G - M = 0 \qquad (1),$$

where R_n is the net radiation, H is the sensible heat flux density, LE is the latent heat flux density from evaporation and transpiration, G is the soil heat flux density, and M is the metabolic flux density, which is small and roughly equal to the error value in measurements. Consequently, M is often ignored in energy balance calculations. For these terms, instantaneous units are commonly [W m^{-2}] and hourly or daily values are expressed in MJ $m^{-2}h^{-1}$ or MJ $m^{-2}d^{-1}$. (1 mm d^{-1} ET=1 kg $m^{-2}d^{-1}$≈2.45 MJ $m^{-2}d^{-1}$).

The equation components are typically obtained with remote sensing technologies or ground-based measurements.

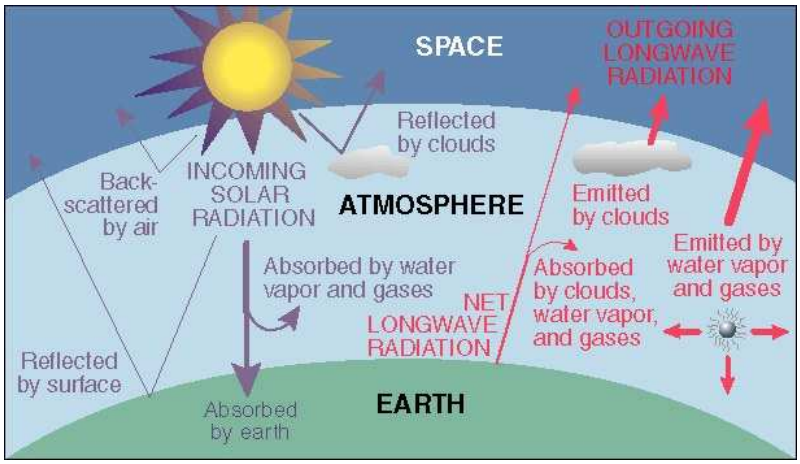

Figure 9. Radiation balance. Radiant energy is electromagnetic energy that can transfer through the atmosphere or through empty space. The amount of energy radiated depends on the temperature of the emitting body. The SI unit for radiant energy is the Joule (J) and the instantaneous flux density is often expressed as J $s^{-1}m^{-2}$ or W m^{-2}. In this picture, most of the incoming solar radiation is absorbed by Earth, but some is back scattered by air, reflected by the Earth surface or clouds. and some is absorbed by water vapour and other gasses in the atmosphere. The absorbed solar radiation increases temperature and radiation is emitted by the earth, clouds, water vapour and other gasses to the atmosphere and the space through the outgoing long wave radiation (http://w3.shorecrest.org/~Lisa_Peck/Physics/All_Projects/photojournal/tina/tina.html).

Radiation is a form of energy due to the rapid oscillations of electromagnetic fields (Oke, 1978), and solar radiation is the climatic driver for energy balance on Earth (Scorer, 1997). It is transferred by photons, or bundles of energy that have properties similar to both particles and waves. The oscillations are like travelling waves characterized by their wavelength (λ), which is thedistance between successive wave crests, and the wave frequency (ν), which is the rate that wave crests pass a point in space. Radiation travels at the speed of light (c), so $c=\lambda\nu$.

Earth receives solar (shortwave) radiation and emits far infrared (longwave) radiation back into space. The incoming shortwave radiation and outgoing longwave radiation are in balance or the entire atmosphere would have to heat or cool. Because there is no appreciable change in energy received from the sun, global temperature rise is due to a redistribution of sensible heat from the upper to the lower atmosphere that is caused by greenhouse gasses intercepting more upwelling, longwave radiation in the lower atmosphere. Intercepted longwave radiation is then reradiated in all directions, but there is an increase in the downward longwave radiation relative to when the Earth had less greenhouse gasses. The result is that the lower atmosphere is warming and the upper atmosphere is cooling. The difference between total incoming and outgoing radiation for the Earth is still zero.

The radiation is measured by a pyranometer and there are many commercial models available. Figure 10 is an example of typical pyranometer:

Figure 10 Pyranometer: a silicon photovoltaic detector is mounted in a cosine-corrected head to provide solar radiation measurements onto a plane that is parallel to the Earth's surface for solar energy, agricultural, meteorological, and hydrological applications. It measures direct solar plus diffuse sky radiation for the spectral range of 300 to 1100 nm. The standard output is 0.2 mV per W m^{-2}, which provides a signal of 200 mV in full sunlight (1000 W m^{-2}) (http://www.campbellsci.com/cs300-pyranometer-specifications).

Net Radiation Estimation

The net radiation term (R_n) as an energy flux density is expressed by the Radiation Balance Eq. (2):

$$R_n = \left(Q\frac{Ap}{A} + q \right)(1-a) + L_u + L_d \qquad (2),$$

where Q stands for shortwave direct radiation at the surface [Wm^{-2}], $A_p/A = \cos\alpha$ for A_p the area of a projection plane that is perpendicular to a direct ray from the sun, A is the horizontal surface area and α is the angle between a ray from the sun and a ray perpendicular to the horizontal surface area. The diffuse shortwave radiation (q) is the flux density [Wm^{-2}] of radiation that was scattered by the atmosphere but reaches the horizontal surface and a is the albedo, i.e., reflectivity of shortwave radiation from the surface. Longwave incoming radiation (L_d) includes all longwave radiation emitted or reflected from the sky that reaches the surface and longwave outgoing radiation (L_u) includes both emitted and reflected longwave radiation from the surface. The instantaneous units for all radiation are J $s^{-1}m^{-2}$ or W m^{-2} and, by convention, all radiation fluxes are positive downward and negative upward. A commonly used equation (Campbell and Norman, 1998) for estimating downward long wave radiation onto a flat horizontal surface (L_d, W m^{-2}) from air temperature (T_a, K) measured in a standard weather shelter is:

$$L_d \approx \varepsilon_a \sigma T_a^4 = \left[(1-0.84c)\varepsilon_{as} + 0.84c \right] \sigma T_a^4 \qquad (3),$$

Where $\sigma=5.67\times10^{-8}$ W $m^{-2}K^{-4}$ is the Stefan-Boltzmann constant, "c" is the sky cloud cover fraction, "ε_a" is the apparent emissivity of the sky, and $\varepsilon_{as} \approx 0.53 + 0.19\sqrt{e}$ is the clear sky

emissivity, which is a function of the vapour pressure (e, kPa) measured in the standard weather shelter. Ideally, the longwave upward radiation from a grass surface would be estimated from the canopy temperature (T_g) and emissivity (ε_g), but T_g is rarely measured at a standard weather station. Instead, the upward longwave radiation is estimated from standard weather shelter air temperature (T_a) as: $L_u \approx \sigma T_a^4$, assuming that the apparent emissivity of the grass surface is approximately ε=1.0. A typical emissivity from a grass surface is ε_g=0.98, so the upward longwave radiation is actually about 2% less than from the L_u equation assuming that T_a is approximately equal to T_g. However, the absorptivity of the grass surface is also 0.98, so the absorbed longwave downward radiation is actually about 2% less than L_d from Eq. 3 due to not adjusting for the absorptivity of the grass. Since the errors in absorption from L_d and emission from L_u are compensating and $L_u+L_d \approx$-100 W m^{-2} under clear skies, the error is small and unimportant for energy balance calculations.

The incoming energy terms of Eq. (2) for R_n are Q, q and L_d; the outgoing terms are L_u and a. The "radiative equilibrium" condition occurs when a surface emits as much energy as it receives from an external source if there is no other source or sink of surface energy (R_n=0).

Ground Heat Flux Density

The conductive heat flux density through a solid, e.g., soil, is designated by the symbol G, which is expressed by Eq. (4), named as the Fourier Heat conduction formula:

$$G = -C_1 \frac{\partial T}{\partial z} = -\rho_s C_p \kappa \frac{\partial T}{\partial z} \quad (4),$$

Where C_1 is the thermal conductivity, which is a function of soil composition, moisture content and structure of the soil [W $m^{-1}K^{-1}$] and κ is the thermal diffusivity [m^2 s^{-1}], which is expressed as:

$$\kappa = \frac{C_1}{\rho_s C_p} \quad (5),$$

Where ρ_s is the apparent soil density [kg m^{-3}], and C_p is the mass specific heat capacity [J $kg^{-1}K^{-1}$].

The sign convention is that a downward flux, i.e., adding heat to the ground, is positive. Note that $\partial T/\partial z = (T_2 - T_1)/(z_2 - z_1)$ where the higher value of the subscripts indicates greater depth in the soil, and the minus sign in equation 4 is included to make the downward flux positive. The thermal conductivity C_1 is an important characteristic that depends on soil mineral fractions and

water content. In the land surface parameterization literature, the most commonly used formulation for predicting soil thermal conductivity is that of McCumber and Pielke (1981, henceforth MP81), which is based on their fit to the dataset of Al Nakashabandu and Kohne (1965). A comparison of soil thermal conductivity values predicted by the MP81 and Johansen (1975, henceforth J75) methods to reference tabulated values is shown in Table 3. Two columns for MP81, corresponding to the differences in soil water retention functions: CH78 for Clapp and Hornberger (1978), and R82 for Rawls et al. (1982). For dry soils, quartz sand has the highest conductivity and peat has the lowest. (Peters-Lidard, 1998).

Tab. 3 Comparison of thermal conductivity values (W m^{-1} K^{-1}). Values of porosity n and quartz content q are given for each soil type. All soils assumed to be fine for J75. (Peters-Lidard C.D., 1998).

Satura-tion	Reference	MP81 + CH78	MP81 + R82	J75
	Sand (n = 0.4, q = 0.95)			
0.0	0.30[c]	0.172	0.172	0.240
0.25	1.05[c]	0.833	3.549	1.116
0.5	1.95[c], 1.76[b]	2.818	5.477	1.779
0.75	2.16[c]	5.749	7.059	2.167
1.0	2.20[c], 2.18[b]	9.536	8.451	2.420
	Clay (n = 0.4, q = 0.25)			
0.0	0.25[a]	0.172	0.172	0.240
0.25	0.63[c]	0.172	0.172	0.724
0.5	1.12[c], 1.17[b]	0.182	0.658	1.090
0.75	1.33[c]	1.358	1.912	1.304
1.0	1.58[c], 1.59[b]	5.643	4.077	1.456
	Peat (n = 0.8, q = 0.0)			
0.0	0.05[a], 0.06[c]	0.172	—	0.038
0.25	0.13[a]	0.172	—	0.315
0.5	0.22[a], 0.29[c]	0.579	—	0.524
0.75	0.33[a]	2.266	—	0.646
1.0	0.5[a,b,c]	6.435	—	0.733

[a] Farouki (1986).
[b] de Vries (1963).
[c] Pielke (1984).

Sensible Heat Flux Density

For molecular diffusion, convective heat flux (C_m, J $s^{-1}m^{-2}$) equals the product of the air mole flux density (F, mol $s^{-1}m^{-2}$) and the heat carried by each mole of molecules (J mol^{-1}):

$$C_m = F\left(-mC_p \frac{\partial T}{\partial z}\ell\right) \qquad (6),$$

Where m is the molecular mass [kg mol^{-1}], C_p is the specific heat at constant pressure [J $kg^{-1}K^{-1}$], and ℓ is the 'mean free path' of the molecule [m].

The number of moles of molecules crossing a unit area perpendicular to the z axis in a unit time (F, mol $s^{-1}m^{-2}$) is expressed as:

$$F = c\left(\frac{N}{3}\right) \quad (7),$$

where c is the speed of the molecules, i.e., approximately the speed of sound and N is the number of moles of molecules per unit volume. At any time, approximately 1/3 of the molecules will have a velocity component in the z direction (the other 2/3s will have components in the x and y directions. The number density considered active in this process is then N/3.

According to this, C_m is determined by Eq. (8):

$$C_m = -c\left(\frac{N}{3}\right)\left(mC_p \frac{\partial T}{\partial z}\ell\right) \quad (8),$$

The product of N (mol m^{-3}) and m (kg mol^{-1}) is the density ρ (kg m^{-3}), so Eq. 8 becomes:

$$C_m = \frac{-c\ell}{3}\rho C_p \frac{\partial T}{\partial z} \quad (9),$$

This molecular diffusion equation is similar to the “flux gradient” relationships, where we define the thermal diffusivity as$\kappa = c\ell/3$ (m^2 s^{-1}), resulting in Eq. (10) for molecular convective heat flux (C) and Eq. (11) for thermal diffusivity (κ) becoming:

$$C_m = -\kappa\rho C_p \frac{\partial T}{\partial z} \quad (10),$$

$$\kappa = \frac{C_t}{\rho C_P}\ m^2 s^{-1} \quad (11),$$

Where (C_t, J $s^{-1}m^{-1}K^{-1}$) is the thermal conductivity. A typical value for thermal diffusivity of air is $\kappa = 2.2*(10^{-5})$ m^2s^{-1}.

For turbulent convective (sensible) heat flux from canopies (H, W m^{-2}), the form of the transfer equation is similar to that for molecular diffusion, except the sensible heat is transferred by turbulence rather than by high speed molecular transfer. The general form for turbulent convective heat transfer is given by Eq. (12):

$$H = -\kappa' \rho C_p \frac{\partial T}{\partial z} = -\rho C_p \frac{\partial T}{(\partial z/\kappa')} = -\rho C_p \left(\frac{T_2 - T_1}{r_H} \right) = -\rho C_p (T_2 - T_1) r_H^{-1} \quad (12),$$

Where $r_h = \partial z/\kappa'$ (s m^{-1}) is the resistance to and g_h (m s^{-1}) is the conductance of convective sensible heat flux density.

Latent Heat Flux Density

The total latent energy transfer from a vegetated surface to the air is the sum of transpiration, i.e., vaporization that occurs in the plant leaves where water diffuses through leaf pores (stomata) to the air, and evaporation, which is vaporization that occurs in the soil or on plant surfaces. Thus, evapotranspiration (ET) from plants is the sum of transpiration (T) and evaporation (E). Plants can control transpiration by closing stomata and the effect is expressed in the conductance or resistance terms in Eq. 12.

The sub-stomatal cavity is the place where transpiration takes place for leaves: here the vapour pressure [$e_s(T_\ell)$] is assumed to be saturated at leaf temperature T_ℓ. Note that saturation vapour pressure $e_s(T)$ is a highly non-linear function of temperature as shown in Fig. 11.

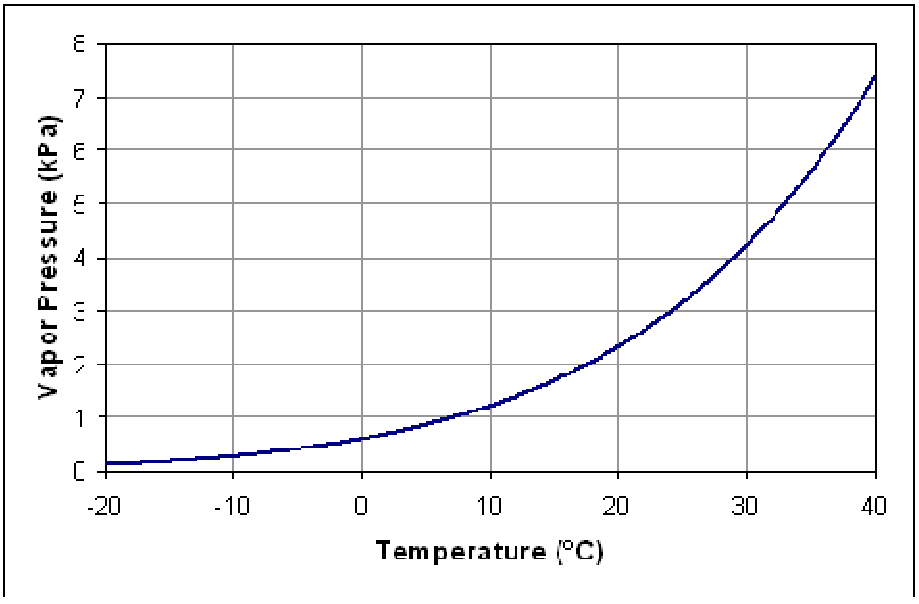

Figure 11. Saturated vapour pressure as function of temperature (Klenzendorf, 2008).

Cuticular resistance to water transfer through cells on leaf surfaces is quite high relative to stomatal resistance, so it is not considered in plant canopy evapotranspiration. During transpiration, water vaporizes from spongy mesophyll cells inside of the stomatal cavities of

leaves and it diffuses through the stomatal opening to the ambient air in the canopy. Stomatal resistance depends on the number of stomata and the area of stomatal opening. In general, closing stomata can restrict the flux of water vapour, and hence it increases stomatal resistance. Canopy conductance g_c is the sum of parallel conductances from soil and wet plant surfaces or the sum of the reciprocals of the parallel resistances. Once a canopy is well developed, however, the soil resistance to water transfer is relatively high, so the conductance is low and the soil resistance is often neglected. Thus, canopy resistance to water vapour flux (r_c) from full canopies is often estimated by considering only the stomatal resistance. For example, the canopy resistance for the standardized reference evapotranspiration, i.e., for 12 cm tall grass, was estimated as the stomatal resistance divided by the effective leaf are per unit soil area, i.e, 0.5×LAI, where LAI is the leaf area index and only have is assumed to be effective at transpiration (Allen et al. 2005). A typical stomatal resistance for grass is 100 s m^{-1} and the LAI for 12 cm tall grass is about 2.88 m^2 of leaf area per m^2 of soil, so the canopy resistance was estimated as 100 s m^{-1} divided by 1.44 m^2 m^{-2} giving a bulk canopy resistance of $r_c \approx 70$ s m^{-1}. A second resistance to latent heat flux occurs when water vapour transfers from the canopy to the atmosphere above the canopy. This is called the boundary layer resistance (r_b) and it depends mainly on the canopy roughness and wind speed, which affects turbulence within the fully adjusted boundary layer over a crop surface. When the surface is smooth or there are calm winds, there is little turbulence and r_b tends to be high. When the surface is rough and there is a high wind speed, there is more turbulence and r_b tends to be low. The canopy and aerodynamic resistances are in series, and resistances in series are additive. Therefore, the total resistance to latent heat flux or vapour flux is $r_v=r_c+r_b$. Therefore, the latent heat flux density due to turbulence is often expressed as:

$$LE = \frac{\rho C_p}{\gamma} \frac{[e_s(T_\ell) - e(z)]}{(r_c + r_b)} \quad (13),$$

Where $L \approx 2.45$ MJ kg^{-1} is latent heat of vaporization (sometimes it is called λ) and E is the instantaneous mass flux of water vapour (kg $s^{-1}m^{-2}$). The left-hand factor is the volumetric heat capacity (ρC_p, J $m^{-3}K^{-1}$) and the psychrometric constant (γ, kPa K^{-1}). The right-hand factor is the difference between the saturation vapour pressure ($e_s(T_\ell)$, kPa) at the mean leaf temperature (T_ℓ) and the actual vapour pressure (e(z), kPa) at some height z (m) above the ground.

Considering the saturation vapour pressure function of temperature (Fig. 11), the following approximation (Eq. 14) was derived by Penman as:

$$e_s(T_\ell)-e(z)=[e_s(T_z)-e(z)]+\Delta(T_z-T_\ell) \quad (14),$$

Where T_z (^oC) is the temperature measured at height z (m) above the ground and Δ is the slope of the saturation vapour pressure curve (kPa K^{-1}). A vapour pressure deficit of the atmosphere (VPD, kPa) term can be defined as follows:

$$VPD=e_s(T_z)-e(z) \quad (15),$$

Combining Eq. (13), (14) and (15), the following expression is obtained for latent heat:

$$LE=\frac{\rho C_p[VPD+\Delta(T_\ell-T_z)}{\gamma(r_b+r_c)} \quad (16),$$

Since T_ℓ is unknown, it can be eliminated by substituting Eq. 17 into Eq. (16) as in Eq. (18):

$$H=\left[\rho C_p(T_\ell-T_z)\right]r_H^{-1} \quad (17),$$

$$LE=\frac{\rho C_p\left[VPD+\left(\frac{\Delta H r_H}{\rho C_p}\right)\right]}{\gamma(r_b+r_c)} \quad (18),$$

Substituting $H=R_n-G-LE$ for H in Eq. (18) gives:

$$LE=\frac{\rho C_p\left[VPD+\left(\frac{\Delta(R_n-G-LE)r_H}{\rho C_p}\right)\right]}{\gamma(r_b+r_c)} \quad (19),$$

Dividing the numerator and denominator on the right-hand side by r_H gives:

$$LE=\frac{\rho C_p\left[VPD+\left(\frac{\Delta(R_n-G-LE)}{\rho C_p}\right)\right]}{\gamma\left(\frac{r_b+r_c}{r_H}\right)} \quad (20),$$

Multiplying through by ρC_p gives:

$$LE=\frac{\rho C_p VPD+\Delta(R_n-G-LE)}{\gamma\left(\frac{r_b+r_c}{r_H}\right)} \quad (21),$$

Transferring the LE components to the left-hand side of the equation gives:

$$LE + \gamma\left(\frac{r_b + r_c}{r_H}\right)LE = \left(1 + \gamma\left(\frac{r_b + r_c}{r_H}\right)\right)LE = \Delta(R_n - G) + \rho C_p VPD \quad (22),$$

Assuming that the boundary layer resistance to latent heat transfer and the resistance to convective heat transfer are equal, we can define the aerodynamic resistance as $r_a=r_b=r_H$, and the equation simplifies to:

$$\left(1 + \gamma\left(1 + \frac{r_c}{r_a}\right)\right)LE = \Delta(R_n - G) + \rho C_p VPD \quad (23),$$

Finally, the latent heat flux is expressed as a function of readily available weather variables and the canopy and aerodynamic resistances in the Penman-Monteith equation (Monteith, 1965).

$$LE = \frac{\Delta(R_n - G) + \rho C_p VPD}{\left(1 + \gamma\left(1 + \frac{r_c}{r_a}\right)\right)} \quad (24)$$

Measurements of R_n and G require relatively simple sensors, but measuring H requires more sophisticated and expensive methods. (Shapland dissertation research, private). There are many methods for estimating H, but only two will be discussed. Both of them are based on the assumption that H is transferred vertically and turbulently to and from the surface. These methods are eddy covariance, widely adopted, and surface renewal.

Measuring LE

The phase change from liquid water to water vapour converts sensible to latent heat, and the process is a major form of cooling to many organisms, plants included. Latent energy is the energy associated with the phase change, which is ‘recovered’ when the phase change is reversed. The rate of phase change is controlled by radiation and turbulent flux exchanges at the surface that affect the water temperature at the surface where the phase change takes place. When a phase change takes place at a surface, the water vapour flux is equivalent to an energy flux, and the energy is lost from the surface. When the water condenses in the atmosphere or on some surface the phase change converts latent heat back to sensible heat.

H MEASUREMENT TECHNIQUES

A. EDDY COVARIANCE SYSTEM

The EC technique consists of measuring at high frequency the vertical wind speed and the concentration of a scalar (like water vapour density or air temperature to obtain latent - LE - or sensible heat – H - flux, respectively). This method is deeply described in Swinbank (1951), Twine et al. (2000), Shaw and Snyder (2003), Villalobos et al. (2009) and Shapland and McElrone (2013). Small air parcels in turbulent flow above the surface of the culture are supposed to carry with them heat, momentum and gases, which are substantially CO_2 and water vapour (Fig.14). The average flux density of one of these quantities in a certain time is the product of the vertical wind speed times the density of the same quantity in the air. This flow will be non-zero only if the fluctuations of velocity and density are related to each other. The sign of the correlation will specify if the flow is to or from the surface.

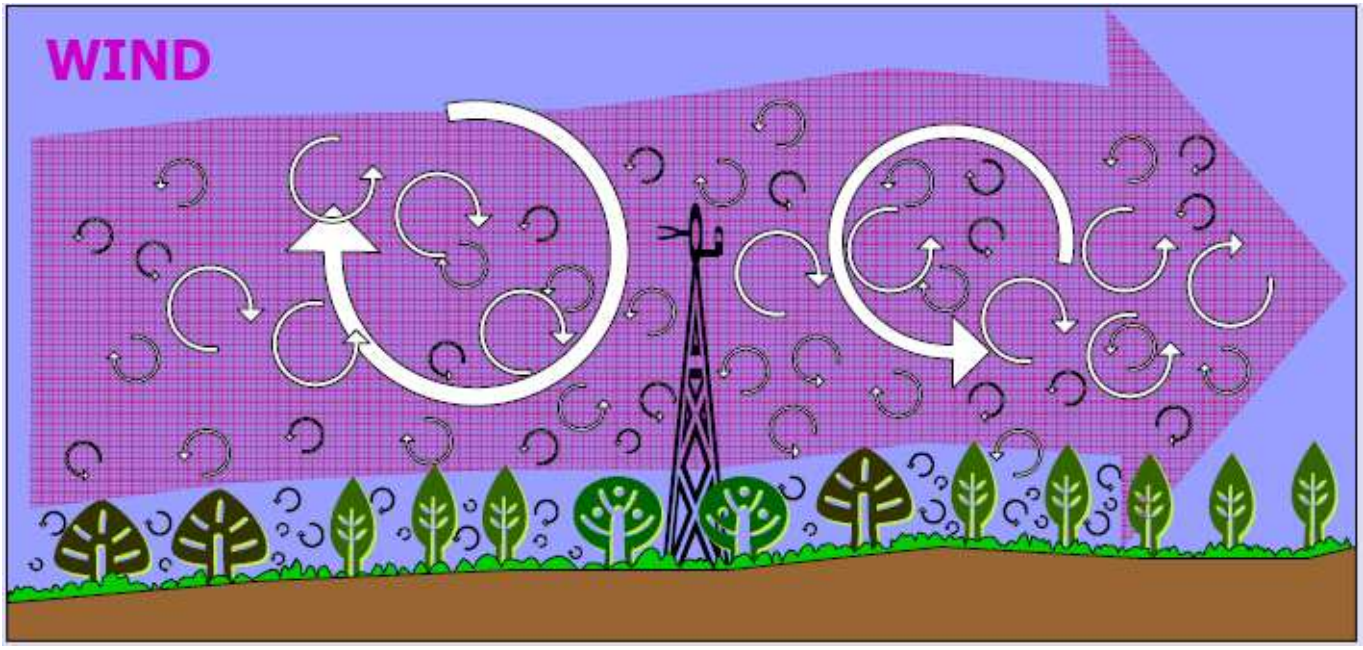

Fig. 12 Air flow in ecosystem. Air flow can be imagined as a horizontal flow of numerous rotating eddies. Small air parcels carry heat, momentum and gases. The product of the vertical wind speed times the density of the same quantity in the air corresponds to the average flux density of one of these quantities in a certain time (http://www.instrumentalia.com.ar/pdf/Invernadero.pdf).

The instrumentation required includes a fast-response three-dimensional sonic anemometer, which is expensive, diligent maintenance, and sophisticated theoretical and programmatic expertise. These reasons make it intractable for commercial applications (Shapland dissertation research, private).

B. SURFACE RENEWAL SYSTEM

Surface renewal system can be used to estimate the exchange of sensible heat, water vapour, and other scalar, requiring only scalar traces (Pau U et al., 2005). This method allows in fact to arrive at H by measuring the energy budget of individual turbulent air parcels (Paw U et al., 1995).

Paw U and Brunet (1991) introduced the method for estimating scalar fluxes based on surface renewal concepts. The observation of canopy turbulence and time-space scalar field associated with spatially extensive, repeated, and identifiable 'turbulent coherent structures' are the paradigms of this method.

Originally developed in chemical engineering field the concept of surface renewal was described by Stull (1984, 1988) and Higbie (1935). The surface-gas interface was supposed to come into contact with liquid elemental volumes and some scalar value characteristic of outer liquid layers. Gas was transferred into the liquid during this contact through molecular diffusion. In order to estimate the energy associated with this gas transfer, standard analytical equation solutions were used, assuming semi-infinite dimensions of the liquid elemental volumes.

With time, numerous modifications to the original concept were applied (Pau U et al., 2005). Current paradigm of turbulence near plant canopies are based on the dominance of turbulent coherent structures, characterized by repeated temporal and spatial patterns of the velocity and scalar field. The exchange rates estimation can be determined by evaluating the dimensions of these ramp structures, by using structure functions.

In surface renewal analysis only two heights are considered, some height above the plant canopy and a height representing the entire plant canopy; high frequency temperature data can be collected using fine-wire thermocouples (Duce et al., 1997).

Surface renewal methods worked successfully from surfaces ranging from bare soil to tall forests. Measuring the scalar trace at one height only, a semi-empirical parameter (α) must be determined by comparison of surface renewal results with independently measured exchange rates. This parameter is height dependent and some problem of over estimation of this parameter can occur because of the rising temperature sensor size, in relation with a sensitivity of the surface renewal method to slower response scalar sensors (Pau et al., 1995; Van Atta, 1977; Snyder et al., 1996; Spano et al., 1997b, 2000; Castellvì et al., 2008).

Surface renewal is less expensive than eddy covariance, because it requires only an inexpensive fast-response air temperature sensor. Moreover, it is simpler, less time-consuming, thanks to the straightforward data processing protocol. These characteristic make the surface renewal technique more amenable to commercial application when compared to eddy

covariance (Shapland dissertation research, private).

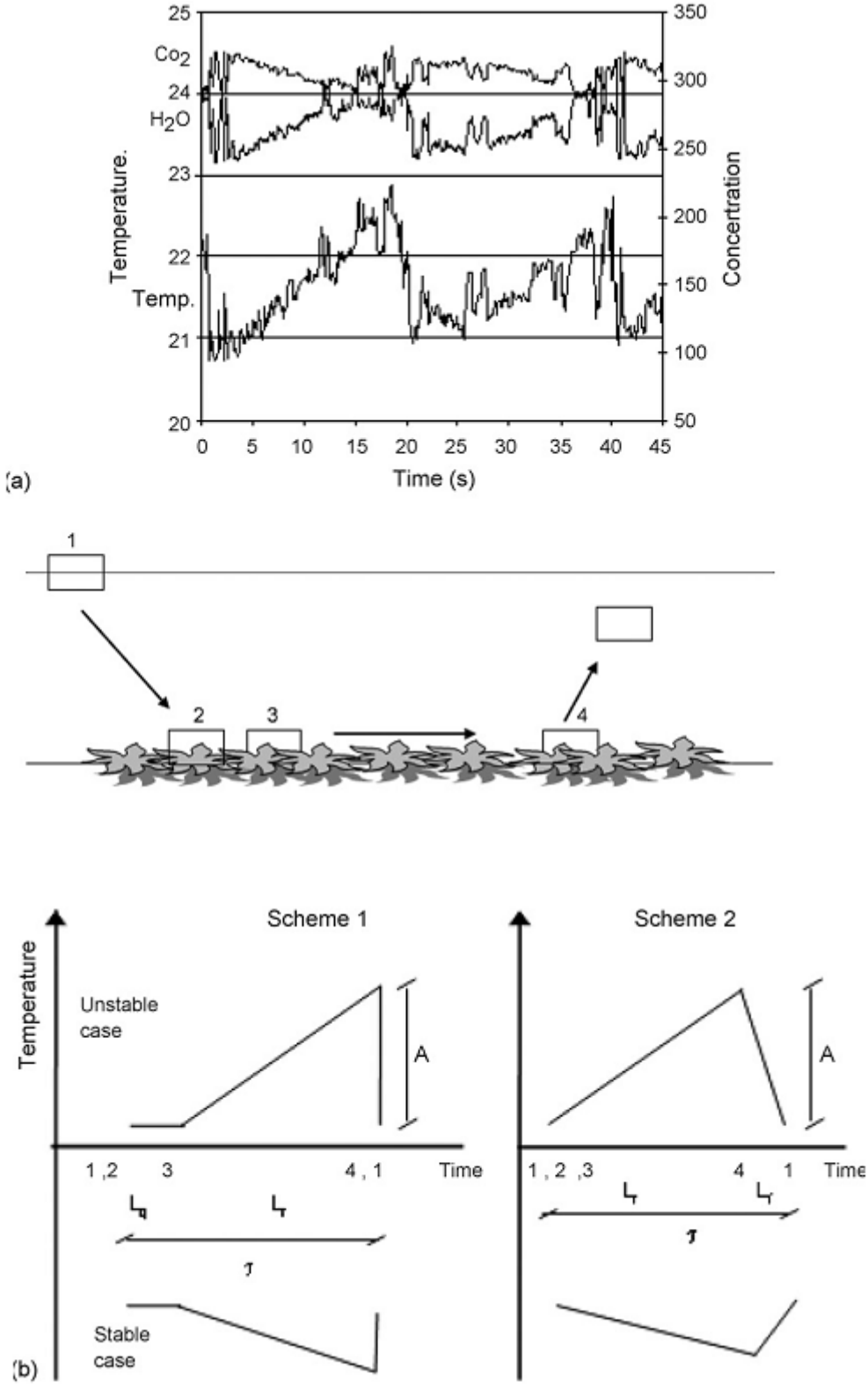

Fig. 13. (a) Temperature (T in °C), water vapour concentration (H2O in mm olm-3), and carbon dioxide concentration (CO2 in x 10-4mol m-3) versus time for a 45 s interval during a sample from 1330 to 1400 h on 14 April. (b) Air parcel diagram of the renewal process.

Figure 13 (a) shows a graph of temperature (℃), wa ter vapour concentration (H_2O in mmol m^{-3}), and carbon dioxide concentration (CO_2 in x 10^{-4}mol m^{-3}) versus time for a 45 s interval during a sample from 1330 to 1400 h on 14 April. For each scalar, two ramps are shown which have durations of about 20 s. The amplitudes are positive for temperature and water vapour concentration and negative for CO_2 concentration. Figure 13 (b) represents a air parcel diagram of the renewal process. The time course of the scalar concentration for the positions shown in the diagram are idealized in two air temperature ramp models. Scheme 1 assumes a quiescent period and a sharp instantaneous drop in temperature. Scheme 2 neglects the quiescent period and assumes a finite micro-front. L_r and L_f denote the warming, quiescent and micro-front periods, respectively. A is the ramp amplitude and τ is the toal ramp duration (Castellvì et al., 2008).

For a brief period, after an air parcel meets the surface its temperature remains the same. The energy flux from the surface to the parcel of air makes this last warm and at the same time, a slow rise in temperature is depicted from the time trace of the air temperature. The warming process stops when the air parcel encounters a cool air parcel, depicting this new event as an abrupt drop, because the heated air parcel is ejected upwards. The shape of the air parcel movement is ramp-like, where the sudden drop refers to the ramp amplitude (a) and the total duration refers to the ramp period (τ). The combination of the ramp amplitude together with the ramp period is used to determine H.

Under many circumstances, surface renewal measurements highly correlate with eddy covariance measurements. However, surface renewal measurements must be calibrated to account for linear bias of the data, which often corresponds to an overestimation.

G MEASUREMENT

Ground heat flux represent an important surface energy component and it can be measured by various instruments, such as the ground heat flux plates for example:

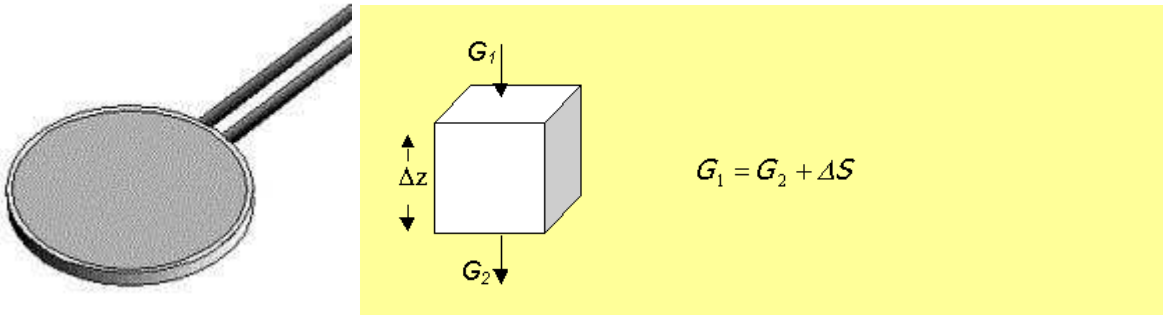

Figure 14 (a) Heat flux plate (http://www.iac.ethz.ch/en/research/riet/instruments.html); (b) schematization of soil heat flux measurement.(source: biomet.ucdavis.edu).

Figure (a) represents a soil heat flux plate, while figure (b) represents the physical principle that allows the soil (or ground) heat flux measurement. The plate, in fact, measures the difference in temperature between the two side of itself, named as G_1 and G_2, while Δz is the thickness of the plate.

2.2. THE SOIL WATER BALANCE

Evaporative loss from transpiration, soil, foliage, and sprinkler spray is expressed by equation (25):

$$E + T = P + I \pm \Delta\theta - R - \mathrm{Pr} \pm \Delta wt \qquad (25),$$

where E is evaporation, T is transpiration (Figure 15), P is precipitation, I is the irrigation, Δθ is the change in soil water content for the medium of interest, and R, Pr, and Δwt are the runoff, the percolation and the water table contribute terms, respectively. The units are water depth per unit of time [mm d^{-1}].

While precipitation term (P) can be measured by a pluviometer (mechanic or electronic), the R, Pr and Δwt depend on the type of soil, from its slope and from the water table characteristics, which can be estimated. Δθ measurement can be or in situ or from remote.

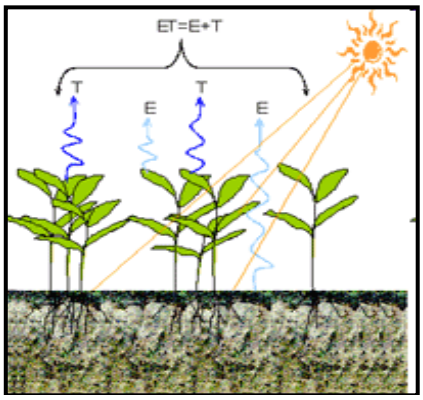

Figure 15- Evapotranspiration process, composed by the evaporation (E) from bare soil and transpiration (T) by plants, due to solar radiation ([2] http.//www.**edis-news.wp.ifas.ufl.edu**.)

E can be measured with micro-lysimeters, to separate E from evapotranspiration (ET) in the soil medium, and T, measured with stem flow gauges, or by having no plants in the system. ET can also be calculated with specific equations (Penman-Monteith or Hargraves-Samani) which will be analyzed later in next paragraph, or measured using energy balance methods.

2.3. EVAPOTRANSPIRATION

Evaporation is defined as the water-vapour flux from a surface towards the atmosphere and it is an important component in soil water and energy balances. (Chanzy, 2003). In a soil-plant-atmosphere system, evaporation occurs from each of the system components (Burt et al., 2005). A plant receives direct sunlight, radiation reflected by clouds, ground surface, and other objects, thermal radiation streaming downward from the atmosphere and thermal infrared radiation streaming upward from the surface of the ground. Energy is transferred to or from the plant by convection if the plant surface temperature is different from air temperature. If the air is cooler than the surface of the plant, energy from the plant will be lost to the air by convection. If the air is warmer than the surface of the plant, energy will be delivered to the plant by convection. Water is lost from the plant by transpiration and from soil by evaporation of soil moisture. Plants can transpire too, not only when the heat loaded on their surface becomes too high, but mainly in order to keep a constant inner water flux, to deliver biochemical components and produce photosynthesized molecules.

As the water available for agriculture becomes limiting due to population growth, competition from other water users, drought and water quality degradation, it is important to ensure that every drop of water (both from rainfall and from irrigation) counts for crop water use. At present and in the future, irrigated agriculture will take place under water scarcity conditions. Insufficient water supply for irrigation will be the norm rather than the exception, and irrigation management will shift from emphasizing production per unit area towards maximizing the production per unit of water consumed, also named water productivity. To cope with scarce water supplies, deficit irrigation, defined as the application of water below full crop-water requirements (evapotranspiration), is an important tool to achieve the goal of reducing irrigation water use (Fereres and Soriano, 2006).

Evaporation from the soil is effected by the environmental conditions, tilth, type, and soil water content, as well as the presence or absence of surface mulches (Sinclair, 2003). Soil evaporation is a three-stage process (Ventura et al., 2006). In stage one, the amount of energy available to vaporize soil moisture in the upper layer of soil is the only limiting factor for the evaporation rate, and it is considered similar to evaporation from a free water surface. Soil hydraulic properties and the lack of water in the upper soil layer are the two limiting factors of evaporation rate, in stage two. Physical and adsorbing soil characteristic are the two main component of stage three, during which evaporation rate is negligible.

Evaporation from the atmosphere (sprinkler droplet evaporation) is associated with sprinkler irrigation methods and it corresponds to the amount of applied water not reaching the soil-plant system, but does not include drift losses. Driving factors in this case are relative humidity, water temperature, droplet size, angle, and distance of droplet travel.

Since, evaporation from plant surfaces is effected by the plant canopy water storage capacity, plants are effected by their water storage capacity, the rain or irrigation length of time affecting the plants, and the water conditions imposed on the plants. Transpiration, in fact, is the process by which water is vaporized from cell walls inside leaves and diffuses from the leaf interior to the bulk atmosphere around plants. It is a complex mechanism, which implies water vapour molecules moving from the leaf interior, through pores in the leaf epidermis called stomata, and then vapour diffuses into the bulk atmosphere. Transpiration rates rapidly and dynamically responds to the environment, since stomata are under active control. Plant canopy transpiration rates calculation starts from the understanding of the influence of both carbon dioxide and water vapour flux density on stomata regulation.

Evapotranspiration (ET) represents the major consumptive use of irrigation water and rainfall on agricultural land (Burt et al., 2005). It is the combination of evaporation from bare soil and transpiration from crop – is related with different weather parameters: the solar energy, the driving factor, the heat transferred to the ground and/or to the air, the metabolic energy used by plants and the energy coming from the evapotranspiration process (Snyder and Pruitt, 1992; Allen et al., 1998). The ability to partition ET into Evaporation and Transpiration components will help irrigation managers to find ways to improve water use efficiency by increasing transpiration and reducing evaporation ([1]http://www-naweb.iaea.org/nafa/news/water-management.html).

The principal weather parameters affecting evapotranspiration (ET) are radiation –which has been already introduced- air temperature, humidity and wind speed. Several procedures have been developed to assess the evaporation rate from these parameters. Moreover, ET is part of the general hydrological cycle and it is affected by several atmospheric parameters, among which we find: temperature, carbon dioxide (CO_2) concentration and humidity. All these factors are differently connected and influenced by each other.

Two are the fundamental cycles in order to understand the atmospheric systems: the solar energy cycle (heat) and the water ones (mass) (Oke, 1978).

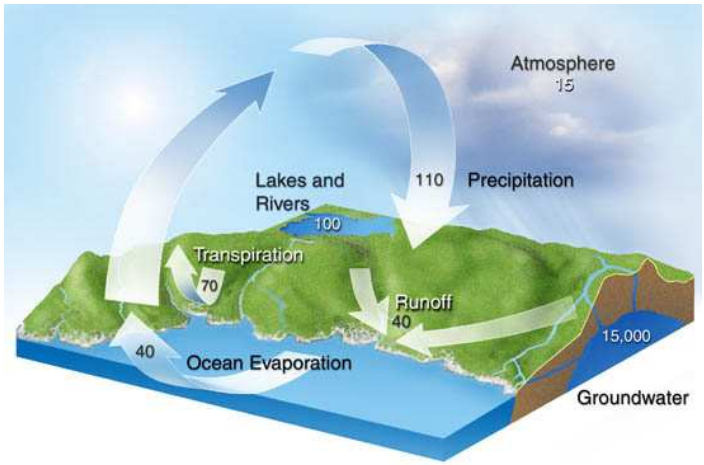

Figure 16 - Water in a changing world: the renewable freshwater cycle ([3]http://www.biology.duke.edu/jackson/fig3.html)

Figure 16 shows the renewable freshwater cycle in units of thousands of km^3/yr, respectively, for pools (white numbers) and fluxes (black numbers). Total precipitation over land is ~110,000 km^3/yr. approximately, two-thirds of this precipitation is water transpired from plants and evaporated from the soil (ET is 70,000 km^3/yr), and whereas one-third is water evaporated from the oceans that is transported over land (40,000 km^3/yr). Total evaporation from the oceans is ~10 times larger than the flux pictured here (approximated 425,000 km^3/yr). Groundwater holds ~15,000,000 km^3 of fresh water, much of which is not in active exchange with the earth's surface (Jackson et al., 2001).

2.4. METHODS TO MEASURE EVAPOTRANSPIRATION

Semi-Empirical and empirical methods apply the only bare soil evaporation. A series of semi-empirical and empirical relationships for E have been developed, but they are non-transferable because very site specific (Ritchie, 1972; Stroonsnjider, 1987; Gallardo et al, 1996; Snyder et al., 2000). The more recent papers found a good semi-empirical relationship between cumulative bare soil evaporation and cumulative reference ET.

Measurements of fluxes by micrometeorological methods can be associated with some group of factors describing how the surface controls or responds to the flux. Considering the canopy as an electrical analogue the rate of exchange of an entity between a single leaf and its environment can be assessed by knowing the potential of the entity at the leaf and in the surrounding air. The other condition for computing the exchange rate is to measure or assess the relevant resistances.

The canopy (or crop, or cover) resistance (r_c) is a parameter which plays the same part in equations for the water vapour exchange of a canopy as the stomatal resistance plays in similar equations for a single leaf.

The two equations most used for calculating the reference evapotranspiration (ET_0) (Fig. 17) are the Penman-Monteith and the Hargraves-Samani equations. The reference evapotranspiration accounts for the weather parameters and it is the first step in order to compute the crop evapotranspiration, theoretical (ET_c) and actual ($ET_{c\ adj}$ or ET_a). The Penman Monteith equation requires a higher amount of data, than the Hargraves-Samani equation. For this reason Penman Monteith equation is considered the most rigorous and it will be discuss in this chapter.

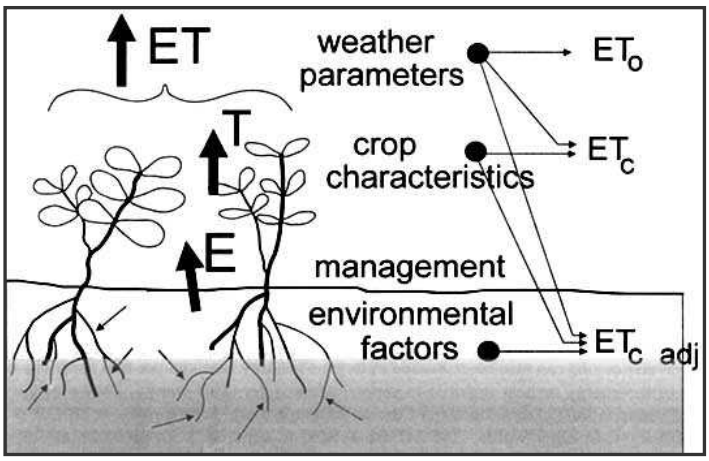

Fig. 17 Reference Evapotranspiration (ET_0), Crop Evapotranspiration (ET_c) and Adjusted Crop Evapotranspiration ($ET_{c\ adj}$) (http://www.fao.org/docrep/W5183E/w5183e07.htm).

Considering the air/plant/soil system as an electronic circuit, this is composed by different resistances. For example, r_c is the canopy or surface resistance and r_a is the aerodynamic resistance, as the figure 18 shows.

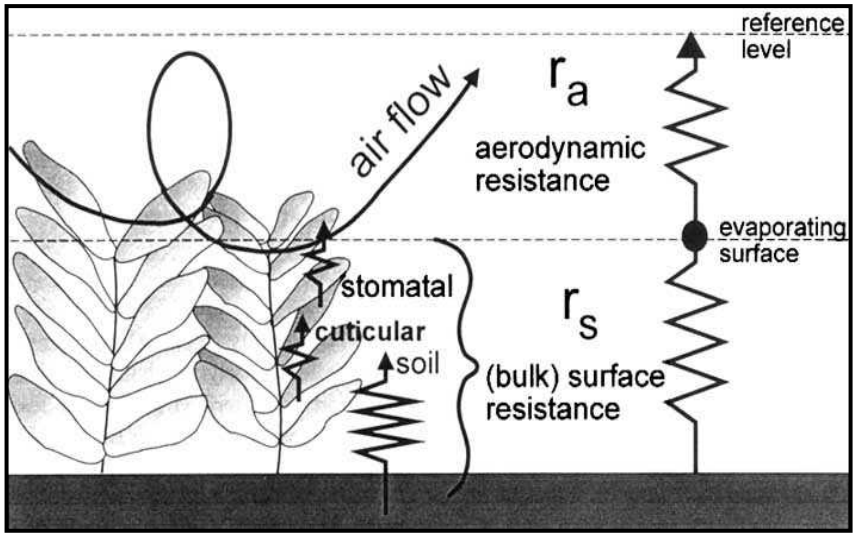

Figure 18- Air/plant/soil system circuit schematization. Rs is the bulk or surface resistance and ra is the aerodynamic resistance ([21]http://www.fao.org/docrep/X0490E/x0490e06.htm).

Eq. (26) is the Penman Monteith equation for latent heat (LE) flux density, which describes the different energy balance variables and how they affect LE.

$$LE = \frac{\Delta\left(R_n - G\right) + \frac{\rho C_p}{\Delta r_h}\left(e_s\left(T\left(z\right)\right) - e\left(z\right)\right)}{1 + \frac{\gamma}{\Delta}\frac{r_w + r_s}{r_h}} \quad (26),$$

where LE is the Latent heat flux [Wm^{-2}], R_n represents the net radiation [Wm^{-2}], G stands for the ground heat flux [Wm^{-2}], ρ is dry air density [kgm^{-3}], C_p is the specific heat capacity of air [J kg^{-1} K^{-1}], and Δ is the change in $e_s(T)$ per change in T [kPa/℃], as reported in Eq. (2 7).

$$\Delta = \frac{\partial e}{\partial T} \quad (27),$$

where r_h represents the aerodynamic resistance to heat flux [s m^{-1}], $e_s(T)$ is the saturation vapour pressure [kPa], T is the absolute temperature [Kelvin], e(z) stands for the vapor pressure at height z [kPa], and γ is the psicrometric constant [kPa ℃ $^{-1}$].

The Penman equation for evapotranspiration assumes that the stomatal resistance r_s is equal to zero, because a well watered condition of the plants is realized by definition. In addition, one could assume that the aerodynamic resistance to water vapour flux and heat flux are very similar ($r_w \approx r_h$).

Over large flat homogeneous terrain, the aerodynamic resistance to sensible heat transfer (r_h) may be approximated by Equation (28).

$$r_h = \frac{\left[\ln\left(\left(z-d\right)/z_0\right)\right]^2}{0.16U\left(z\right)} \quad (28),$$

where U(z) stands for the wind speed at height z [m s-1], z_0 is the roughness of the terrain (≈0.13*canopy height), and d is the zero plane displacement (≈0.63* canopy height).

For the Penman-Monteith ET_0 equation, T and e should be measured at 1.5 to 2.0 m height above the ground over a grass surface and the wind speed should be measured at 2.0 m height over a grass surface (u_2). Using these heights, the aerodynamic resistance simplified to the equation is equal to the ratio of 208 divided by the wind speed.

Based on typical leaf stomatal resistance and the effective LAI for a 0.12 m tall grass canopy, the surface resistance is assumed to be r_s = 70 s m^{-1}, when using daily data in the Penman-Monteith equation for ET_0.

In agrometeorology, the measurements of ecosystem-scale energy and mass flux density are very important, especially as climate change, environmental policy, and growing urban

demands limit agricultural water resources (California Department of Water Resources, 2005). In order to improve water use efficiency of irrigated crops, agrometeorologists measure ET to evaluate experimental treatments. The aim is to provide growers with crop ET information through the concept of crop coefficients, and to optimize regional water management practises (Moratiel and Martinez-Cob, 2011; Doorenbos and Pruitt, 1977; Snyder et al., 2005). Crop coefficients are values, which allow switching from the reference ET (ET_0) to the crop ET (ET_c) and vice-versa. ETc is defined as the ET from a specified vegetative surface in good agronomic condition, extensive area, under optimum soil water conditions and achieving full production under the given climatic conditions. ET_c varies according to meteorological variables (primarily radiation, vapour pressure deficit and wind speed) and according to canopy characteristics (leaf surface area, the plant height and roughness, reflection and ground cover of the leaves). This last group of factors changes with season and growth stage, for all this reason it is difficult to quantify. Therefore, ET equations are rarely used in a single step. Instead, a crop coefficient approach is used, giving an integration of the effects of the canopy characteristics that distinguish the crop from the reference surface (Pereira et al, 1999; Peacock and Hess, 2004).

The Food and Agriculture Organization of the United Nation (FAO) provided a procedure for calculating reference and crop evapotranspiration (ET_c) from meteorological data and crop coefficients (K_c). This procedure is presented in FAO Irrigation and Drainage paper No. 24 'Crop water requirements', and updated in FAO Irrigation and Drainage paper No. 56 (Allen et al., 1998). The conjunction of these two values is useful also for estimating the partitioning of ET into E and T (Burt et al., 2005).

FAO Irrigation and Drainage paper No. 56 reports the approximate date of planting and the duration in days of the four growth stages of various crops. As well, K_c values vary during these growing periods:

A - seeding or planting, corresponding to the change from bare soil to a minimum ground cover;

B- rapid growth or leaf out, during which the canopy increases the ground cover;

C- maturation, during which kc value is fixed,

D- senescence or leaf drop.

Crop coefficient lines represent K_c values varying during the growing period.

Three values for K_c are required to describe and construct the crop coefficient curve (Fig. 19): those during the initial stage ($K_{c\ ini}$), the mid-season stage ($K_{c\ mid}$) and at the end of the late season stage ($K_{c\ end}$).

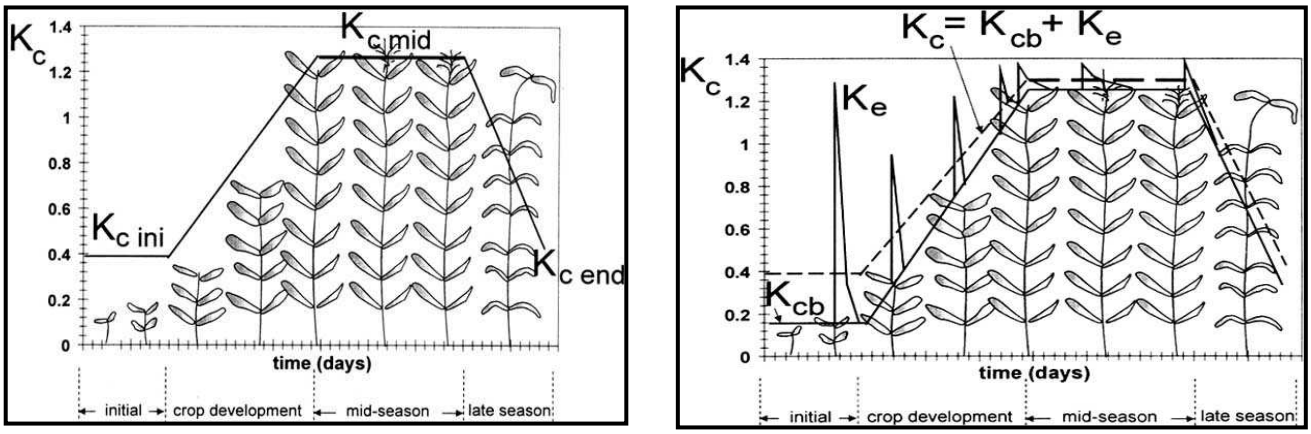

Figure 19 Schematization of “single” and “dual” Kc curve, according to FAO-56 paper (Allen et al., 1998).

In FAO-56 two methods are described for ET_c calculation (Eq. 29) and they are called the ‘single’ and the ‘dual’ method. The ‘single’ crop coefficient (K_c) approach is the method mostly adopted to quantify the consumptive water use for irrigated crops (Allen et al., 1998; Allen, 2002).

$$ET_c = K_c ET_0 \quad (29),$$

The K_c term in Equation (29) can be replaced as a dual crop coefficient to partition E and T, as follows in Equation (30):

$$K_c = K_s K_{cb} + K_e \quad (30),$$

where K_s is the reduction coefficient for crop stress, K_{cb} is the basal crop coefficient, or the ratio of ET_c to ET_0 for dry surface soil conditions in which the water content in the underlying soil does not limit the full plant transpiration needs, and K_e is a soil water evaporation coefficient. Generally, evaporation is computed by multiplying K_s by ET_0 and transpiration is obtained by multiplying K_e by ET_0.

According to this procedure, K_c is an empirical crop coefficient and ET_o is the reference evapotranspiration for a grass or alfalfa reference crop. Since it is very difficult to apply water balance approach, for studies where ET_c is computed as residual, the K_c ET_o method has been the primary approach for predicting water consumption for irrigation projects. In effects, deep percolation components are complicated to measure and this implies a large approximation in ET_c computed from the water balance. The approximation is due to many factors: representativeness and quality of weather data used to estimate ET_o, uncertainties regarding planting, growth stage, harvest dates, precipitation events, agronomic practices implied in the K_c

factor. Therefore, a big variety of K_c value are present in literature for every crop and this uncertainties line out the question if K_c ET_o will over or under predict actual ET_c.

In Snyder et al. (2010) data from 18 California Irrigation Management Information System or CIMIS stations for the 2006 year were used for the analysis of the possible effect of climate change on ET_0. The stations cover a wide range of climate conditions and vary from cool, moist coastal to hot, dry desert locations. The elevation varies from well below sea level (-55 m) to a high mountain valley (1271 m). The climate is Mediterranean but with a wide range of micro-climates due to proximity to the cold ocean and high mountains. Monthly means of daily climate data from 2006 were used to make the daily mean ET_0 calculations. The daily ET_0 means were multiplied by the days per month to obtain monthly totals, and the monthly totals were summed to obtain annual total ET_0 for each location. Reference ET was computed using a modification of the equation based on Monteith (1965), developed by the American Society of Civil Engineers–Environmental Water Resources Institute (EWRI) (Eq. 7). This equation allows computing the standardized reference ET for short canopies (ET_0) to quantify evaporative demand (Allen et al., 2005). The following monthly version of the ET_0 equation (Eq. 31) was used for the analysis in Snyder et al. (2010).

$$ET_o = \frac{0.408\Delta(R_n - G) + \frac{900\gamma(e_s - e)u_2}{T + 273}}{\Delta + \gamma(1 + 0.34u_2)} \quad (31),$$

where Δ [kPaK^{-1}] is the slope of the saturation vapour-pressure-curve at the mean daily air temperature. Rn [MJm^{-2}d^{-1}] is the net radiation over well-watered grass. G is the soil heat flux density [MJ m^{-2} d^{-1}]. γ [kPa K^{-1}] is the psychrometric constant. T [℃] is the mean daily air temperature at 1.5 – 2.0 m height. u_2 [ms^{-1}] is the wind speed measured at 2 m above the ground, and e_s and e [kPa] are the saturation and actual vapour pressures of the air. Equations about R_n, G, and Δ computation have already been provided in previous paragraphs.

The aerodynamic resistance to sensible and latent heat transfer (r_a) occurs in two locations in Eq. (31). The 0.34 in the denominator comes from the following Eq. (32):

$$\frac{r_c}{r_a} = \frac{70}{208/u_2} \approx 0.34u_2 \quad (32),$$

where r_c equals 70 sm^{-1} and r_a equals $208/u_2$. In Eq. (34), the right-hand side of the numerator could be written as Eq. (33):

$$\frac{900\gamma(e_s - e)u_2}{T+273} = \frac{187200[\gamma(e_s - e)]/(T+273)}{208/u_2} = \frac{187200[\gamma(e_s - e)]/(T+273)}{r_a} \quad (33),$$

Therefore, the 208 coefficient is also included in the 900 in the numerator of Eq. (33).

The r_c=70 sm^{-1} was derived by estimating the typical stomatal resistance r_s=100 sm-1 (corresponding to stomatal conductance g_s=0.010 m s^{-1}=10 mm s^{-1}) for the actively transpiring C3 grass leaf surface, which was estimated as half of the LAI = 2.88. Therefore, the canopy resistance for 0.12 m tall C3 species grass r_c was calculated as equation (34):

$$r_c = \frac{r_s}{0.5 \cdot LAI} = \frac{100\, s\, m^{-1}}{0.5 \times 2.88} = 69 \approx 70 \;\; s\; m^{-1} \quad (34),$$

Assuming that the $r_c \approx 70$ sm^{-1} applies under the current 372 ppm atmospheric CO_2 concentration, estimating a new r_c value for higher CO_2 concentration provides a method to estimate possible impacts of higher CO_2 on ET_0.

Tab. 4 Variables used to modify the current climate data and obtain scenarios for climate change projections for 2050. T_x is the maximum temperature, T_n is the minimum temperature, T_d is the dew point temperature and r_c is the canopy resistance (Snyder et. al. 2010).

Scenario	T_X (^oC)	T_n (^oC)	T_d (^oC)	r_c (sm^{-1})
1.a.	+0	+0	+0	70
1.b.	+0	+0	+0	87
2.a.	+2	+4	+0	70
2.b.	+2	+4	+0	87
3.a.	+2	+4	+4	70
3.b.	+2	+4	+4	87

Table 4 shows the different combinations of variation of four variables, which are: maximum temperature (T_x), minimum temperature (T_n), dew point temperature (T_d), and canopy resistance (r_c), that were used to modify the current climate data and obtain scenarios for climate change projections to 2050.

The same temperature and r_c modifications were applied equally to data from all months and at all locations, so there was no attempt to adjust for possible seasonal or regional differences in climate change. This could be improved to more accurately estimate ET_0 changes if a reliable regional downscale model from a global model were available. However, the study does show how an equivalent climate change might affect ET_0 depending on initial conditions. Based on climate trends (Roderick and Farquar, 2002) and plant stomatal response to CO_2 (Long et al., 2004), scenario 3.b. is the most likely to occur on a global scale. Therefore, the relationship

between current annual ET_0 (i.e. scenario 1.a., Figu. 20-21) and scenario 3.b. was investigated to determine if the ET_0 responses to climate change might vary depending on initial climate conditions.

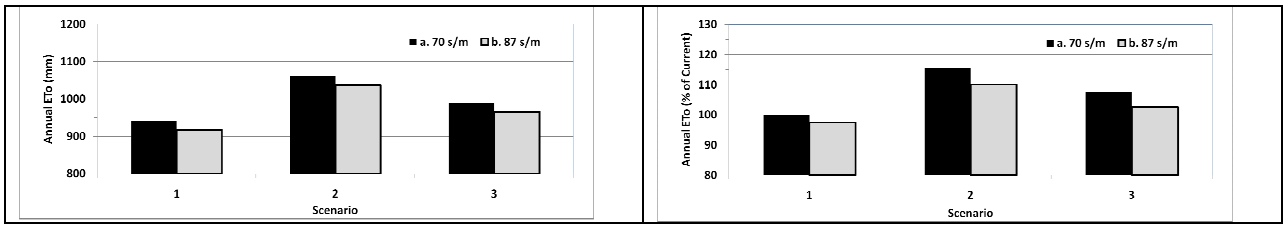

Fig. 20 and 21 Annual total ET_0 (mm) and annual ET_0 as a percentage of current annual ET_0 (scenario 1.a.) by scenario for Oakland, California. Note that the black columns are for r_c=70 s m^{-1} and the gray are for r_c=87 s m^{-1}.

According to Snyder et al., 2010, climate change is likely to increase temperature and stomatal resistance of plants, and all of those parameters affect ET_0. The results of that study indicated that the change would have little impact on annual ET_0 assuming that the T_d rises at the same rate as T_n and the canopy resistance increases to 87 sm^{-1}. The annual ET_0 would increase slightly in non-windy regions, and it actually would decrease in windier locations. However, the absolute magnitude of variation from the current annual ET_0 would be small in all locations when T_d and r_c compensated for higher temperature.

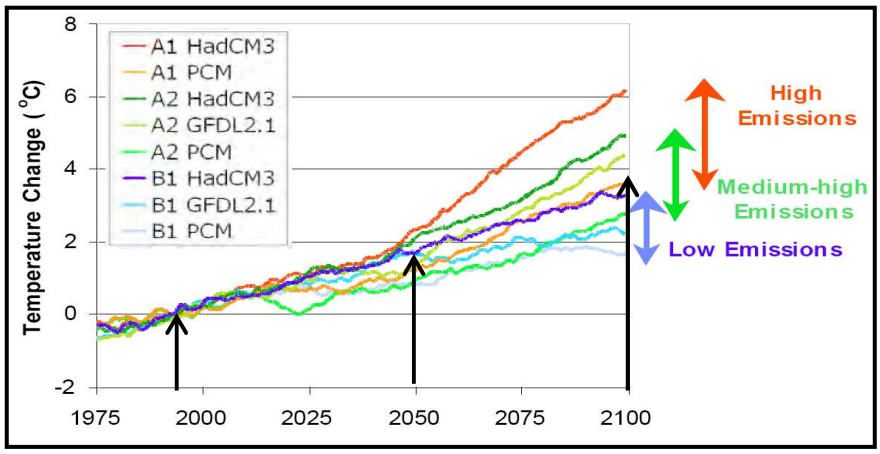

Figure 22 Change in California Annual Average Daily Mean Temperature Relative to 1971–2000, in three different scenarios (4California EPA Report to the Governor and Legislature (Dec. 8, 2005).

Figure 22 shows the mean daily temperature changes versus the time, with measured data related to 1971 – 2000 period, the other are projections. These projections are based on 3 different hypothetical scenario types:

1. High emissions: red colour.
2. Medium-high emissions: green colour.
3. low emissions: violet colour.

Even in the more optimistic cases, there still be a 2° C temperature increase by the end of the century. If we consider the medium high emission scenario, this increase corresponds to 3℃: this is the scenario choosen from Snyder et al. (2011) for the first projections of impacts on plant evapotranspiration due to climate changes study.

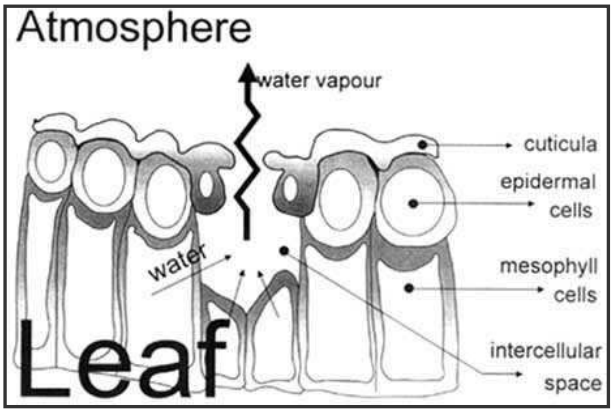

Figure 23 Schematic representation of a stoma (5http://www.fao.org/docrep/X0490E/x0490e04.htm

Plants need CO_2 in order to make photosynthesis, so opening the stomata, CO_2 can enter into the leaf, but this implies that the leaf looses water vapour (Fig. 23). Opening stomata is for plants a compromise between water loss and uptake of CO_2 from ambient air (Farquhar et al., 1980; Mott, 1990; Wolfe, 1994; Stanghellini and Bunce, 1994; Leuning, 1995). A partial stomatal closure is in general the response of plants to elevated concentrations of CO_2 (Fig 24), trying to keep constant the ratio between the inside (C_i) and the outside (C_a) concentration. (Mott, 1990; Goudriaan and Unsworth, 1990). In steady state conditions, the ratio (C_i/C_a) is equal to 2/3 and ¼ for C3 and C4 plants respectively, because of the higher affinity for CO_2 for C4 plants, and reflects the more efficient water use for these plants (Goudriaan and Unsworth, 1990; Kimball et al., 1993; Kimball et al., 1995). For a given water vapour deficit there is a constant ratio (C_i/C_a) with the atmospheric concentration. Such a regulation would directly lead to the partial stomatal closure at elevated CO_2, as observed in many studies using porometers (Tyree and Alexander, 1993; Morison and Gifford, 1983; Morison, 1987). Measuring photosynthesis and water relation, Jackson et al. (1994) found out that, with a small rise tendency, the value tends likely to be conserved, for native grassland.

The required CO_2 supply and the photosynthesis rate are directly correlated with light intensity. From this, one can derive that stomata conductance is highly correlated to light intensity (Leuning, 1995) and this relation is connected with environmental conditions, such as water stress.

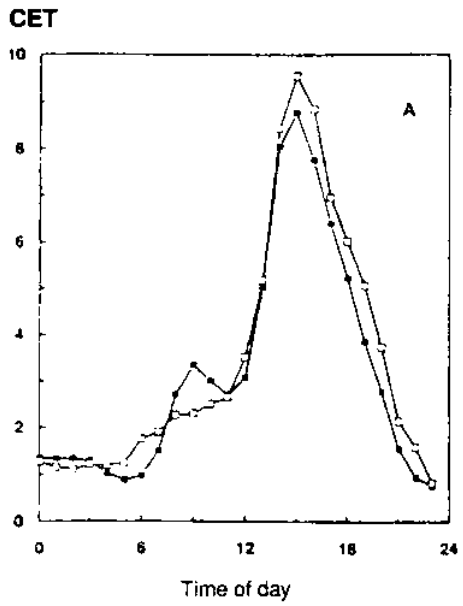

Figure 24. Effect (1992) (6http://www.fao.org/docrep/W5183E/w5183e07.htm).

Theoretically, with increasing temperature, evaporation from water surfaces also increases, which means higher atmospheric water vapour concentration, and higher humidity. Increasing atmospheric humidity, the atmospheric gradient that allows plant to transpire, will decrease. This implies that with higher humidity and higher temperature, plants will transpire less, increasing their heat stress. According to McKenney and Rosenberg (1993), the atmospheric evaporative demand would raise up about 5 to 6% per degree warming as determined by the vapour pressure deficit. Even if the main effect of a higher temperature alone can be translated in an intensification of the hydrological cycle, the combination of higher temperature and higher evaporative demand, a partial stomata closure counteracts this (Fig. 25). Moreover, a higher vapour pressure leads to different atmospheric conditions, including relative air humidity, soil available water and precipitation pattern.

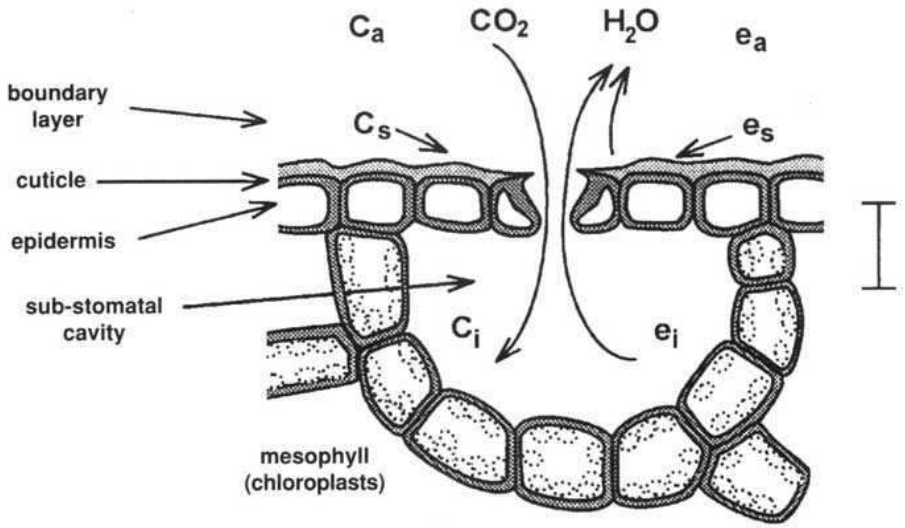

Figure 25 - Schematic cross-section of a stomata of a leaf showing the pathway of CO_2, and H_2O of a leaf exposed to light. C_i, C_s, C_a: internal, surface and ambient CO_2 concentration; e_i, e_s, e_a: internal, surface and ambient air humidity. Bar indicates 100 μm ([6]http://www.fao.org/docrep/W5183E/w5183e07.htm)

In addition to the sensitivity of stomata to photosynthesis and CO_2 concentration, Jacobs (1994) introduced an additional correlative relationship between the humidity deficit at the leaf surface and the C_i/C_a ratio. An estimated overall decrease of the regional transpiration by 10 to 30% is reported in that study. Surface roughness is determined by the vegetation type, temperature, and air humidity. Arable crops, especially in the temperate regions in general, have a low surface roughness, and in that case the transpiration is primarily determined by the radiation energy. This is also true for pastures. In rangelands with sparse higher vegetation the higher roughness leads to a stronger coupling, a situation comparable to forests and mixed vegetation (McNaughton and Jarvis ,1991; Hollinger et al., 1994; McNaughton, 1994).

Thus, while climate change is likely to increase air temperature, the effect of higher humidity and CO_2 concentration could partially offset the temperature effect on ET of C_3 plants.

Since water crop requirements are strictly related with the climate and irrigation scheduling is mostly based on crop evapotranspiration, the starting point of this study was a previous research on the possible impacts of climate change on ET. The study was conducted according to the different climate of California, a state of USA characterized by many different climate zones. The aim of the study was to understand in which type of climatic area the impacts will be more or less important.

Figure 26 shows an evapotranspiration map of California, where the different colours represent the different inches of water evaporated per month, on a zone scale which goes from 1 (=violet) to 18 (=red). From this map we can see how ET can be different, according to the climate of the region. So that the impact of climate change differs depending on the “initial” conditions, and for this reason the impact assessment includes climate data from locations having a wide range of micro-climates.

According to the projections of climate change for the Euro-Mediterranean region obtained from global models, the region may be subjected to a substantial warming, which in the Mediterranean basin would be more pronounced in summer and at the end of the twenty-first century it could reach a 4℃-5℃ increase in the se asonal mean surface temperature compared to the end of the twentieth century. The warmer temperature would be accompanied by an increased in winter precipitation in the north of the Alps, while southern Europe and the Mediterranean region would suffer a drastic reduction in precipitation, more pronounced in summer (-25-30%). In addition, the global projections indicate that the signal of climate change is clearly visible also in the variability among various years, which shows a marked tendency to increase as does the occurrence of extreme events (heat waves) and drought (IPCC, 2007).

In Emilia-Romagna the increase of temperature from 2000 to 2016 means a modest increase in the domestic water demand. The irrigation season in Emilia-Romagna is the summer. The demand for irrigation water depends from a lot of factors: temperature, precipitation, wind etc. For summer a weak trend for an increase in precipitation and quite no increase in temperature are forecasted. The Water Protection Plan of the Emilia-Romagna Region has an approach to water resources planning mainly based on the sustainable development and the 'twin-track' strategies (better water balance, reduction of water losses in the irrigation network, water saving by irrigation techniques, and the promotion of appropriate irrigation technologies and timing through advice, demonstration of best practices.

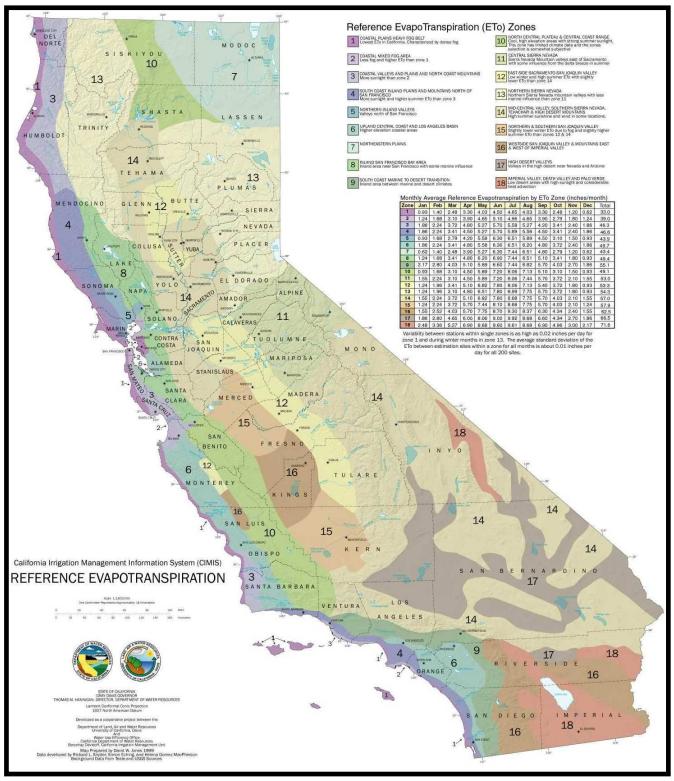

Figure 26 Data from 18 California Irrigation Management Information System or CIMIS (Snyder and Pruitt, 1992) stations from 2006 were used for the analysis. The stations cover a wide range of climate conditions and vary from cool, moist coastal to hot, dry des

3. PROJECT MOTIVATION AND OBJECTIVES

The motivation for this project is my personal high interest in the deep relation existing between environment, and its natural resources, and human beings and their fundamental needs, which are food and water availability. Agriculture is the link between environment and human life. And water is a key factor for the wellness of both.

After founding an internet article (FAO, 2003), a contribution to the World Water Assessment (UNESCO-WWAP) that attempted to answer the question of How can the world food production be made more efficient without compromising the environment? Global food production has kept pace with population growth in recent decades; there is an high percentage of people in undernourished nutrition conditions and world population is growing, meaning an increased need of food and thus more water. At the same time, climate seems changing its pattern, making water availability in some part of the world more difficult.

A literature research on crop water needs, made me arrive at the concept of evapotranspiration and crop coefficients, which are considered one of the key method to do irrigation planning. The problem is those crop coefficients present in literature are different, according to the different weather conditions of the specific site where they are measured. What was not present in literature was a method to obtain crop coefficient values valid for different climates, in particular for climate having wind speed different from 2 ms^{-1} and relative humidity different from 45%. Crop evapotranspiration is just one example of irrigation scheduling approach, so I decided it would be interesting to investigate this method further. Having never taken a course or studied biometeorology in depth, this project gave me good excuse to become more educated on the topic and form a better expertise on facing the subject as a whole. To do this, this study focused on the need of improving water use efficiency in agriculture, in relation to actual climate and future climate change impact on irrigated crops. The objectives of this study were:

to investigate crop coefficients (Kc) values already existing in literature, measured in different part of the World and so in different climate, in order to understand whether they are similar or not to Kc provided in FAO Irrigation and Drainage paper no. 56, which contains the guidelines for computing crop water requirements most accepted until now from scientists;

to provide a K_c values report and a data base for the different crops reviewed, which contains information that can be useful either for practical and study purposes;

to develop a K_c model that allows to use actual, or historical, or future weather generated, bio-meteorological data to compute crop evapotranspiration (ET_c), both by using the dual and the single K_c approach. The model includes the climate correction for wind speed and relative humidity, cover crop contribution, type and frequency of irrigation, immature trees correction, through the Penman-Monteith or the Hargraves-Samani equation, depending on the data set availability;

To test the model by using measured K_c values for different crops (maize, lettuce, broccoli, kiwifruit) in order to validate and improve the ET_c calculation;

The developed crop coefficient model will contribute to improve the irrigation scheduling, in order to actual and future climate change, its effect on world food production and water use efficiency in agriculture.

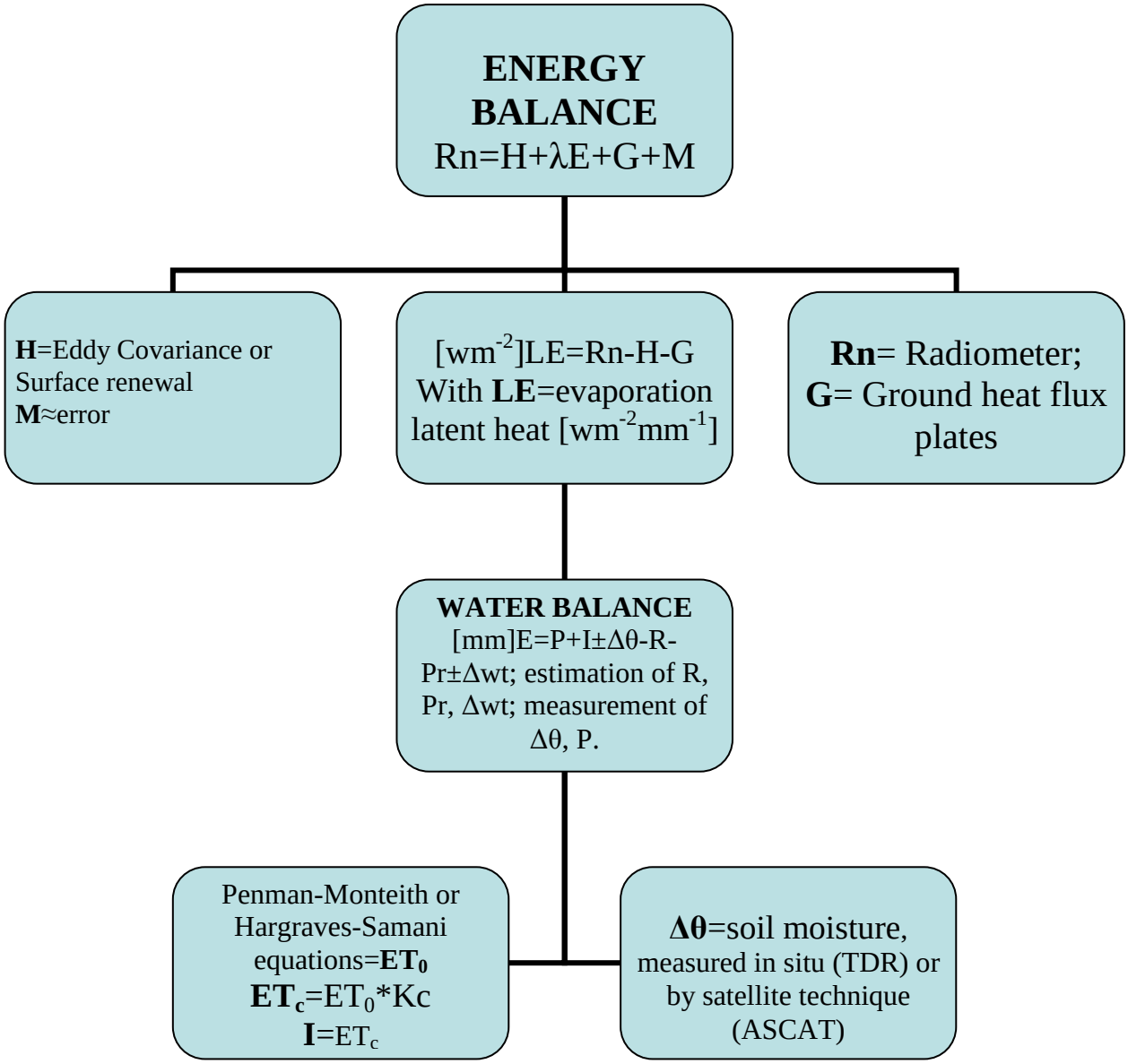

Figure 27 Flow chart of the study topic, methodologies and objectives

2.1. CROP COEFFICIENTS LITERATURE REVIEW AND DATA BASE

The first step for the creation a literature measured Kc values report was the repartition of the various papers regarding this topic in specific categories, according to the difference between herbaceous crops versus trees, perennial or seasonal leaves. Basing the distinction among crops on these assumptions, the more than 100 articles reviewed, investigating crop coefficient values of about 70 different crops, where grouped in four different categories. The first category, called 'seasonal field crops', group together all the field crops, characterized by crop development changing during the season. The second one is named 'annual field crops': their leaves do not change during the seasons. The crops of the third group are trees and vines, which have seasonal leaves. The fourth category is subtropical trees, whose leaves are present during all the year. Therefore, to summarise, there are two herbaceous crops (seasonal and annual, field- and row-crops) and two trees categories (deciduous trees and vines and subtropical trees).

For field and row crops (category n. 1) K_c are calculated using a method similar to that described by Doorenbos and Pruitt (1977). According to their method, the season separated into initial (date A-B), rapid (date C-B), midseason (Date C-D), and late season (date D-E) growth periods. During phases A-B and C-D, K_c values are initially constant. When the canopy increases from about 10 to 75% of ground cover, during phase B-C, K_c value linearly increases. During phase D-E, at the end of the season, K_c linearly decreases (Snyder et al., 2007). Some field crops are harvested before senescence, such as silage corn and fresh market tomatoes, and there is no late season drop in K_c curve. For annual crops (category n. 2), among which there are turfgrass and pasture, it is possible to use a fixed K_c value all over the year, with little loss in accuracy (Snyder et al., 2007),

Deciduous trees and vines crops (category n. 3), without a cover crop, have similar K_c curves, but without the initial growth period. The season begins with rapid growth at leaf out. The midseason period corresponds at ground cover reaching the 62% approximately. Then, for mature crops, K_c value doesn't change during phase C-D, after which senescence occurs and in phase D-E crops are characterized by leaf drop or by transpiration almost negligible immature deciduous trees and vine crops use less water than mature crops and a correction is applied to

adjust K_c values as a function of percentage ground cover. When a cover crop is present, K_c values for deciduous trees and vines are increased, according to the amount of cover.

For mature subtropical orchards, for example citrus, olive, palm, (category n. 4), fixed kc values during the season provide acceptable ET_c estimates. For immature orchards, the mature Kc values are adjusted for their percentage ground cover, by using a specific equation (Snyder et al., 2007).

In parallel with the crop coefficient literature review, a data base of all crop coefficient values corresponding to the initial, mid season and end season stages for each crop, described in each paper, was created, specifying an identification number of the crop, an identification number of the article, the values, the title of the paper, the author and the comment to the results obtained. In this way, it is easier to compare the different methods used in literature and the different values obtained.

2.2. CROP COEFFICIENT MODEL DESCRIPTION

Improved irrigation scheduling is needed to enhance efficient water use in agriculture, and the importance is increasing due to climate change and drought variability (Metz et al., 2007). Using crop coefficient (K_c) values with reference evapotranspiration (ET_o) to estimate crop evapotranspiration (ET_c) is a well-known and widespread method to estimate soil water depletion and schedule irrigation (Doorenbos and Pruitt, 1977; Jensen et al., 1990; Allen et al., 1998). In this method, the ET_c is estimated as the product of ET_o and K_c values, where ET_o represents the evaporative demand, and K_c values adjust for differences in crop, management, and climate. It is generally accepted that crop coefficients are somewhat universally applicable; however, the two main United Nations-Food and Agriculture Papers on evapotranspiration (Doorenbos and Pruitt, 1977; Allen et al., 1998) both presented methods to correct for climate impact on midseason K_c values. Although the climate corrections were presented, widespread usage is minimal and research results often neglect the climate effect in their K_c recommendations. Clearly, a more reliable procedure is needed to adjust for climate and to help scientists present their crop coefficient information in a more usable format.

Literature on crop coefficients shows considerable difficulty in reaching consistent K_c values mostly where advection is an important factor affecting evaporation (Pruitt et al., 1972; Grattan, 1998; Kang et al., 2003; Madeiros et al., 2001; Kuo et al., 2006; Lage et al, 2003; Tolk et al, 2001; Colaizzi et al., 2006). The UN-FAO publication 24 (Doorenbos and Pruitt, 1977) gave a

range of midseason Kc values for crops that varied depending on local wind and humidity conditions. They also presented a method to correct reference evapotranspiration for daytime and nighttime wind differences, which is not included in more recent publications. Also, the UN-FAO publication 56 (Allen et al., 1998) introduced an equation for correcting midseason K_c values as a function of wind speed and humidity. The Eq. (35) provides a method to adjust for the aerodynamic contribution of sensible heat flux to evapotranspiration. The correction for midseason K_c values (K_{cmid}) from Allen et al. (1998) was presented as:

$$K_{cmid} = K_{ctab} + [0.04(u_2 - 2) - 0.004(RH_n - 45)]\left(\frac{h_c}{3}\right)^{0.3} \quad (35),$$

where K_{ctab} is a tabular value for the midseason crop coefficient in a climate with u_2=2.0 ms^{-1} and a daily minimum relative humidity RH_n=45%. In the climate correction (Eq. 40), the K_{cmid} is increased if u_2>2.0 ms^{-1} and it is decreased for u_2<2.0ms^{-1}. The K_{cmid} is decreased if RH_n>45% and it is increased if RH_n<45%. The equation is weighted to adjust for the canopy height by multiplying by 1/3 of the canopy height raised to the 0.3 power.

To test the FAO 56 climate correction, the K_{cmid} was calculated using Eq. (35) and the mean daily climate data (Table 4) from 49 California Irrigation Management Information System (CIMIS) stations (Snyder and Pruitt, 1992) using the canopy heights 0.12, 0.5, 1.0, 1.5, 2.0, 2.5, 3.0, and 4.0 m. For each canopy height, the calculated correction factors, i.e., the right-hand component of Eq. (40), were plotted versus the July mean daily reference evapotranspiration (ET_o) for short canopies (Allen et al., 2005) for each station. For this data set, the regression lines all intersected the zero correction factor at a mean monthly ET_o =5.3 mm d^{-1}. The slopes were all positive and varied from 0.017 for h_c =0.12 m to 0.049 for h_c=4.0 m height. The plot for h_c=0.12 m height is shown in Fig. 31. The results, however, show a problem related to use of Eq. (35).

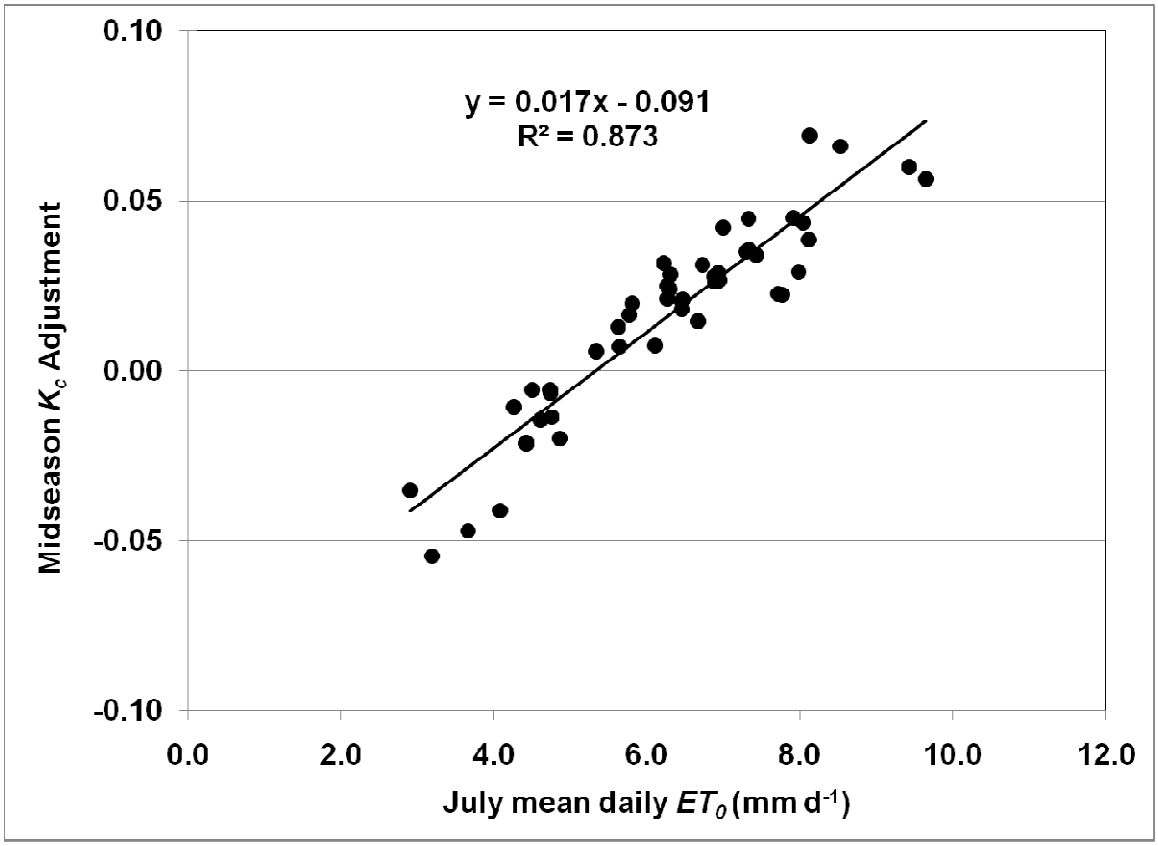

Figure 28 Midseason Kc adjustment, based on the FAO 56 correction method, versus July mean daily ETo for a canopy height hc = 0.12 m

Assuming a K_{ctab}=1.00 for h_c=0.12 m, the results in Fig. 28 show that the K_{cmid} will increase as the ET_o rate increases. For example, K_{cmid}=1.08 for ET_0=10.0 mm d^{-1}. However, the reference surface should have a K_c=1.00 regardless of the climate, so a climate correction equal to zero is appropriate for h_c =0.12 m. Thus, a different midseason K_c climate correction is clearly needed. In this study, we develop a new K_c climate correction based on the daily ET_o rate rather than wind speed, humidity and canopy height. The correction applies to crops with midseason during the summer months.

It is possible to estimate crop evapotranspiration using Eq. (21) (see previous paragraphs) directly by varying the net radiation, canopy resistance, and aerodynamic resistance to match characteristics of the crop of interest. This was the procedure used to develop the standardized reference evapotranspiration equation for tall canopies (Allen et al., 2005).

Assuming little or no physiological stress, the main climate factor affecting the variations in midseason K_c=ET_c/ET_o is the aerodynamic resistance, where ET_c is the well-watered crop evapotranspiration. Assume that the aerodynamic resistance for a crop canopy is approximated by an inverse function of the wind speed, as Eq. (36) shows:

$$r_a = \frac{c_n}{u_2} \quad (36),$$

where, u_2 is the wind speed measured over a broad expanse of well-watered grass, c_n can be varied to estimate ET_c and $K_c=ET_c/ET_o$ to identify a particular value for K_c as a function of c_n (208). It is assumed that the c_n values will not vary with climate, but climate differences in temperature, humidity, and wind speed will affect the ET_c calculation. Temperature affects the values for Δ and e_s, humidity affects the value for e, and wind speed affects the r_a in the numerator and in the denominator (Eq. 38). Although there may be some exceptions, it is unlikely that the relative difference in canopy resistance between most well-watered crop canopies and the standardized reference canopy will vary greatly with climate. Crop coefficients already account for the difference in net radiation between a crop and the reference surface, and climate differences should have little impact on the net radiation contribution to the crop coefficient unless there is a big change in the crop net radiation due to light interception. Therefore, net radiation changes due to climate are unlikely within mid-latitudes. Based on these concepts, the main factor influencing climate change impact on crop coefficients is the sensible heat flux, which is affected by the canopy height and roughness, the wind speed, and the temperature profile.

The numerator of the right-hand component of Eq. 21, (Paragraph 2.1) is equal to equation (37):

$$\rho_a c_p \left(e_s - e\right) r_a^{-1} \quad (37),$$

and it has the unit $Jm^{-2}d^{-1}$. The air density is expressed by equation (38):

$$\rho_a = \frac{1000P}{T^* R} \quad (38),$$

and the specific heat at constant pressure is equal to Eq. (39):

$$c_p = \frac{\gamma \varepsilon \lambda}{P} \quad (39),$$

where P (kPa) is the barometric pressure, ε = 0.622 is the ratio of molecular mass of water vapor to dry air, $T^* \approx 1.01(T_a+273)$ is the absolute virtual temperature (K), and R = 287 J kg1K^{-1}

is the universal gas constant. The expression is multiplied by 86,400 sd^{-1} and divided by λ to convert to $kgm^{-2}d^{-1}$ in Eq. (40)

$$\left(\frac{86{,}400}{\lambda}\right)\frac{\rho_a c_p (e_s - e)}{r_a} = \left(\frac{86{,}400}{\lambda}\right)\left(\frac{1000P}{1.01(T_a + 273)R}\right)\left(\frac{\gamma\varepsilon\lambda}{P}\right)\left(\frac{e_s - e}{r_a}\right) = \gamma\left(\frac{86400000 \times 0.622}{[1.01(T_a + 273)]287}\right)\left(\frac{e_s - e}{r_a}\right) \quad (40),$$

which simplifies to Eq.(41)

$$\left(\frac{185396}{T_a + 273}\right)\left(\frac{e_s - e}{r_a}\right) \quad (41),$$

The aerodynamic resistance is specified in Eq. (42):

$$r_a = \frac{208}{u_2} \quad (42),$$

So, by inverting and multiplying, the right-hand component becomes as Eq. (43) shows:

$$\gamma\left(\frac{891}{T_a + 273}\right)u_2(e_s - e) \quad (43),$$

For simplicity, the value 900 was substituted to 891 in Eq. (43). The denominator of Eq. (44), comes from the substitution:

$$\gamma\left(1 + \frac{r_c}{r_a}\right) = \gamma\left(1 + \frac{70}{208/u_2}\right) \approx \gamma(1 + 0.34u_2) \quad (44),$$

Thus, Eq. (21) (Paragraph 2.1.) provides an estimate of the ET from a vegetated surface having r_c=70sm^{-1} and an r_a equal to Eq. (44), (see Paragraph 2.1.3. K_c Model description). The 900 in the numerator of Eq. (31) (see Paragraph 2.6. PM Equation) is approximately equal to 187200/208. Thus, the ET_c for a crop having the same physical characteristics of ET_o (i.e., c_n=208 and K_c=1.00) is expressed as Eq. (45) points out:

$$ET_c = \frac{0.408\Delta(R_n - G) + \gamma\left(\frac{187200}{T_a + 273}\right)\left(\frac{u_2}{c_n}\right)(e_s - e)}{\Delta + \gamma\left(1 + \frac{70}{c_n}u_2\right)} \quad (45),$$

Then, we can vary the value for c_n to calculate ET_c for different canopies and to calculate K_c by dividing the results from Eq. (39) by the results from Eq. (46). Using the K_c value determined from field research in a "base" climate, one can use trial and error substitution to determine the c_n that gives an ET_c and K_c that corresponds to the observed K_c for the "base" climate. It is assumed that R_n, r_c, and c_n are unchanged for the same crop canopy when estimating K_{cmid} values in another climate. The sensible heat flux density, however, does change because of the effect of temperature and/or wind speed on aerodynamic resistance. In a hotter or windier climate the K_{cmid} will increase and it will decrease in a cooler, calmer climate.

The c_n values required to obtain particular K_c values were determined for July using climate data from Davis, California, as the "base" climate. This location was used because many of the K_c values presented in FAO-24 and later in FAO-56 were developed in Davis, and because the Penman-Monteith equation (Monteith, 1966) was tested using the Davis lysimeters (Pruitt and Angus, 1960). Moreover, the daily standardized ET_o equation was partially validated with the Davis lysimeter data.

The July mean daily reference evapotranspiration rate is ET_o=7.3 mm d^{-1} in Davis (CIMIS, 2011). The c_n values were varied to identify the K_c values corresponding to 0.80 to 1.30 in increments of 0.05 (Table 5).

Table 5 Values for c_n and corresponding $K_{ctab}=ET_c/ET_0$ values for Davis, CA, having July mean daily ET_0=7.3 mm d^{-1}. The b values are slopes of the regression of K_c versus ET_0 based on July climate data from 49 CIMIS stations using the same values for c_n to calculate ET_c.

c_n	K_{ctab}	b
517	0.80	-0.0530
385	0.85	-0.0396
303	0.90	-0.0263
248	0.95	-0.0131
208	1.00	0.0000
177	1.05	0.0134
154	1.10	0.0260
135	1.15	0.0389
119	1.20	0.0521
106	1.25	0.0648
95	1.30	0.0775

To investigate how climate might affect the K_c values, the same c_n values were used to calculate ET_c and K_c using July mean climate data from 49 CIMIS stations (Table 6) that represent a wide range of climate zones in California.

Table 6 CIMIS station locations and mean daily solar radiation (R_s), maximum (T_x), minimum (T_n), dew point (T_d) temperature, wind speed (u_2), and reference ET (ET_a) data from July 2003.

Station	Lat.	Lon.	Elev.	R_s	T_x	T_n	u_2	T_d	ET_o
	deg.	deg.	m	MJ $m^{-2}d^{-1}$	^oC	^oC	m s^{-1}	^oC	mm d^{-1}
Arvin Edison	35.2	-118.8	152	26.8	36.3	21.1	1.1	11.4	6.3
Barstow	34.9	-117.0	622	25.2	39.7	24.0	3.1	9.7	9.4
Belridge	35.5	-119.7	125	26.8	37.2	19.5	1.6	12.3	6.9
Bishop	37.4	-118.4	1271	26.2	34.7	12.9	1.4	7.1	6.2
Brentwood	37.9	-121.7	14	28.6	34.5	15.1	1.6	13.3	6.5
Browns Valley	39.3	-121.3	287	27.2	35.3	20.0	1.7	12.4	6.9
Buntingville	40.3	-120.4	1221	28.4	32.4	11.5	2.3	6.4	7.0
Calipatria	33.0	-115.4	-34	26.4	41.0	24.4	2.3	21.5	7.8
Camarillo	34.2	-119.0	40	23.3	26.2	16.6	1.8	16.9	4.4
Castroville	36.8	-121.8	3	21.5	17.2	12.3	2.8	13.0	2.9
Concord	38.0	-122.0	-11	27.4	31.2	14.1	2.1	11.6	6.3
Cuyama	34.9	-119.6	698	25.7	34.5	14.9	2.4	8.4	7.3
Davis	38.5	-121.8	18	28.5	34.7	15.5	2.4	12.2	7.3
Deleno	35.8	-119.3	91	25.7	37.1	20.1	1.4	13.9	6.5
Denair	37.6	-120.8	46	27.5	34.0	16.4	2.3	13.4	6.9
Escondido2	33.1	-117.0	119	24.2	30.5	14.9	2.0	15.7	5.3
Fair Oaks	38.7	-121.2	81	28.2	35.4	17.9	1.8	12.5	6.9
Fresno State	36.8	-119.7	103	27.1	36.2	19.7	2.2	12.6	7.4
Glendale	34.2	-118.2	339	22.1	28.8	17.1	1.5	17.1	4.6
Goleta	34.4	-119.8	9	24.5	26.1	16.2	1.6	15.0	4.8
Hastings Tract	38.3	-121.8	3	28.4	31.6	15.8	5.2	12.9	8.1
Indio	33.8	-116.3	12	24.1	40.5	28.5	3.2	13.2	9.6
Irvine	33.7	-117.7	125	25.3	27.7	17.1	1.7	17.7	4.9
Lindcove	36.4	-119.1	146	27.9	37.5	19.5	1.4	16.5	6.7
Lodi West	38.1	-121.4	8	27.6	32.4	14.6	1.1	13.2	5.6
Madera	37.0	-120.2	70	27.3	34.9	17.1	2.4	12.1	7.3
McArthur	41.1	-121.5	1009	28.4	31.3	10.9	1.9	9.5	6.3
Meloland	32.8	-115.5	-15	24.8	41.4	25.9	2.6	21.1	8.0
Morgan Hill	37.2	-121.6	117	28.1	32.7	12.5	2.2	11.0	6.7
Oakville	38.4	-121.4	58	26.8	30.7	11.6	1.8	13.1	5.6
Oasis	33.5	-116.2	4	24.2	40.2	27.2	2.3	14.8	8.1
Orland	39.7	-122.2	60	27.3	33.7	17.5	1.6	16.5	6.1
Otay Lake	32.6	-116.9	177	23.3	26.2	16.6	1.8	16.9	4.4
Oxnard	34.2	-119.2	15	22.3	22.5	16.1	1.6	17.2	3.7
Parlier	36.6	-119.5	103	25.5	36.1	19.1	1.7	15.6	6.5
Patterson	37.4	-121.1	56	25.9	22.1	11.4	2.1	12.1	4.3
Pt San Pedro	38.0	-122.5	2	28.7	22.9	11.6	2.3	12.3	4.7
Santa Monica	34.0	-118.5	104	23.4	24.2	18.0	1.9	18.5	4.1
Seeley	32.8	-115.7	40	26.3	41.6	24.3	1.9	20.2	7.7
Sisquoc	34.8	-120.2	163	24.8	25.6	11.3	1.8	13.4	4.5
Siuson Valley	38.2	-122.1	11	28.1	29.8	14.8	2.8	13.8	6.3
SLO_West	35.3	-120.7	87	25.9	22.1	11.4	2.1	12.1	4.3
Stratford	36.2	-119.9	59	26.8	36.7	19.1	2.7	12.3	8.0
Temecula	33.5	-117.2	433	24.3	31.8	15.4	1.9	13.5	5.8
Torrey Pines	32.9	-117.3	102	19.6	19.4	16.2	1.7	15.4	3.2
Tracy	37.7	-121.5	25	28.9	33.8	16.5	2.9	10.5	7.9
Tulelake	42.0	-121.4	1232	27.4	29.6	10.1	1.9	10.9	5.8
Twitchell	38.1	-121.7	0	27.7	32.0	17.2	4.5	10.4	8.5
Union City	37.6	-122.1	5	26.2	24.8	13.1	1.8	12.9	4.7

For each c_n value, the regression of K_c versus ET_o was determined for the 49 stations to determine the slope (b). A sample plot, for c_n=119 and K_c=1.20 is shown as the dots in figure 2. The solid regression line of the dots in figure 2 crosses the K_c=1.20 line at ET_0=7.3 mm d^{-1}, which is the mean daily July ET_0 rate for Davis, California. The plotted points are not shown, but the dotted and dashed lines shown in figure 2 are the regression lines for K_c=0.90, 1.00, and 1.10 that were calculated from ET_0 and ET_c using equation 4 and c_n=303, 208, and 154, respectively. Note that all of the regression lines cross the base climate K_c values when ET_0=7.3 mm d^{-1}, which is identified by the vertical dashed line in Figure 29.

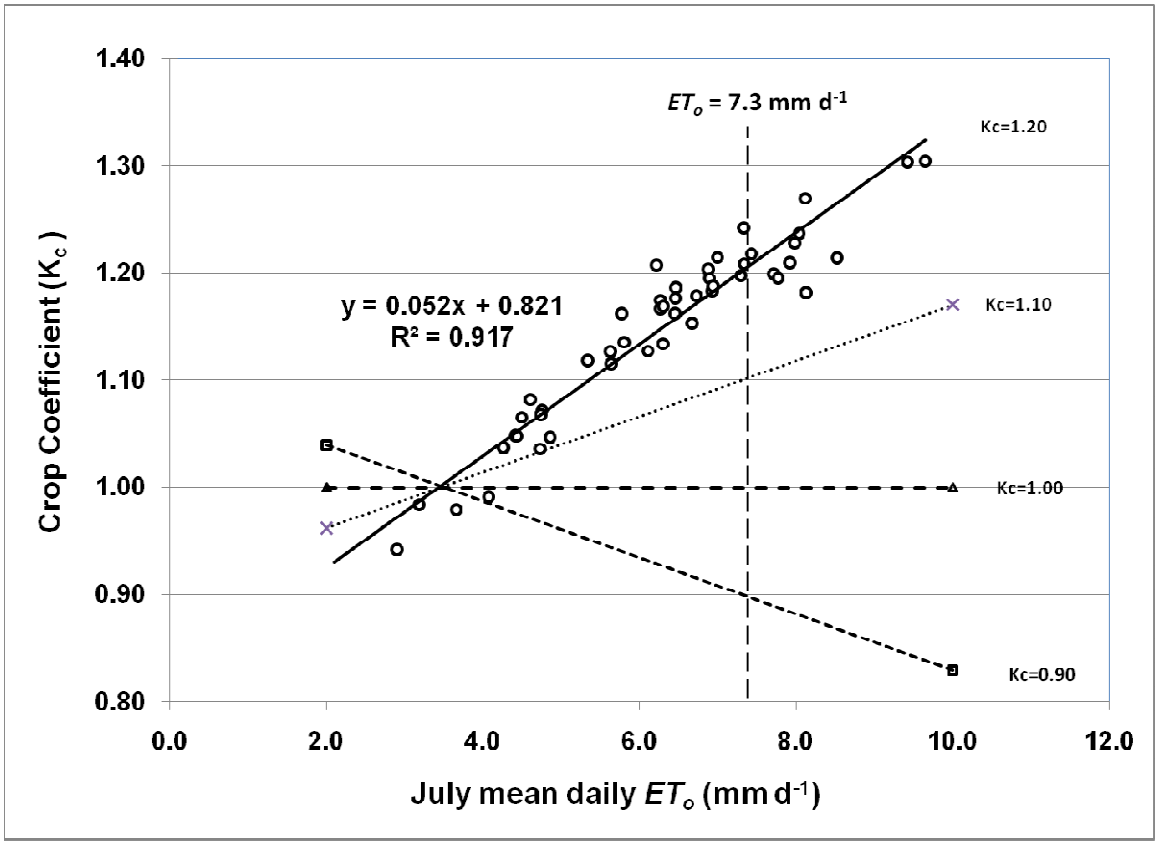

Figure 29 Crop coefficients versus July mean daily ET_0 for the 49 CIMIS stations.

To determine the K_{cmid} value for a given ET_0 rate, find the difference between the given ET_0 rate and 7.3 mm d^{-1}, multiply by the interpolated slope values from table 5, and add the product to the base climate K_{ctab} value (Tab. 5) as in Eq. (47):

$$K_{cmid} = K_{ctab} + b\left(ET_0 - 7.3\right) \qquad (47),$$

For each corresponding value of K_{ctab} and c_n in Table 5, ET_o and K_c were calculated using data from the 49 CIMIS stations. The regression of K_c versus ET_o was computed for each K_{ctab}, and the slopes (b) were plotted versus the K_{ctab} values (Fig. 30).

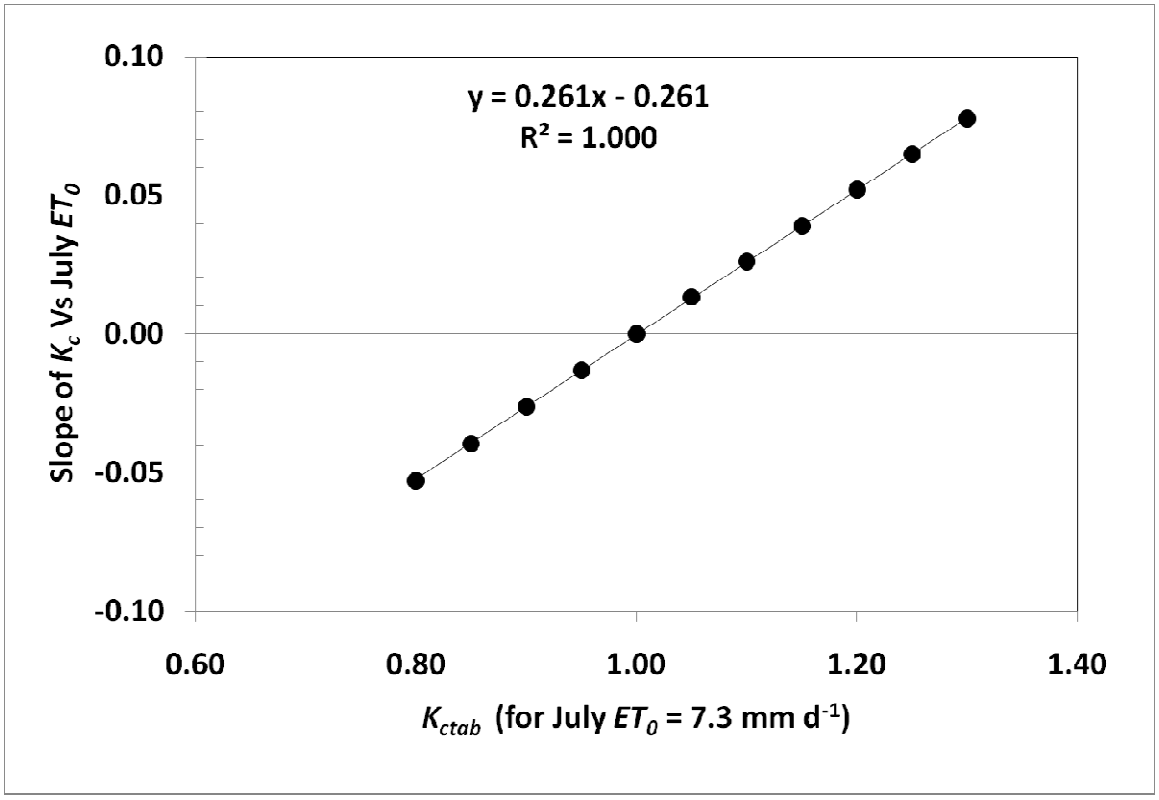

Figure 30. Plot of the Kc versus ET_0 rate regression line slopes versus the K_{ctab} values corresponding to ET_0=7.3 mm d^{-1}

The regression line for the plot of b values versus K_{ctab} has a slope of 0.261 with R^2=1.00. Therefore, the climate adjusted K_c value (K_{cmid}) can be estimated as the sum of K_{ctab} and the difference (d) in ET_0 rate from the "base" climate (d=ET_o-7.3) multiplied by the regression line slope b=0.261 (K_{ctab} -1), as in Eq. (48):

$$K_{cmid} = K_{ctab} + (ET_0 - 7.3)\left[0.261\left(K_{ctab} - 1\right)\right] = K_{ctab} + 0.261\left(ET_0 - 7.3\right)\left(K_{ctab} - 1\right) \quad (48),$$

In the case where ET_0=7.3 mm d^{-1}, K_{cmid}=K_{ctab}. If K_{ctab}=1.00, then K_{cmid}=1.00 regardless of the ET_0 rate, so the K_c for the reference surface does not change with climate. The following paragraph provides a sample calculation.

For ET_0 =10.0 mm d^{-1} and K_{ctab}=1.20, Fig. 30 indicates a value b=0.050. The value for d=10.0*7.3=2.7 mm d^{-1}. Therefore, K_{cmid}=1.20+ 2.7*0.050=1.34.

Alternatively, using Eq. (49) adjusting Observed Midseason K_c to K_{ctab}

K_{cmid} =1.20+0.261(10.0-7.3)(1.20-1)=1.34 (49),

For this correction to be useful, the tabular K_c values should be appropriate for use in a "base" climate where the midseason ET_o = 7.3 m d^{-1}. Therefore, K_c values developed in other climates should be adjusted to the midseason K_{ctab} corresponding to ET_0=7.3 mm d^{-1} before inclusion in the K_c table. Rearranging Eq. (49), we obtain Eq. (50) to determine the K_{ctab} corresponding to ET_0 =7.3 mm d^{-1} as a function of the observed midseason K_c (K_{cobs}) and the midseason peak ET_o from a "non-base" climate:

$$K_{ctab} = \frac{K_{cobs} + 0.261(ET_0 - 7.3)}{1 + 0.261(ET_0 - 7.3)} \quad (50),$$

For example, if a K_{cobs} = 1.34 Eq. (51) is observed in a climate with ET_0=10.0 mm d^{-1}, then:

$$K_{ctab} = \frac{1.34 + 0.261(10.0 - 7.3)}{1 + 0.261(10.0 - 7.3)} = \frac{2.045}{1.705} = 1.20 \quad (51),$$

and, therefore, Eq. (51) provides a method to determine the tabular K_c values from research in "non-base" climate. Eq. (50) is used to compute K_{cmid} values from K_{ctab} regardless of the climate.

The KcMod.xls application program was written using Microsoft Excel software. The application has three main climate-weather data input worksheets. The "Climate" worksheet allows for the input of montlhly mean weather data for calculating monthly mean standardized reference evapotranspiration. Then a cubic spline procedure is used to estimate daily values for ET_0. A soil evaporation model based on the ET_0 rate and rainfall frequency is used to estimate a baseline crop coefficient. The "Weather" worksheet is used to input daily ET_o data for use in the irrigation scheduling program to determine the dual Kc curve. Thje worksheet "DailyMet" allows for input of daily weather data that are then used to compute the monthly means used in the "Climate" worksheet.

KcMod has a "YTD" worksheet that is used to compute the yield threshold depletion (YTD) to help with irrigation scheduling. The YTD is determined by inputting the root depth on different dates, the water holding characteristics, allowable depletion, and adjustments for the irrigation system. After determining the YTD, a rough irrigation schedule is determined by calculating the soil water depletion on each date and irrigating when the depletion level reaches the YTD or some management allowable depletion (MAD) that is typical for the crop and region. The

worksheet displays a figure showing the cumulative ET_c and the cumulative irrigation depths. The last irrigation is applied when an irrigation results in a cumulative irrigation application approximately equal field capcity (FC) minus the YTD. This forces the derived irrigation schedule to be similar to what a farmer might use in the region of interest and it defines the irrigation dates.

Finally, the "Input" worksheet is used to determine the dual and single K_c curve for a particular crop. First, a crop number is found in the "Kc Info" worksheet, and the crop number is input into the "CropList" worksheet for use developing the K_c curves. The number corresponding to a particular crop is entered into the "Input" worksheet. If needed the beginning date and ending date can be modified from those read from the CropList worksheet. The beginning date corresponds to planting for field (type 1 and 2) crops, to leafout for deciduous orchard and vine crops (type 3), or 1 January to 31 December for subtropical and other orchard crops that do not lose their leaves (type 4). The dual K_c curve is computed using the tablular (basal) K_c curve read from the CropList tabular values, the methodology from FAO 24 an FAO 56, and the bare soil K_c method described by Ventura et al. (2006) to estimate a basal Kc curve with spikes resulting from the rainfall and irrigation dates. For field crops, the single K_c curve is determined by fitting linear approximations to the dual K_c curve for each of the four growth periods (i.e., early, rapid, midseason, and late season). The procedure is to determine a horizontal K_c representing the mean of the dual K_c curve during initial growth and again during midseason growth. Then a linear fit from the end of the initial to the beginning of the midseason growth is computed. Finally, a linear fit from the end of the midseason period K_c that passes through the mean of the late season period to the ending date is computed. Then, plots and tables of the results are generated. These plots and tables can be given to growers to provide them with the single method K_c curves that are specific to typical management and climate in the region of interest.

For deciduous orchard and vine crops, the procedure is similar to the field crop method. First, the dual K_c curve is determined using the basal K_c curve adjusted for spikes due to rainfall and irrigation events. Then, a midseason K_c curve is computed as a horizontal line through the mean of the dual K_c values during midseason. The K_c values from leafout to the beginning of midseason are computed so that the Kc line passes through the mean rapid growth K_c value at the midpoint of the rapid growth period and connects with the Kcmid at the beginning of the midseason period. The same approach is used to determine the late season K_c line. The line goes from the end point K_c of the midseason period through the mean K_c of the late season dual K_c values and ends on the ending date.

For subtropical and other orchards that do not lose their leaves, the dual K_c method works the same as for the other methods. The basal K_c curve is combined with the spikes due to rainfall and irrigation events to identify the dual K_c curve. The linear approximation method to determine the single Kc curve does not work with subtropical crops, so the mean K_c of each month was used with a cubic spline method fit to determine the daily K_c curve. When linear fitting was used, the K_c lines often gave unrealistic values during the transition from winter rainy period to dry summers, and the cubic spline method eliminated that problem.

2.3. CROP COEFFICIENTS MODEL VALIDATION

KcMod was tested using measured Kc values for different type of crops: a) maize, b) broccoli, c) lettuce, d) tomato, e) olive and f) kiwifruit.

A) MAIZE

The first data set for K_c values was for maize and they were measured near Milan (Italy). The experiment was conducted by the Università degli Studi di Milano and Politecnico di Milano (Facchi et al., unpublished). The purpose of the research was to measure the K_c pattern for maize grown in the Lombardia region. Kc was derived from two experimental maize fields (Landriano and Livraga) for years 2006, 2010 and 2011 (Table 7) as the ratio between actual ET_c (ET_a) in well watered conditions and ET_0. Crop data, management and meteorological condition data were used to run KcMod.

ETc was measured using the eddy-covariance technique, while ET_0 was determined from agro-meteorological data registered by two standard meteorological stations close to the experimental areas (Landriano and Bertonico). Weather date were used as input for the Penman-Monteith equation. ET_0 was used as input in KcMod to simulate 'single' and 'dual' ET_c values, as well as the daily and the monthly weather data, the irrigation time, amount, type and frequency data.

Table 7. Dates of seeding, harvesting and irrigation practices for maize (Landriano and Livraga, 2006-2011) (Facchi et al., unpublished).

Practice	Landriano 2006	Landriano 2010	Livraga 2010	Landriano 2011
Seeding date	30/05 (second crop)	29/04	26/04	09/04
Harvesting date	10/10	11/09	10/09	01/09
Irrigation	08/06 sprinkler, 14/07 surface	18/07 surface	14/06, 14/07, 31/07 surface	not irrigated

B) BROCCOLI

Broccoli were grown in Ventura, California (1995-1996). Crop management details are summarized in Table 8. Purpose of the research was to measure the Kc pattern for broccoli, to derive a model that allow to predict the different contribute of evaporation from bare soil and transpiration from crop to crop evapotranspiration (Ventura et al, 2001). ET_c was measured using the eddy-covariance technique, while ET_0 was determined from agro-meteorological data registered by Port Heuneme (n.97) CIMIS meteorological station, close to the experimental area.

ET_0 was used as input in KcMod to simulate 'single' and 'dual' ET_c values, as well as the rainfall and irrigation time, amount, type and frequency data.

Table 8 Date of transplanting, harvesting, irrigation practices and soil characteristics for broccoli (Ventura, 1995-96).

Practice	Date
Soil type	Pico sandy loam
Transplanting	12/19/95
Harvesting	4/15/96
Irrigation	01/16/96 furrow 01/16/96 furrow

C) LETTUCE

Lettuce was grown in Imperial Valley, California (1996-1997). Crop management details are summerized in Table 9. Purpose of the research was to measure the Kc pattern for lettuce, to derive a model that allow to predict the different contribute of evaporation from bare soil and transpiration from crop to crop evapotranspiration (Ventura et al, 2001). ET_c was measured using the eddy-covariance technique, while ET_0 was determined from agro-meteorological data registered by Meloland (n.87) and Calipatria (n.41) CIMIS meteorological stations, close to the experimental areas. ET_0 was used as input in KcMod to simulate 'single' and 'dual' ET_c values, as well as the rainfall and irrigation time, amount, type and frequency data.

Table 9 Date of transplanting, harvesting, irrigation practices and soil characteristics for lettuce (Imperial Valley, 1996-1997).

Practice	Date
Soil type	Very fine sandy loam
Planting	9/17/96
Germination	10/16/96
Thinning	11/12/96
Harvesting	2/5/97
Irrigation	10/16/96 sprinkler
	10/17/96 sprinkler
	10/18/96 sprinkler
	10/19/96 sprinkler
	10/20/96 sprinkler
	10/21/96 sprinkler
	10/22/96 sprinkler
	10/23/96 sprinkler
	10/28/96 sprinkler
	11/1/1996 furrow
	12/4/1996 furrow
	12/12/1996 furrow
	11/1/1996 furrow
	1/8/1997 furrow
	1/23/1997 furrow

D) KIWIFRUIT

Kiwifruit is a native species of medium-low solar radiation and humid environments. In Mediterranean environments, like Italy, this crop needs, high amount of irrigation to compensate the high flow of evapotranspiration. The goal the research was to improve crop evapotranspiration estimates by identifying specific local crop coefficients. Crop water requirements estimation improvement may allow substantial reductions in water consumption.

The study was conducted by CER (Consorzio per il Canale Emiliano Romagnolo-Emiliano Romagnolo Channel Consortium- Anconelli et al, 2009) in a kiwi orchard in Brisighella, (Ravenna, Italy, 44°12.23 lat N, 11°45.26 lon E, 15 1 m of elevation.) The meteo station was 1 km far from the orchard. Water needs were satisfied with a drop irrigation system. The Eddy Covariance technique was used to measure evapotranspiration fluxes and energy balance. Table 10 summarizes the major date for kiwi growing season.

Table 10 Kiwifruit phenological stages.

Date 2008	**Phenological stage**	**Date 2009**	**Phenological stage**
16 Mar	Gems breaking	25 Mar	Gems breaking
21 May	blooming	10 May	blooming
29 May	fruit	29 May	fruit
≈20 Jul	pruning	18 Jul	pruning
22 Oct	harvesting	20 Oct	harvesting

Irrigations were frequent, in particular in 2008, they were almost daily starting from 21st June until 12th September. In 2009, irrigations started before than in 2008, and in particular they started the 3rd June, until 12th September. The reason was that rainfall were more abundant during spring 2008, so water storage were higher, while in 2009 the amount of rainfall were lower and air temperature was higher then during kiwifruit growing season 2008.

Crop coefficient simulations start from considering specific table Kc values, according to FAO 56 paper (Allen et al. 1998). For crops used for the model validation, the table Kc used are those in Table 11.

Table 11 Table Kc values from FAO 56 and adjusted for the climate with KcMod for the crops used during the model validation tests.

Growing Season K_c	K_c Ini		K_c mid		K_c end	
Crops	Table	Adjusted	Table	Adjusted	Table	Adjusted
Maize	0.20	0.20	1.00	0.20	1.00	0.20
Broccoli	0.30	0.30	1.00	1.00	0.80	0.80
Lettuce	0.80	0.80	0.80	0.87	0.80	0.87
Kiwifruit	0.30	0.30	1.05	0.99	1.00	1.00

These values were corrected from the program to be adjusted for the specific climate and for the age of crops, in case of tree crops.

CHAPTER 3. RESULTS AND DISCUSSION

3.1. K_c REPORT & DATA BASE

The products of this research step include:

A Word file reporting more than 100 articles about 69 crops reviewed and 6 other types of different transpiring surfaces, that are not included in any crop categories. They include for example wetland, and lake evaporation. Each review starts with an introduction (generally the aim of the study description), the methods used for the measurements (including the location, time and type of treatment of the experiment), the calculations, and the results obtained for each paper revised. Every article has a number of identification (from 1 to 110), as well as every crop (from 1 to 69), as Figure 37 shows.

An Excel file reporting all the K_c values of the papers corresponding to each crop for each referenced article, specifying the number of identification of the paper and the name and the number of identification of the crop, the name of the author, the Country, the year of publication and a note, which is a comment to the results of the study.

The following flow chart shows how the Word report on crop coefficients values – a review of literature - is structured. In this example, the article crop is maize, which is crop n. 22. The articles reviewed which provided K_c values for Maize were paper numbers 20, 29, 7, 8, 40, 45, 55, 57, 50, 59 and 819 (Fig. 38). Article n. 8 is the example reported in Figure 39. The review of the article is separated into the aim of the study, methodology and results.

A) REPORT ON Kc LITERATURE REVIEW

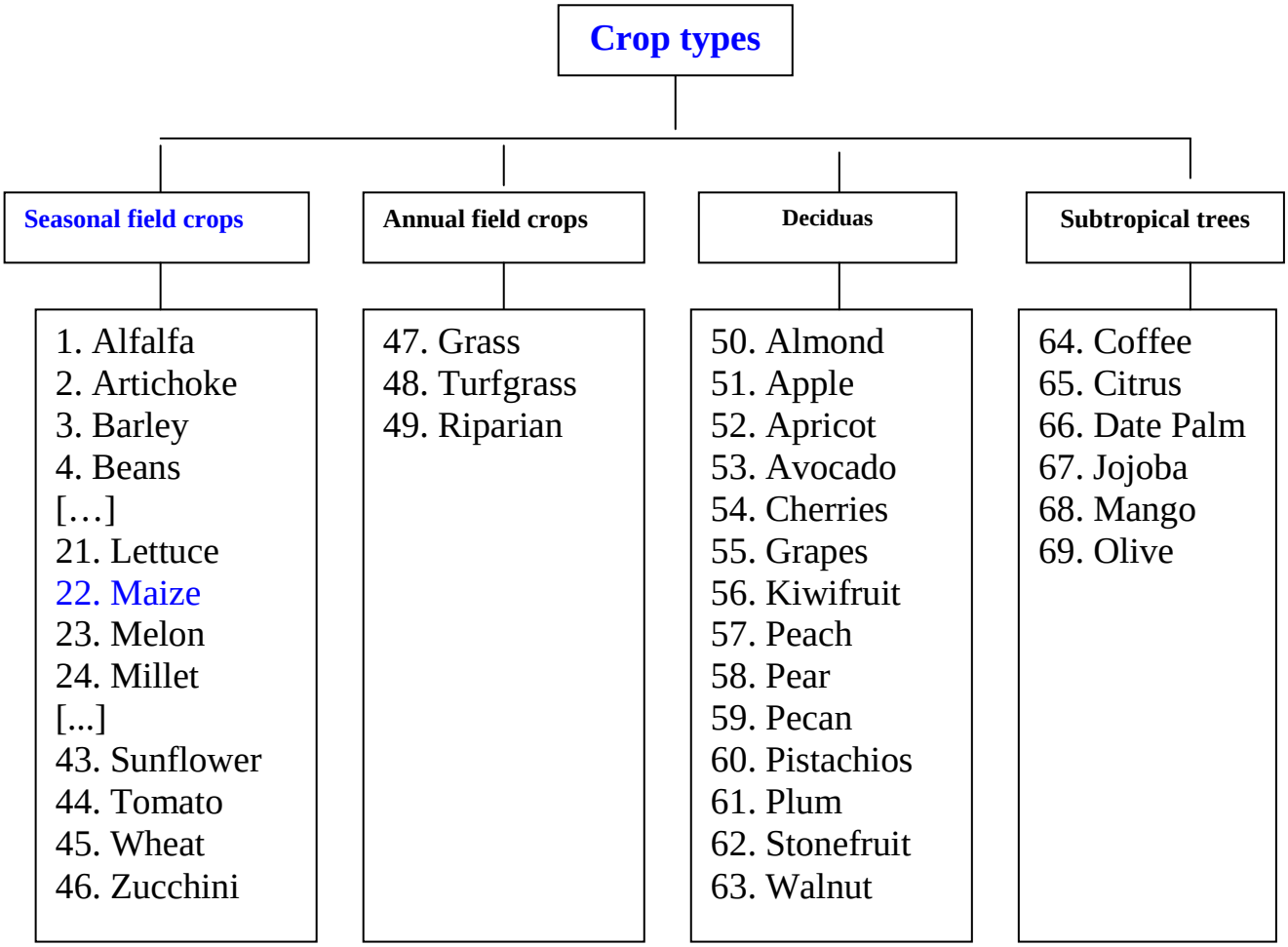

Figure 31. Flow chart of the different crops that were object of all the literature review on crop coefficients values. All the crops object of the articles reviewed were divided in 4 groups: Seasonal field crop, annual field crops, Deciduas and subtropical trees.

22. **Maize**

Articles:

20. TRANSFORMATION OF YIELD RESPONSE FACTOR INTO JENSEN'S SENSITIVITY INDEX

29. WATER UPTAKE AND USE BY MORPHOLOGICALLY CONTRASTING MAIZA/PEA CULTIVARS IN SOLE AND INTERCROPS IN TEMPERATE CODITIONS

7. WATER USE BY CROPS AFFECTED BY CLIMATE AND PLANT FACTORS

8. DETERMINATION OF EVAPOTRANSPIRATION FOR MAIZE AND BERSEEM CLOVER

40. ESTIMATION IRRIGATION WATER REQUIREMNTS WITH DERIVED CROP COEFFICIENTS FOR UPLAND AND PADDY CROPS IN CHIANAN IRRIGATION ASSOCIATION, TAIWAN

45. EVAPOTRANSPIRATION OF IRRIGATED AND RAINFED MAIZE-SOYBEAN CROPPING SYSTEMS

55. PEAK CROP COEFFICIENT VALUES FOR SHAANXI, NORTH-WEST CHINA

57. CROP COEFFICIENT AND RATIO OF TRANSPIRATION TO EVAPOTRANSPIRATION OF WINTER WHEAT AND MAIZE IN A SEMI-HUMID REGION

50. CHANGES IN SEASONAL EVAPOTRANSPIRATION, SOIL WATER CONTENT, AND CROP COEFFICIENTS IN SUGARCANE, CASSAVA, AND MAIZE FIELDS IN NORTHEAST THAILAND

59. MEAN CROP CONSUPTIVE USE AND FREE WATER EVAPORATION FOR TEXAS

81. CROP COEFFICIENTS

Figure 32. Sample list of the articles reviewed for maize, which is crop n. 22.

8. DETERMINATION OF EVAPOTRANSPIRATION FOR MAIZE AND BERSEEM CLOVER

1. INTRODUCTION

The first objective of this study was to measure daily, weekly and seasonal ETc of maize and berseem directly from weighing type lysimeters.
The second objective was to develop crop coefficients for maize and berseem from ETc measurements and weather data.

1. MATERIALS AND METHODS

Period of the Experiment
Started in: June, 1996
Ended in: April, 1998
Seeding date: maize (hybrid Ganga-5), 2 and 24 June (1996, 1997); berseem (Mescavi), 18 and 16 October (1996, 1997)
Cutting dates: maize, 4 and 26 September (1996, 1997); berseem, 1st cut: after 9 weeks, 2nd: 14 weeks, 3rd: 19 weeks, 4th: 23 weeks, 5th: 26 weeks.
Duration: 24 months.

Place of the Experiment
Location of the farm: Central Soil Salinity research Institute, Karnal, India (latitude, 29˚43' N; longitude, 76˚58'E);
Elevation: 245 m MSL;
Regional climate: semi-arid with highest monthly temperature of 39.7˚C recorded in May and the lowest one of 5.7˚C, recorded in January. Sunshine hours range is between 9 and 10.7 h/day from April till October and between 6.8 and 8.9 h/day in the rest of the months. Annual rainfall average is 787 mm (the 71% is received from July to September).

Lysimeters
Each lysimeters comprised 2 rectangular tanks: the inner tank was 1.985x1.985x1.985 m and the outer one was 2.015x2.015x2.015 m. They were located in the centre of a 1.5 ha field.
Their accuracy and resolution range was from 0.05 to 1 mm; measurements and micro-meteorological data were made by a Campbell Scientific 21X datalogger (programmed to determine lysimeters mass every hour) and AM32 multiplexer. Load cell measurements were made for 3 min at 0.5 Hz.
Evapotranspiration during a 60 min period was computed as the difference between two adjacent mass averages.

Figure 33 (a) Review for article n. 8, which reports Kc values for maize (crop n.22). The review of the article is divided in aim of the study, methodology and results.

Weather Station
Location was within 10 m of the lysimeters and included:

- 2 anemometers
- 2 humidity sensors
- 1 pyrometer
- 1 net radiometer
- 1 tipping bucket rain gauge
- 1 wind direction sensor
- 2 soil heat flux plates.

Hourly and 24 h values of ETc and weather data were stored in the datalogger for a week. A program named TAPCARD was used to analyze the data and prepare hourly and daily summaries of ETc and weather data. ETo was estimated by the method described by Allen (1991).

Treatments
Irrigations were scheduled to maintain the soil water profile adequately supplied and soil water contents were measured at 8-days intervals, using a neutron probe at 0.15 m depth increments over a 1.5 m deep soil profile. Deep percolation water collected at the bottom of the lysimeters was pumped periodically. The recommended doses of fertilizers were given to all crops.

Calculations
Percolation and rainfall/irrigation were accounted for ETc computations. The leaf area index was measured by a LAI-2000 plant canopy analyzer: measurements were in a minimum of 10 number and five values of the canopy transmittance were calculated by dividing all the 10 values from corresponding pairs.
ETo was computed by six-climate-based ETo estimation method:

- Penman-Monteith (Smith et al. 1992; Allen et al, 1990)
- FAO-ID-corrected Penman (Doorenbos and Priutt, 1977)
- Original Penman (Penman,1963)
- FAO_ID-radiation (Doorenbos and Priutt, 1977)
- FAO+ID-Blaney and Criddle (Doorenbos and Priutt, 1977)
- US class A pan evaporation (Hargraves and Samani, 1985).

Penaman-Monteith gave the most consistent ETo estimates (Smith et al., 1992).

3 RESULTS AND DISCUSSION

The estimated Kc values for Maize by Penman-Monteith method at the four crop growth stages were respectively: initial=0.55, crop development=1.00, mid-season=1.23 and maturity=0.64. The corresponding values for berseem were 0.76, 0.82, 1.11 and 1.24.
For these two crops actual Kc values were different from those suggested by FAO (Allen at al. 1998).

Figure 33 (b) Review for article n. 8, which reports Kc values for maize (crop n.22). The review of the article is divided in aim of the study, methodology and results.

B) K_C VALUES DATA BASE

The K_c values data base reports all of the K_c values of the 110 papers corresponding to each of the 69 crops, specifying the number of identification of the paper and the name and the number of identification of the crop, the name of the author, the Country, the year of publication and a note, which is a comment to the results of the study. Table 12 and Figure 34 show the K_c values for the initial, midseason and end period for maize crop and the box plot compare the values reviewed with FAO-56 Kc values from a statistical point of view.

Figure 33 (c) Review for article n. 8, which reports Kc values for maize (crop n.22). The review of the article is divided in aim of the study, methodology and results.

Tab le 12. Initial ($K_{c\ ini}$), midseason ($K_{c\ mid}$) and end season ($K_{c\ end}$) Kc values for maize crop.

Paper n	Country	Kc ini	Kc mid	Kc end
7	California, USA	0.2	1.2	0.5
20	Kenya, Africa	0.5	1.0	0.8
8	Karnal,India	0.6	1.1	0.6
29	Wokingham, UK	-	0.8	-
40	Taiwan	0.4	0.8	0.7
45	Nebraska, USA	0.3	1.2	0.3
55-57	Shaanxi, China	0.2	1.1	0.6
50	Khon Kae, Tailand	1.0	1.2	1.1
59	Texas, USA	0.3	1.1	1.0
81	Idaho, USA	0.2	0.9	0.7

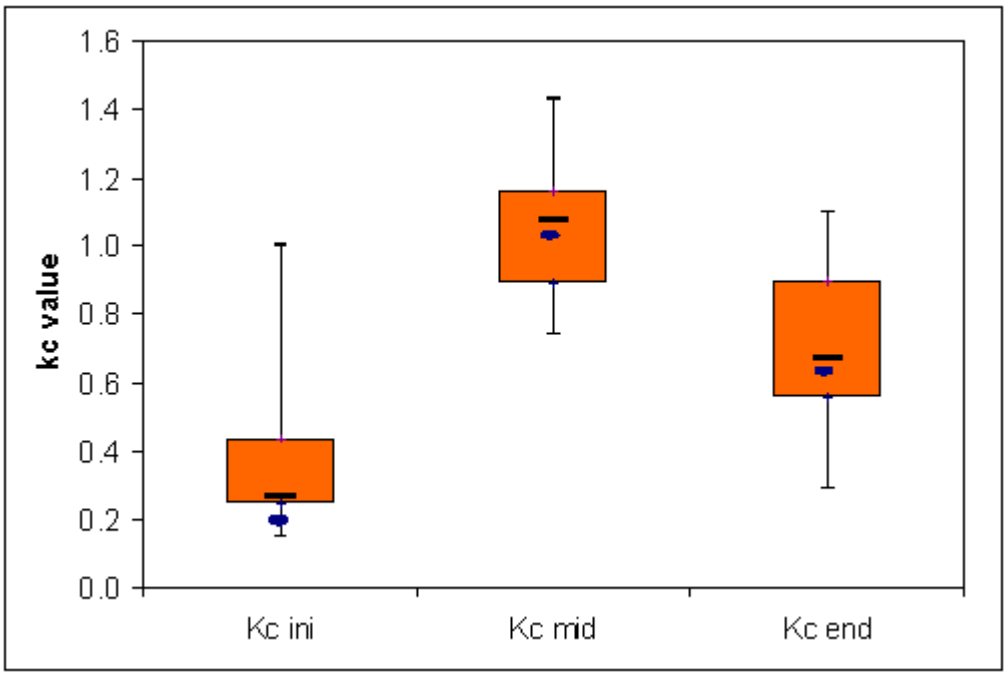

Figure 34. Box plot of Kc values for maize including: initial Kc, mid season Kc and Kc end. The minimum, maximum, mean or 50° (median), 25° (Q1) and 75° (Q3) are calculated from all the K_c values reported in 10 reviewed articles. According to this graph, there is a high variation about Kc values measured in different locations, but the mean values are similar to FAO 56 Kc values recommended for maize, as the blue spots underline.

From a statistical point of view, it is clear that the initial crop coefficient presents the highest variability, both between articles reporting maize crop coefficients, and between crop coefficient present in literature and table crop coefficients proposed by FAO 56. For midseason crop coefficients, the range of values is smaller and for the end season crop coefficient the values are close to the mean crop coefficient values reported in the articles on maize.

3.2.K_c MODEL VALIDATION

Field data were obtained by direct measurements on different crops: a) maize, b) broccoli, c), lettuce, d) olive and e) kiwifruit, as described in Materials and Methods section.

A) MAIZE: The experiment was conducted by the University of Milan and Politecnico di Milano (Facchi et al., 2013). The purpose of the research was to measure Kc for maize grown in the Lombardia region. Kc was derived for two experimental maize fields (Landriano and Livraga) for years 2006, 2010 and 2011 (Table 9) as the ratio between actual evapotranspiration (ET_c) in well watered conditions and reference evapotranspiration (ET_0). Crop data, management and meteorological condition data were used to run KcMod, obtaining simulated 'dual' and 'single' K_c and ET_c values. Then, simulated data were tested against the measured ET_c ($=ET_0*K_c$) values, where Kc are the crop coefficient measured values and ET_0 was computed with the standardized Penman-Monteith equation using weather measured data, from the closest ARPA Lombardia weather station, (Landriano and Bertonico, respectively).

The results include a visual comparison (Fig. 35) of the bare soil, dual and table Kc curves produced by the model, the ETc temporal graph (Fig. 36) and the statistical tests for 'dual' and 'single' ET_c (Fig. 43-44) for Landriano 2006.

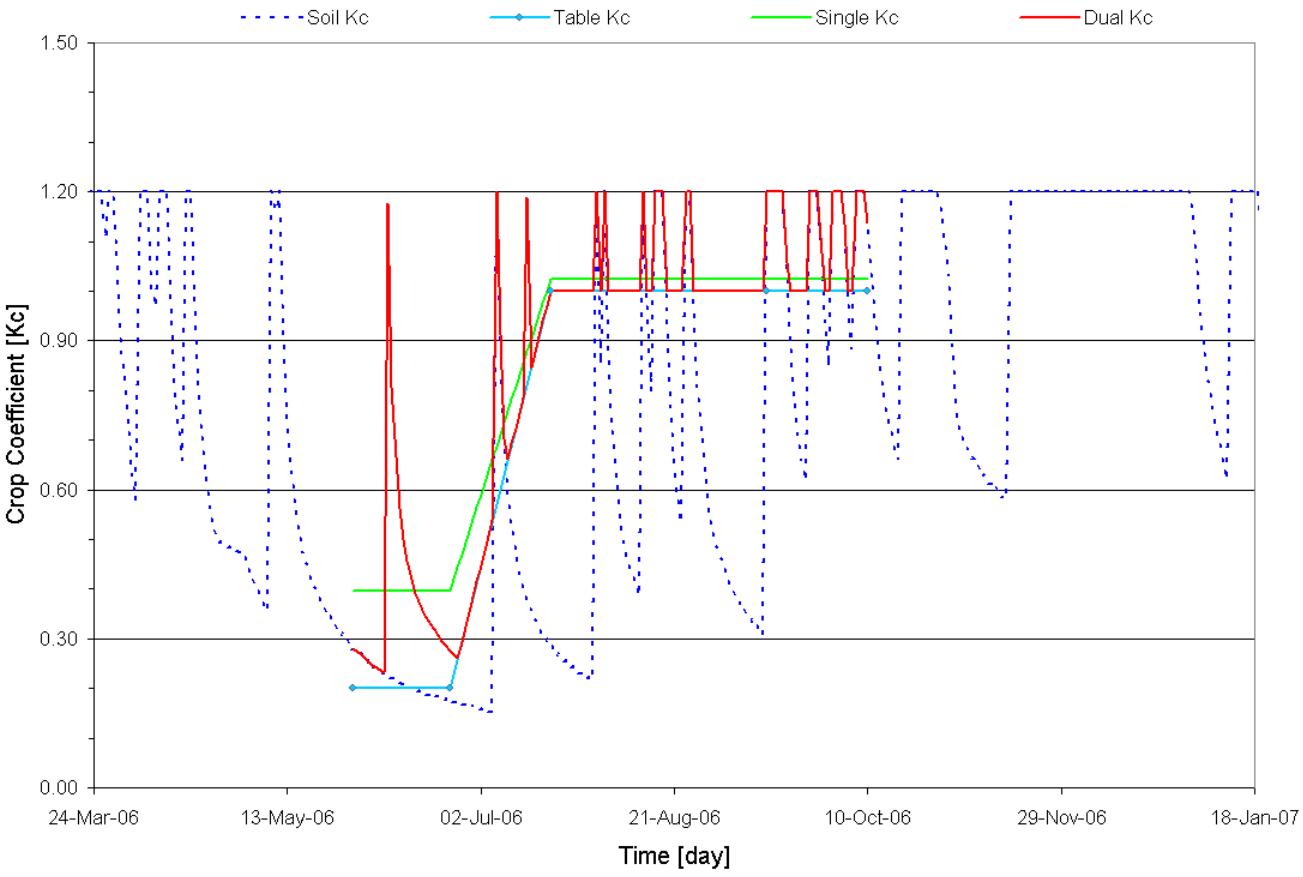

Figure 35 Simulated bare soil K_c (dashed blue line), Table K_c (blue line), Single (green line) and Dual (red line) K_c values, using ET_0 Penman-Monteith equation, computed from weather data for maize (Landriano, 2006). Spikes correspond to either rainfall or irrigation events.

Simulated K_c curves in Figure 35 include bare soil evaporation curve (dashed dark blue), FAO 56 table K_c line (light blue), single K_c curve (green), and dual K_c line (red) versus date. The time period corresponds to the growing season period (see Materials and Methods paragraph for details) plus a brief interval before the planting date and after the harvesting date, in order to easily see the rainfall spikes during the entire period. The two figures show K_c spikes at each precipitation event, corresponding to a soil evaporation spike, before the crop growing season starts. Then, during the crop growing season, to every irrigation or precipitation event corresponds a dual K_c spike. The single crop coefficient curve simply follows the average between the dual K_c curve and the table crop coefficient line. The first K_c plateau (30 May-24 June) represents the initial growth stage, just after crop emergence, and the main contribution to evapotranspiration is due to bare soil evaporation (K_e). From 25 June untill 20 July, the rapid growth stage of maize presents two spikes, one for irrigation and one for rainfall. There is a high water table in the experimental area, so irrigation is needed but less frequently than in other parts of Italy, especially when abundant rainfall contributes to the water storage. During

summer, the number of spikes is related to the number of rainfall events that allows the plant available water to remain higher than the permanent wilting point, even without irrigation. This period, which goes from 21 July till 14 September, corresponds to the mid season growing period, during which maize blooming occurs. The last part of the crop coefficient curve is called late season and correspond to the maturation of caryopsides. Harvesting begins before senescence is completed. The maximum simulated K_c value is 1.20 and occurs at almost every irrigation or rainfall date for the dual method (single max K_c=1.02) The minimum simulated K_c value is 0.23 and occurs for the dual method when no rainfall or irrigation occurs (single min K_c=0.40), while the average K_c values are 0.85 and 0.84 for the dual and single K_c, respectively. Table K_c corresponds to 0.20 for the initial period and to 1.00 for the mid and end season periods. Since the crop is harvested before the senescence stage, (due to the fact that crop is silage maize) the K_c value does not present any decrease in the last part of the growing period. From a qualitative point of view the 'dual' K_c curve fits better with the corresponding peaks of rainfall and irrigation events and this is evident during the entire growth stage, when 'dual' K_c curve has high and low values, depending on soil moisture level, while the 'single' K_c curve is more approximate, sometimes overestimating and sometimes underestimating the real crop evapotranspiration.

Figure 36 represents the temporal graph for measured, dual and single simulated ET_c values. The maximum ET_c is equal to 5.94 mm d^{-1} and it belongs to the dual series. The minimum ET_c value corresponds to 0.17 mm d^{-1} and it is part of the single ET_c values. The average values are 3.7 mm d^{-1}, 3.4 mm d^{-1} and 3.5 mm d^{-1}, for the measured, dual and single data respectively. In general, the simulated ET_c values show a good agreement, even if they slightly underestimated the measured ET_c, in particular during the mid season growing period. Both simulated lines follow the experimental data trend, all over the growing season.

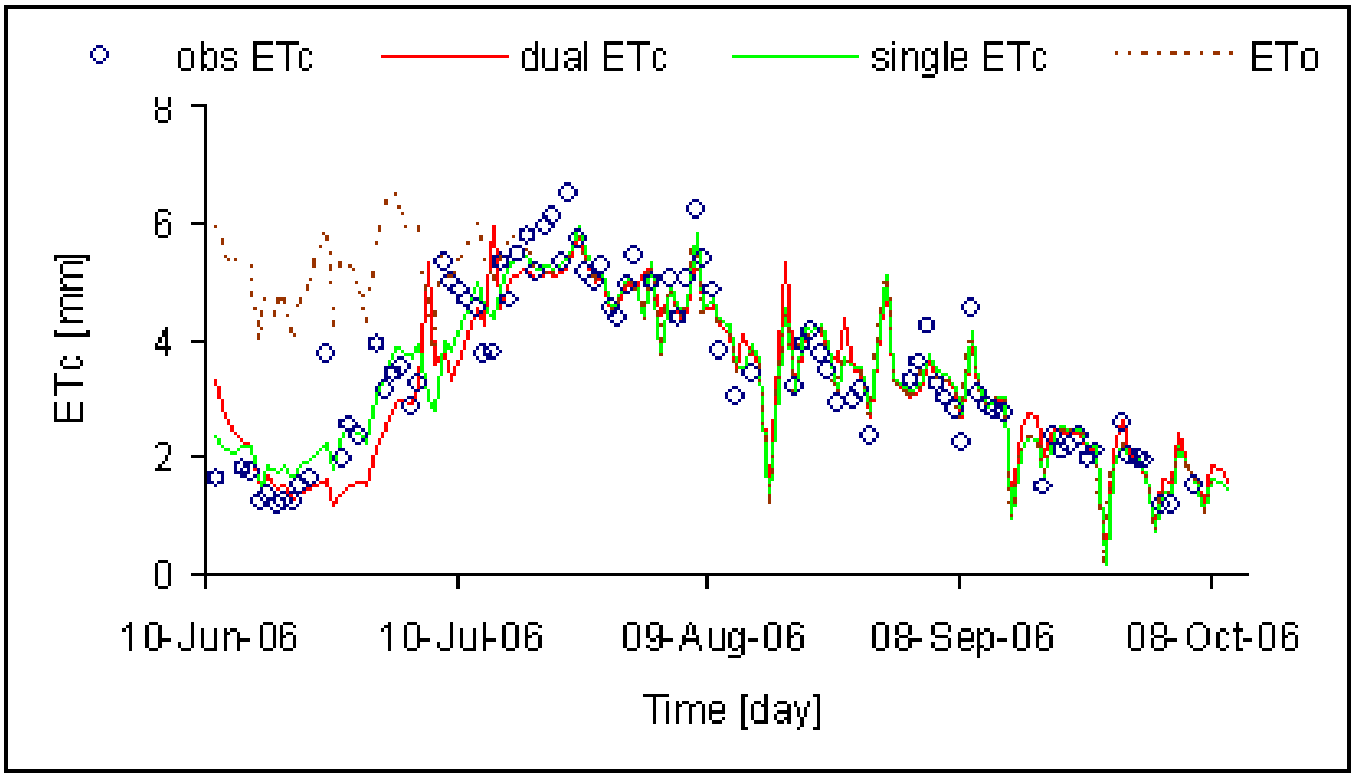

Figure 36 Temporal graph of measured (obs ET_c=observed ET_c) versus simulated single and dual ET_c calculated with ET_o weather data for maize (Landriano, 2006).

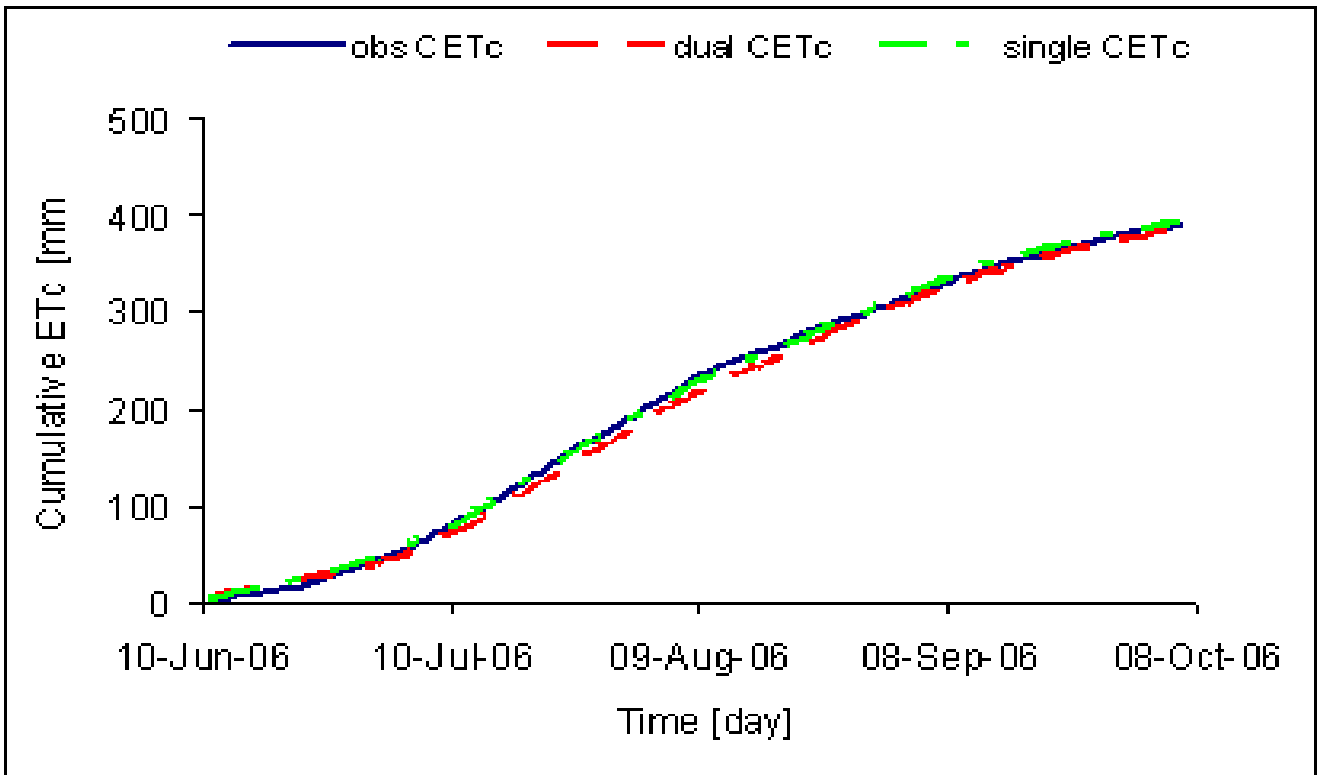

Figure 37 Temporal graph of measured, dual and single simulated cumulative ET_c for maize (Landriano, 2006).

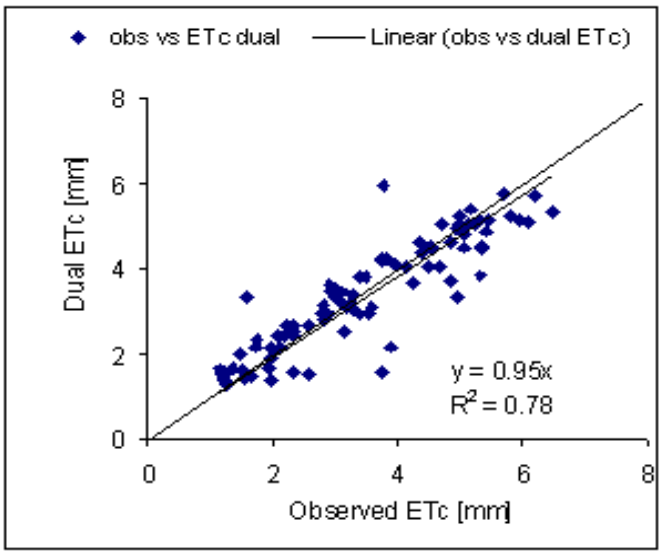

Figure 38 Scatter plot of measured versus simulated dual ET_c for maize (Landriano, 2006)

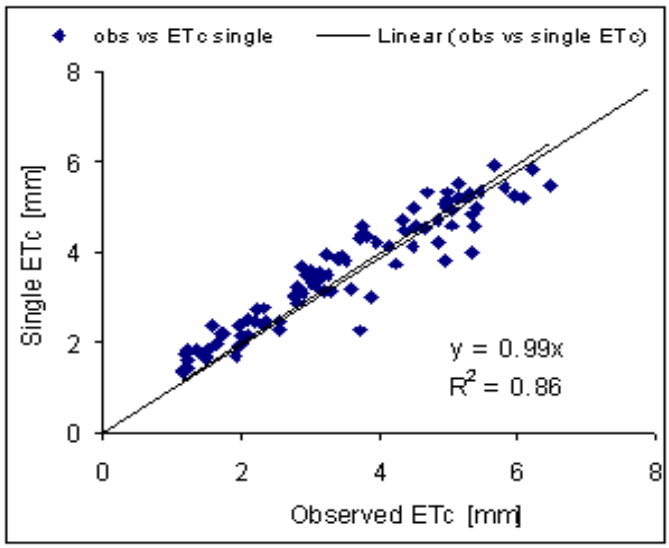

Figure 39 Scatter plot of measured versus simulated single ET_c for maize (Landriano, 2006).

Graph of figure 37 shows the cumulative ET_c for measured, simulated single and dual methods. The curves are almost equivalent during all growing season. The cumulative ET_c at the end of the season was 391 mm, 392 mm, and 398 mm, respectively for measured, dual and single methods, with a difference of only 1 mm and 7 mm, respectively. Figures 38 and 39 show observed ET_c data versus simulated ET_c data, for the dual (Fig. 38) and single (Fig. 39) method. We can see that using dual ET_c values provides a better correspondence with measured ET_c values than the ET_c simulated with the single method. The Root Mean Square Error was calculated, to provide an additional statistical comparison. With this last test, the 'single' method provides better results, with a lower RMSE, in respect to the 'dual' ET_c method (RMSE 'single'=0.48 mm d^{-1}; RMSE 'dual'=0.64 mm d^{-1}).

To summarize, for data set of Maize, Landriano, 2006, the 'single' ET_c obtained from KcMod run with ET_0, calculated with Penman-Monteith equation, by using meteorological data, showed a better comparison with measured data than the dual ET_c.

The same tests were performed simulating crop coefficients (K_c) and crop evapotranspiration (ET_c) values, to compare them with measured ET_c values, for Landriano 2010 and 2011, Figure 40 shows the temporal graphs of 2010 for simulated K_c, and Figure 41 represents the temporal graph for dual and single simulated and measured ET_c. Cumulative measured ET_c curves are presented only for data sets with a number of data equiparable to the simulated ones.

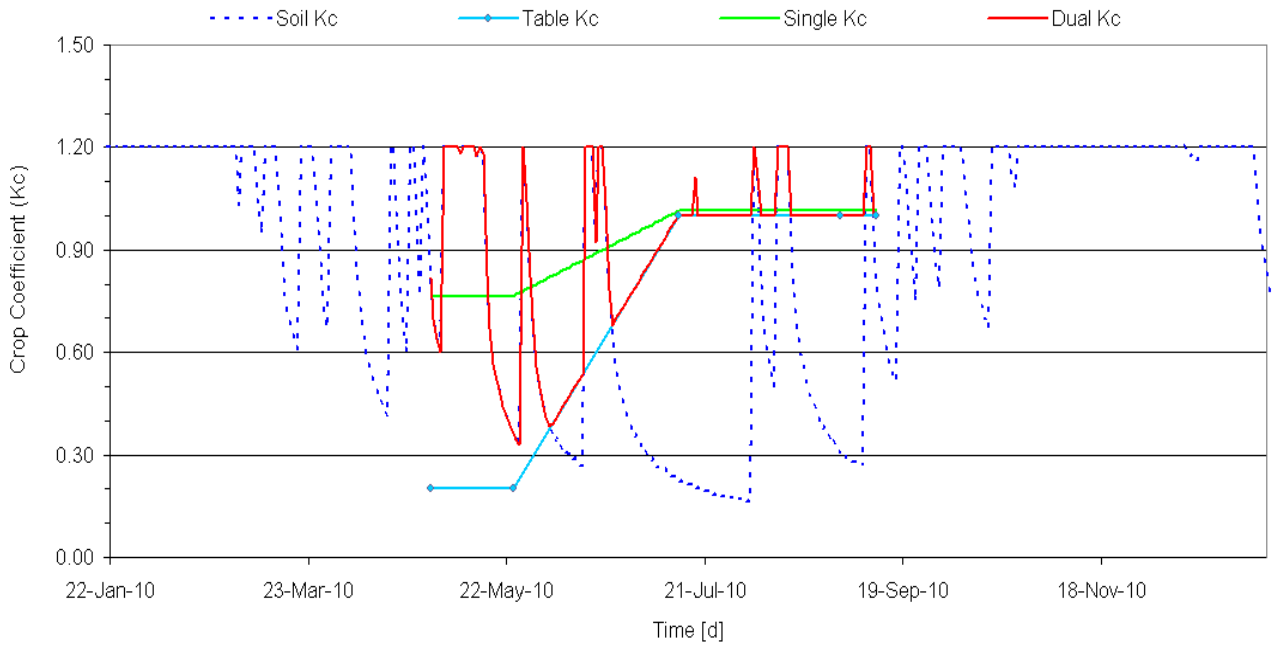

Figure 40 Simulated bare soil Kc (dashed blue line), Table K_c (blue line), Single (green line) and Dual (red line) K_c values for maize, (Landriano, 2010), using ET_0 Penman-Monteith equation, computed from weather data. Spikes correspond to either rainfall or irrigation events.

During 2010, the growing season started on April 29 and ended on September 11. The rapid growth stage went from May 24 to July 13 and the end season started on 31 August. Also for this year, 'dual' K_c fits better with the corresponding peaks of rainfall and irrigation events, and this is remarkable in particular for the initial stage. The maximum simulated K_c value is 1.20 and occurs at almost every irrigation or rainfall date for the dual method (single max K_c=1.01) The minimum dual K_c value was 0.33 and it occurred following a long period with no rainfall or irrigation during rapid growth (single min K_c=0.77), while the average K_c values are 0.90 and 0.92 for the dual and single K_c, respectively. Figure 41 represents the temporal graph for measured, dual and single simulated ET_c values. The maximum ET_c is equal to 7.84 mm d^{-1} and it came from the single K_c curve. The minimum ET_c value corresponds to 0.45 mm d^{-1} and it is part of the single ET_c values. The average values are 2.8 mm d^{-1}, 3.5 mm d^{-1} and 3.9 mm d^{-1}, for the measured, dual and single data respectively. In general, the simulated ET_c values show a good agreement, even if they slightly overestimated the measured ET_c, in particular for the single method, during the mid season growing period. For the single and dual cumulative ET_c curves (Fig. 42), the estimated values show a good agreement (single CET_c is 50 mm higher than dual ET_c).

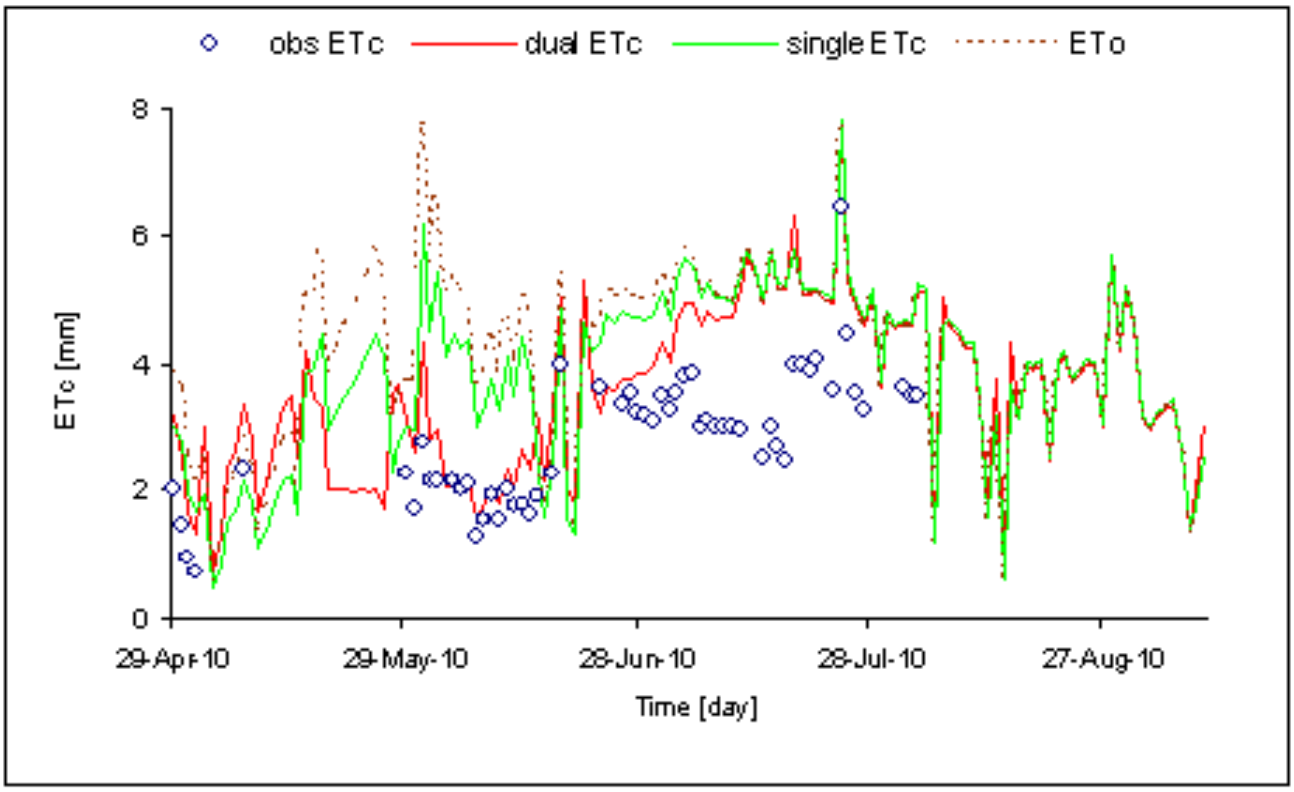

Figure 41 Temporal graph of measured versus simulated single and dual ET_c calculated with ET_0 weather data for maize (Landriano, 2010).

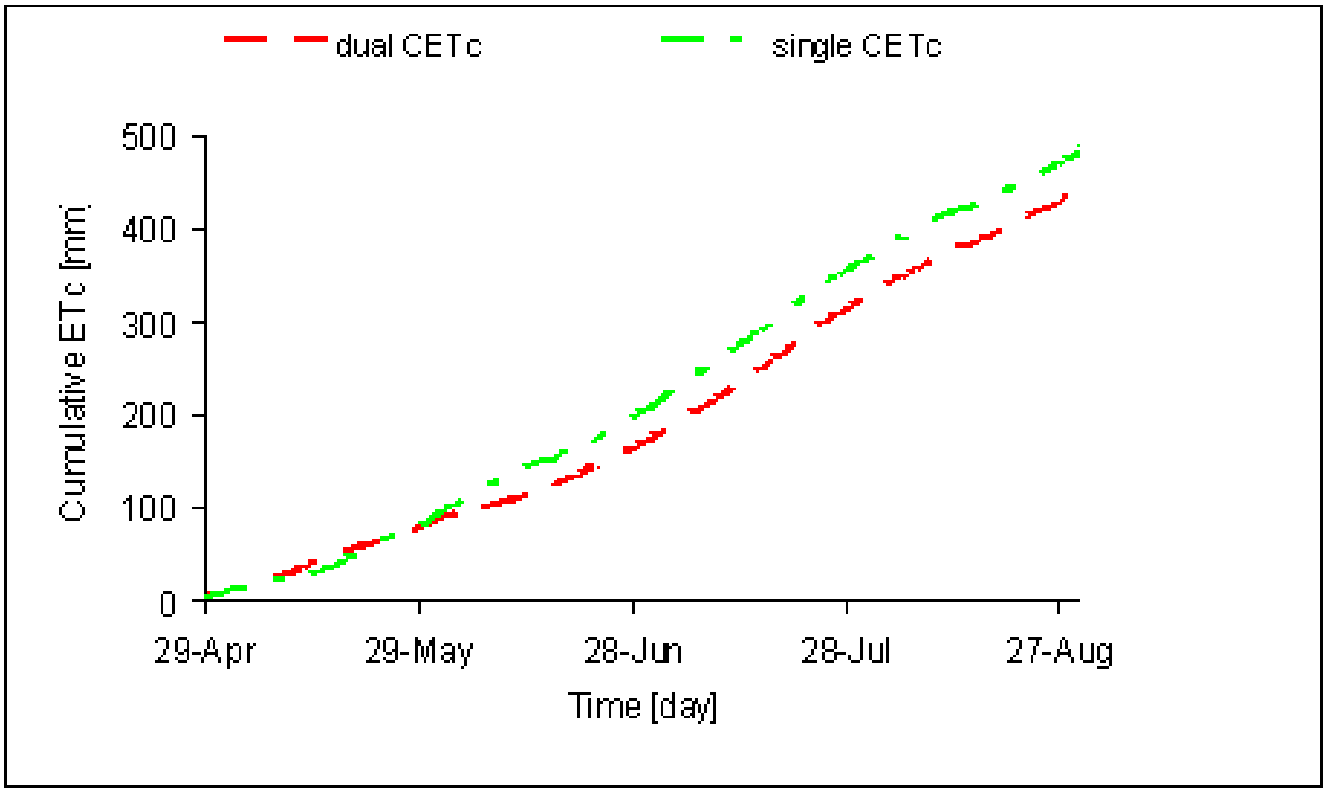

Figure 42 Temporal graph for the cumulative ETc simulated with dual and single method for maize (Landriano, 2010).

Figures 43-44 represent the statistical results for 'dual' and 'single' versus measured ET_c for maize, grown in Landriano 2010. For the RMSE test, the 'dual' method with ET_c provides better results, with lower error (RMSE dual=1.25 mm d^{-1}; RMSE single=1.80 mm d^{-1}). In both cases the model overestimate the measured date, as it is possible to see also in figures 41 in the central part of the graph, which is the mid season growing period.

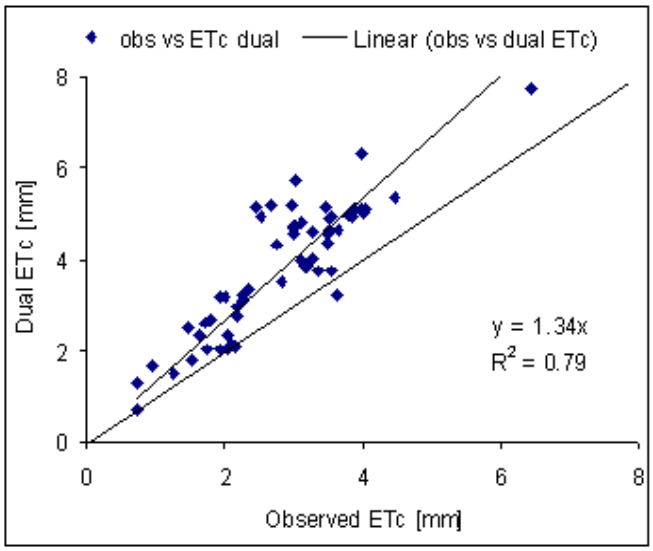

Figure 43 Scatter plot of measured versus simulated dual ET_c for maize (Landriano, 2010).

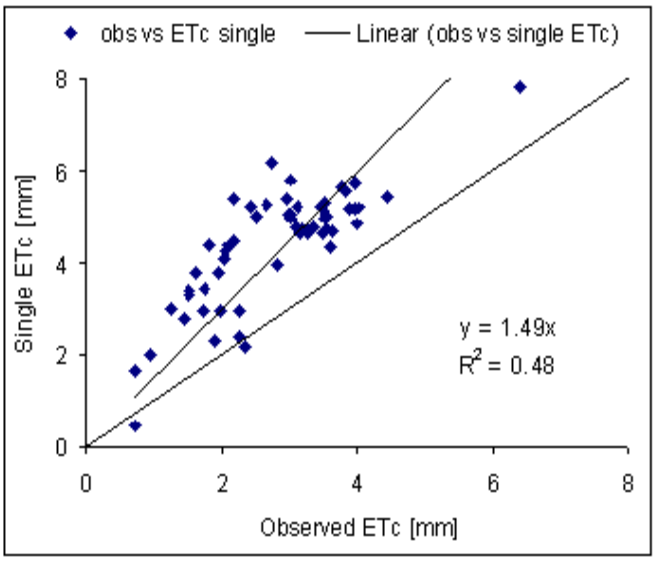

Figure 44 Scatter plot of measured versus simulated single ET_c for maize (Landriano, 2010).

To summarize, for data set of Maize ET_c, Landriano, 2010, the 'dual' ET_c showed a better correlation than the 'single' method. The following Figures, 45, 46, 47, 48 and 49 represent the simulated K_c curves, the measured and simulated dual and single ET_c and ET_o temporal graphs, the dual and single cumulative ET_c, and measured versus dual and single ET_c scatter plots, respectively, for maize crop, grown in Landriano, during 2011.

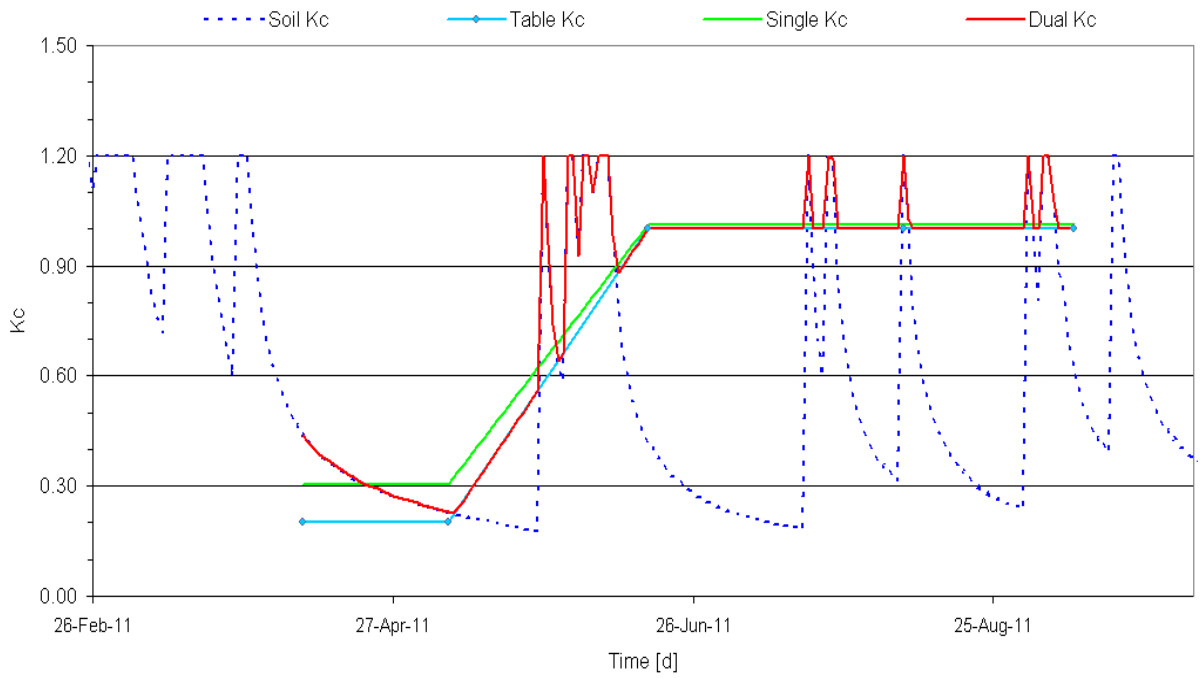

Figure 45 Simulated bare soil K_c (dashed blue line), Table K_c (blue line), Single (green line) and Dual (red line) K_c values, for maize, (Landriano, 2011), using ET_0 equation, computed from weather data. Spikes correspond to either rainfall or irrigation events.

Looking at Figure 45 of simulated K_c curves for Landriano, 2011, as for the previous years, there is almost no difference with ET_c calculated from dual or single method, excepted for the initial growth period. The average is 0.88 mm d^{-1} and 0.86 mm d^{-1}, for the dual and the single method respectively.

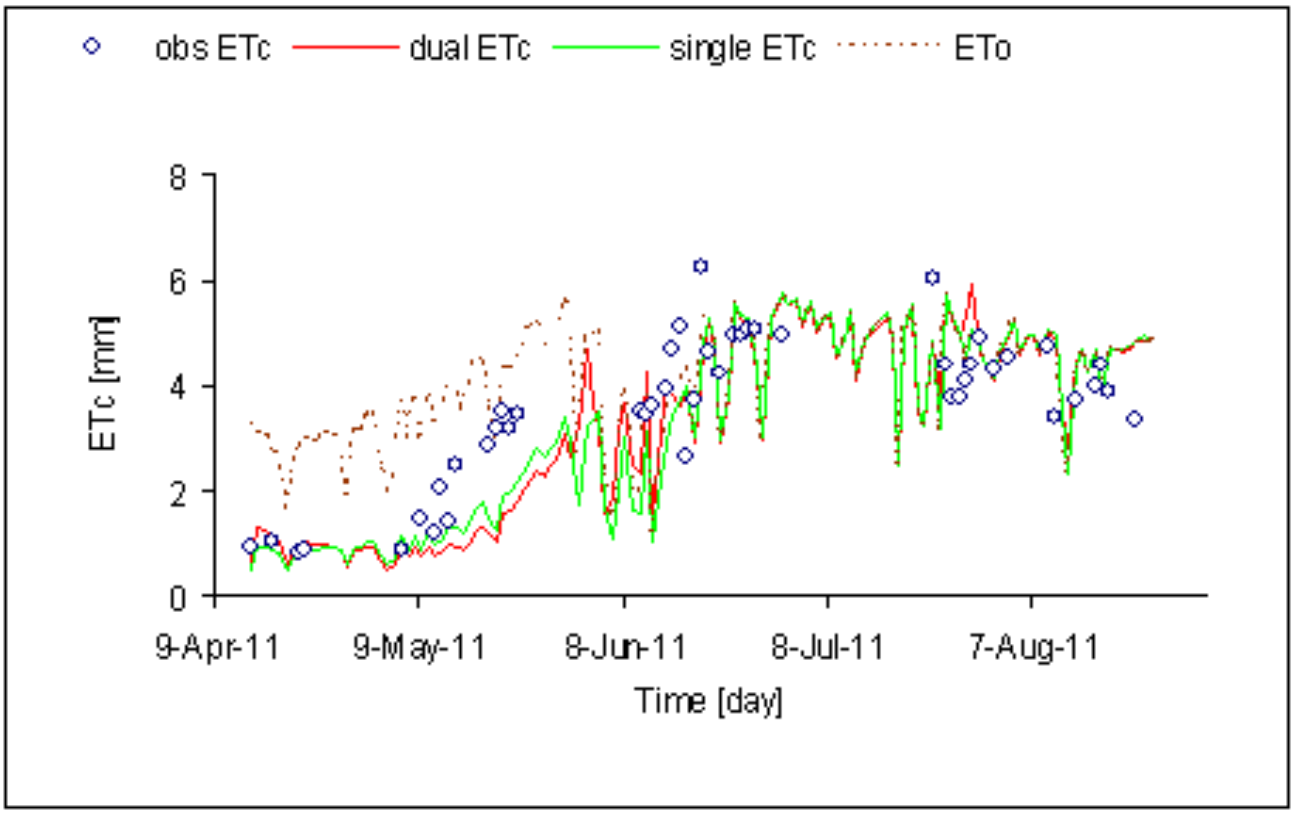

Figure 46 Temporal graph of measured versus simulated single and dual ET_c calculated with ET_0 weather data for maize (Landriano, 2011).

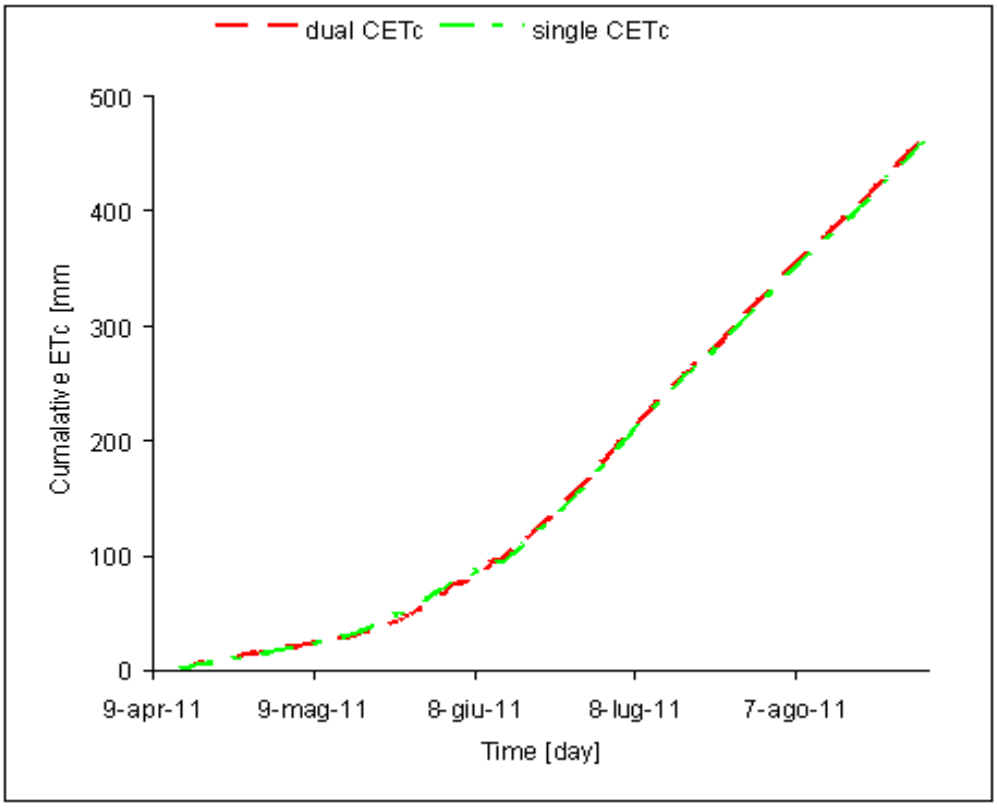

Figure 47 Temporal graph for the single and dual cumulative ET_c for maize (Landriano, 2011).

From the ET_c temporal graph (Fig. 46) there is instead a little difference between computing ET_c using dual or single method. The maximum ET_c is 6.25 mm d^{-1} and it is for the measured series (5.93 mm d^{-1} and 5.77 mm d^{-1} for the dual and single K_c series respectively). The minimum value for ET_c is 1.04 mm d^{-1} for the single, versus 1.49 mm d^{-1} and 2.15 mm d^{-1} (dual and measured K_c values series, respectively). The average values are: 4.26 mm d^{-1}, 4.32 mm d^{-1} and 4.24 mm d^{-1} for the measured ET_c, dual and single simulated ET_c. The cumulative ET_c curves are almost identical by using dual and single method (Figure 47). The higher agreement of the single ET_c values with the measured ones is more evident from the scatter plots results (Fig. 48-49). In particular, simulated single ET_c values showed a higher agreement with measured ET_c, in the initial growth stage, while during end season period simulated dual ET_c values showed a higher agreement with measured ET_c.

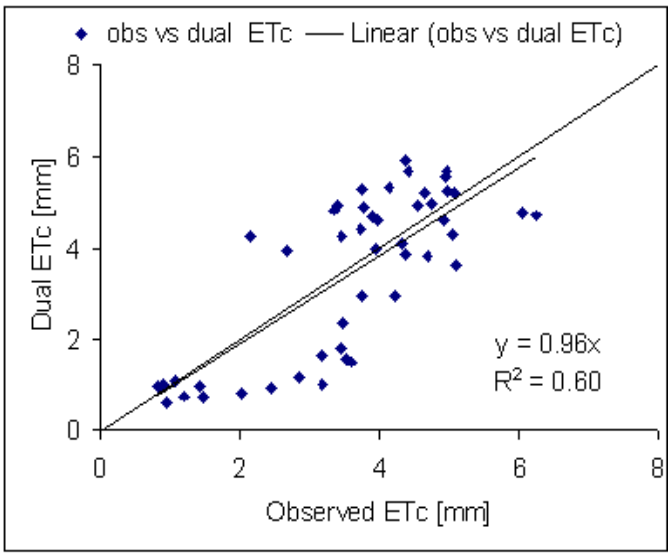

Figure 48 Scatter plot of measured versus simulated dual ET_c for maize (Landriano, 2011).

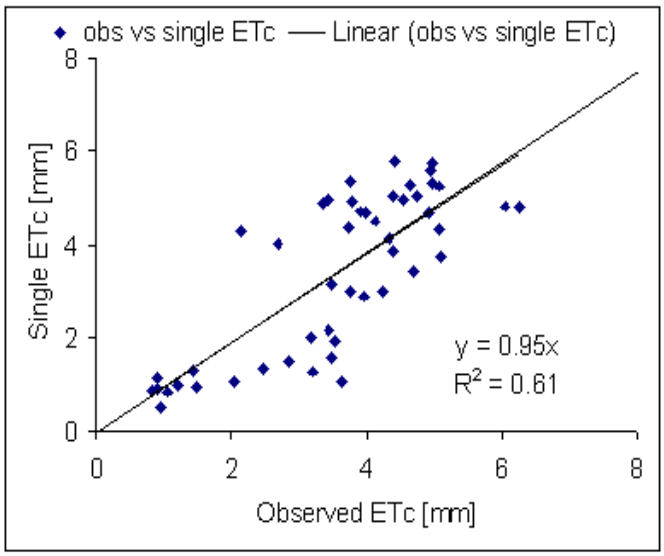

Figure 49 Scatter plot of measured versus simulated single ET_c maize (Landriano, 2011).

The root mean square error data are not very good, neither for the dual and single data. In fact all the values are higher than 1.00 mm d^{-1} and in particular: RMSE dual=1.11 mm d^{-1}; RMSE single=1.05 mm d^{-1}.

Maize experimental data were measured in two sites. The second experimental field was located in Livraga. In this field maize was grown for biogas use. Penman Montetih ET_0 was calculated using weather data measured from the closest ARPA Lombardia station (16.1 km), located in Bertonico, for year 2010. After using the measured weather, ET_0, soil and crop data

as input, (as described in Materials and Methods section), and run the KcMod program, simulated K_c, and ET_c values were tested against the measured ET_c values. Figure 50 shows the K_c curves of bare soil evaporation, FAO-56 table line, 'single' and 'dual' K_c simulated curves for maize, grown in Livraga, in 2010.

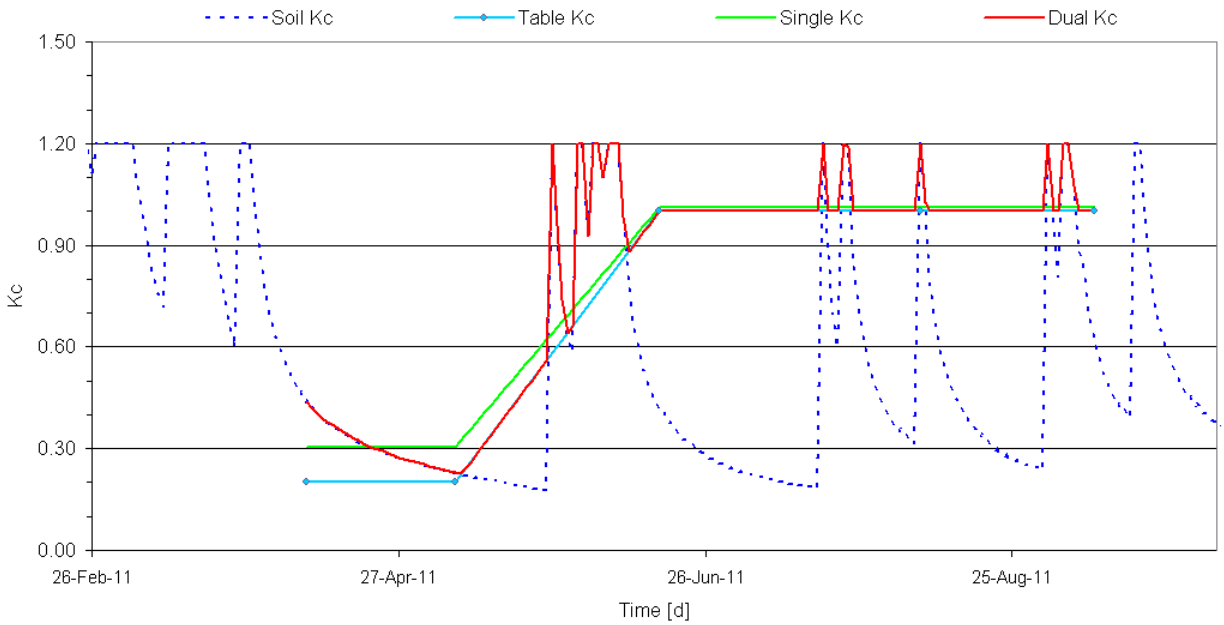

Figure 50 Simulated bare soil K_c table K_c dual, single, and curves for maize, (Livraga, 2010), calculated using ET_0 Penman-Monteith, computed from weather data. Spikes correspond to either rainfall or irrigation events.

The maize growing season was from April to September 2010. Table K_c corresponds to 0.20 for the initial period and to 1.00 for the midseason period. Since the crop is harvest before the senescence stage, K_c value does not present any decrease in the last part of the growing period. Also in this case, during the initial and rapid growth period, the table line is lower than the simulated curves. During all growing season period, the dual K_c is the method of calculation that provides a more precise estimation of the crop coefficient values, following closely every wetting surface event.

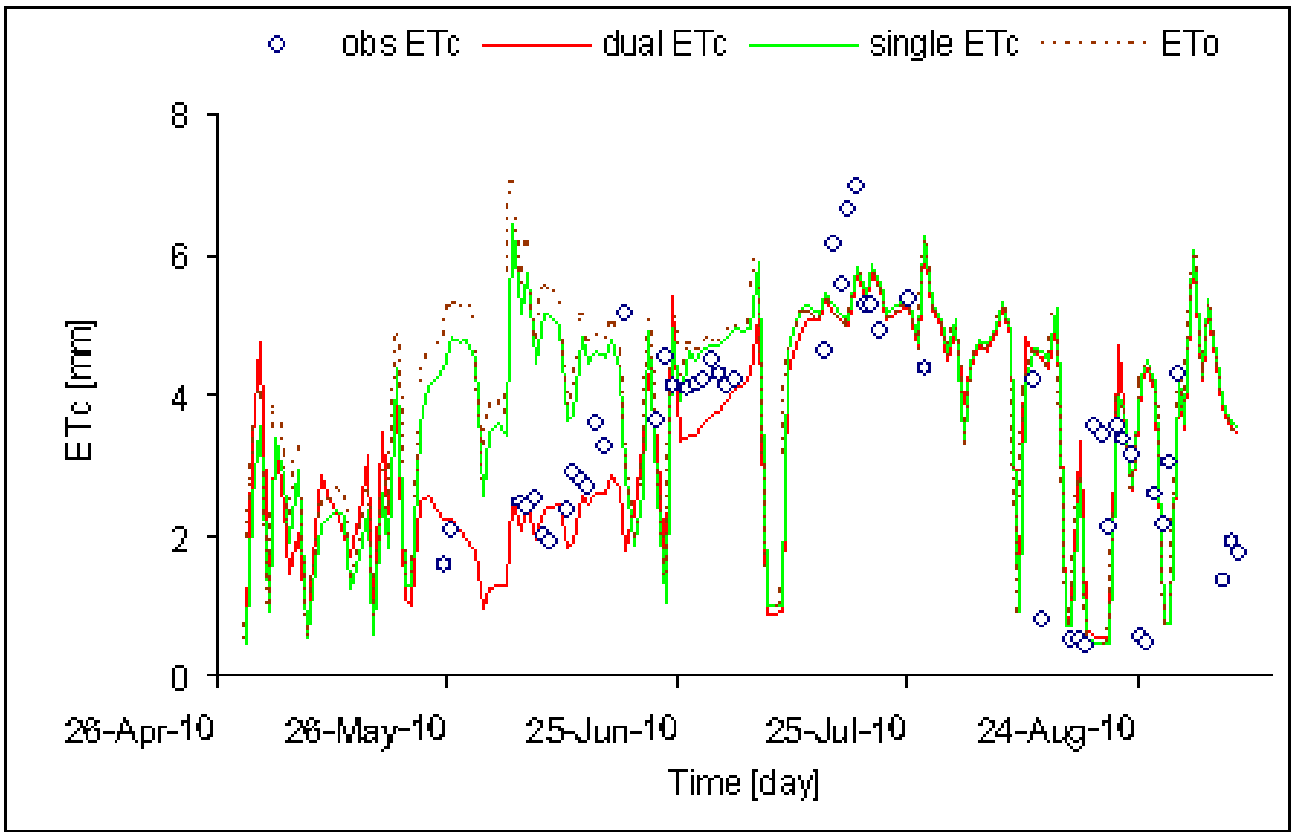

Figure 51 Temporal graph of measured, dual and single simulated ET_c calculated with ET_0 for maize (Livraga, 2010).

Figure 51 shows the temporal graphs for maize, for the measured, 'dual' and 'single' simulated ET_c. In general, the observed ET_c are higher then the simulated ET_c values, in particular during the rapid growth period. The dual and single K_c estimates of ET_c are almost identical during midseason. During the end season growing period, both the dual and the single methods equally well simulated the measured values.

The cumulated simulated dual and single ET_c show a difference equal to 60 mm, considering the maize growing season (Figure 52).

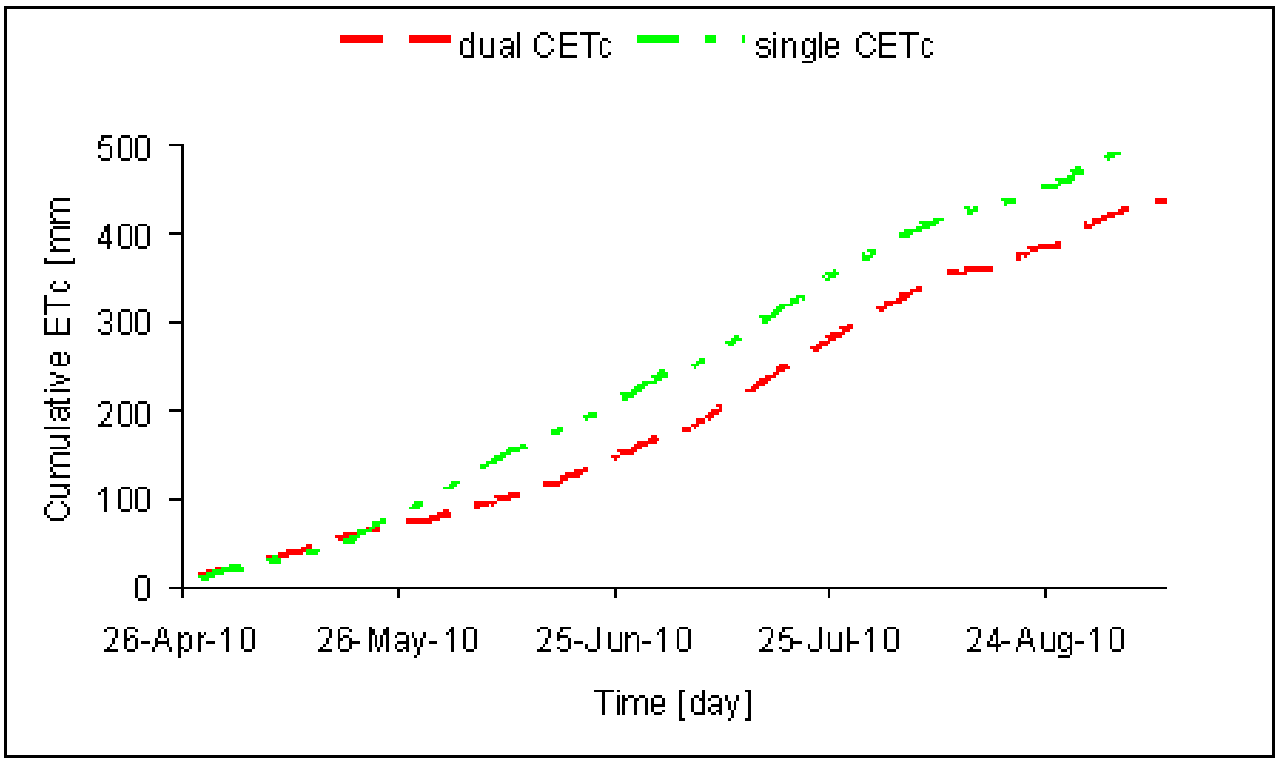

Figure 52 Simulatred dual and single cumulated ET_c for maize (Livraga, 2010).

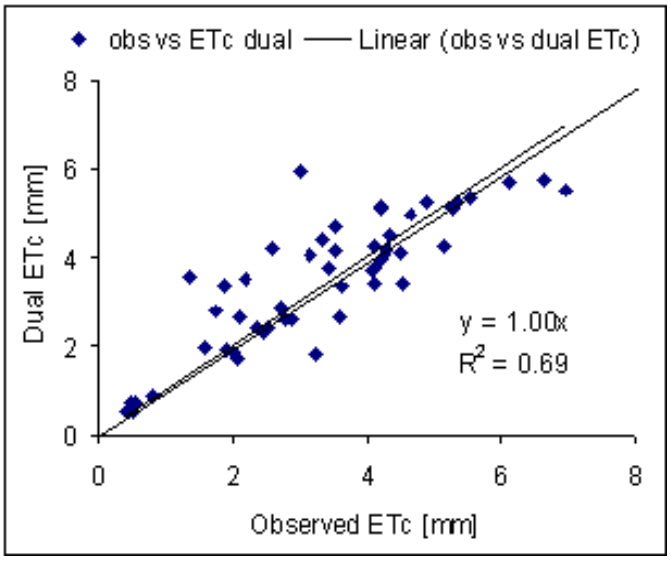

Figure 53 Scatter plot of measured versus simulated dual ET_c for maize (Livraga, 2010)

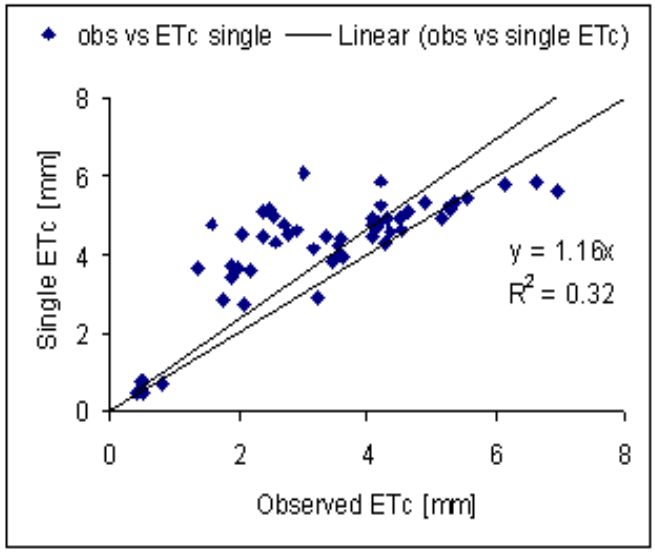

Figure 54 Scatter plot of measured versus simulated single ET_c for maize (Livraga, 2010)

Figures 53-54 report the statistical results for measured against simulated 'dual' and 'single' ET_c values for maize (Livraga, 2010). The RMSE provided good results for the dual, less for the

single method (dual ET_c= 0.57 mm d^{-1}, single ET_c=1.27, mm d^{-1}). In general, the dual method for crop coefficient calculation showed the best performance, if compared to the single method.

B) BROCCOLI: After using the measured weather, $ET_{0,}$ soil and crop data as input, as (described in Materials and Methods section), and run the KcMod program, simulated K_c, and ET_c values were tested against the measured ET_c values. Figure 55 shows the K_c curves of bare soil evaporation, FAO-56 table line, 'single' and 'dual' K_c simulated curves for broccoli grown in Ventura, California.

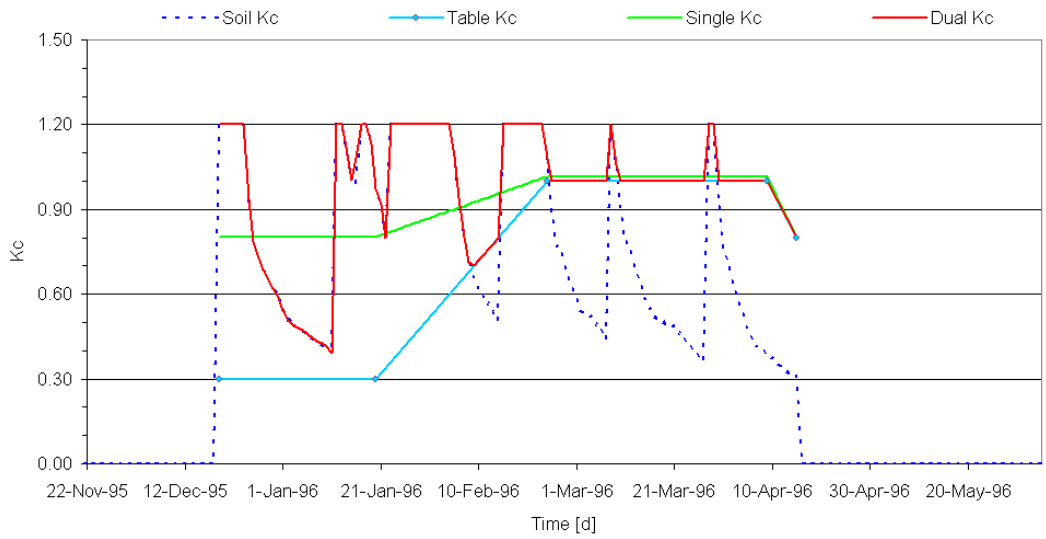

Figure 55 Simulated bare soil (blue dashed), FAO-56 Table Kc line (light blue), single Kc (green), and dual Kc (red) curves for Broccoli, grown in Ventura (California, 1996).

Among the simulated K_c curves generated from KcMod, using the Table K_c curve underestimated more, in particular during the initial growth period. When the main contribute to evapotranspiration was due to the bare soil evaporation, spikes at each rainfall and irrigation event raised the dual K_c relative to the Table K_c values. During the midseason period the Table, Dual and Single K_c curve are almost equivalent.

Figure 56 shows the temporal graph to compare the simulated single and dual ET_c with the measured ET_c for broccoli. Figure 57 represents the temporal graph to compared single and dual simulated cumulative ET_c.

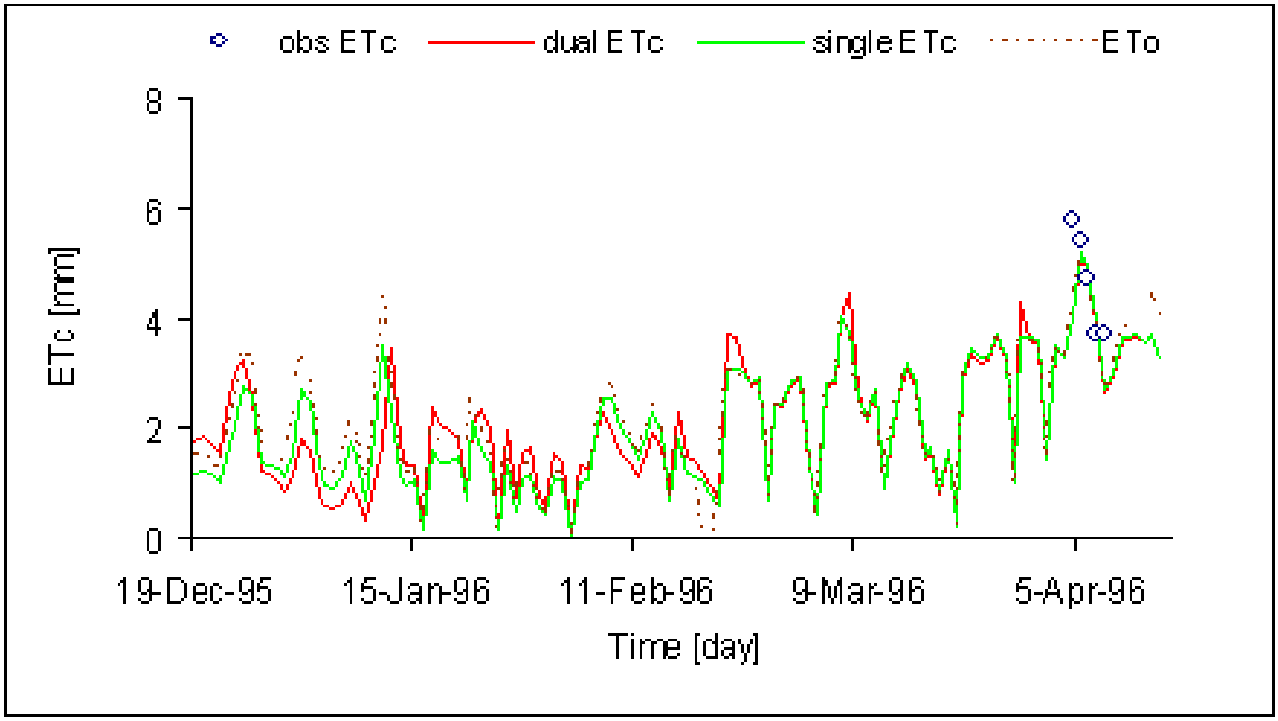

Figure 56 Temporal graph of measured, dual and single simulated ET_c and ET_0 for broccoli (California, 1996).

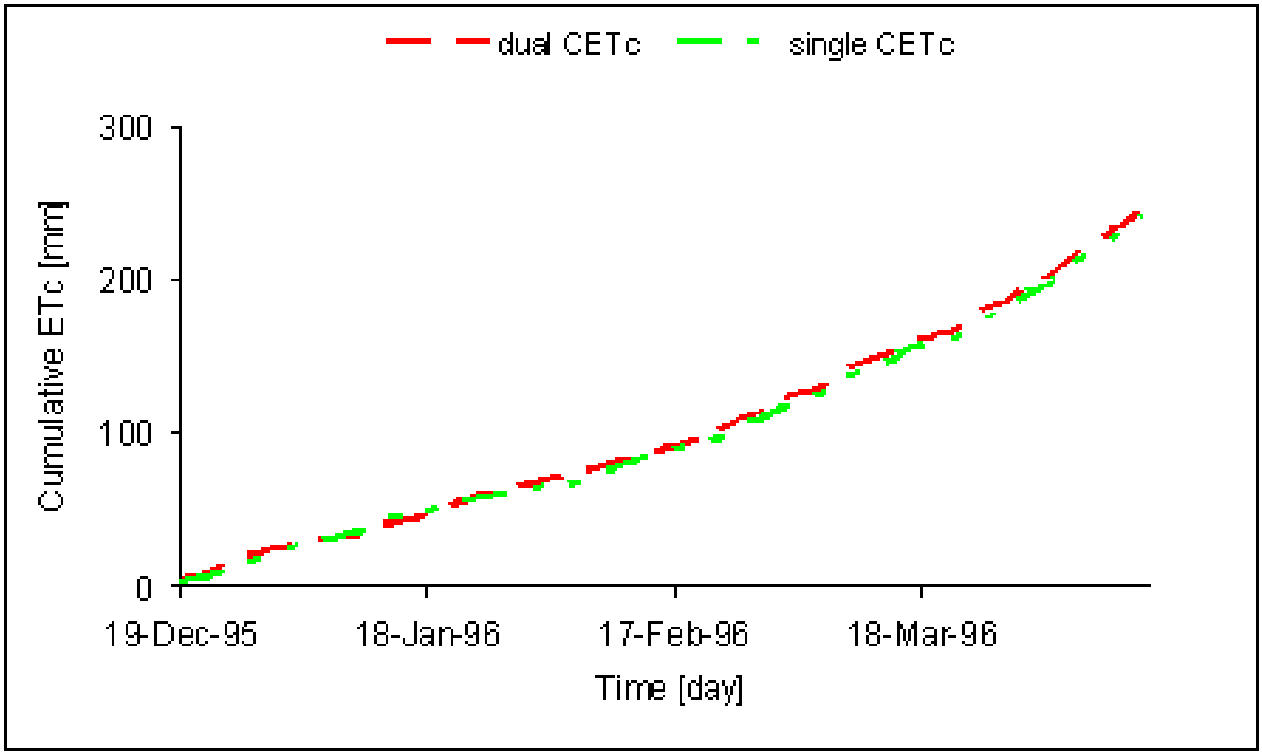

Figure 57 Temporal graph for simulated sigle and dual cumulative ET_c for broccoli (California, 1996).

The observed data are limited to the late midseason growing period (Figure 56). Both the single and dual ET_c estimates showed a good agreement with measured ET_c values. The high value

for April 5 does not correspond to any irrigation or rainfall event. The simulated evapotranspiration on that date was computed using K_c=1.2, and the ET_c was still a bit lower the observed ET_c. The simulated cumulative ET_c for dual and single method show good agreement during all the broccoli growing season (Figure 57). The statistical results of measured against simulated 'dual' and 'single' ET_c values for broccoli were satisfying. Figures 58-59 show good results, in particular the single method provided a lower RMSE (dual ET_c=0.78 mm d^{-1}, single ET_c=0.71, mm d^{-1}).

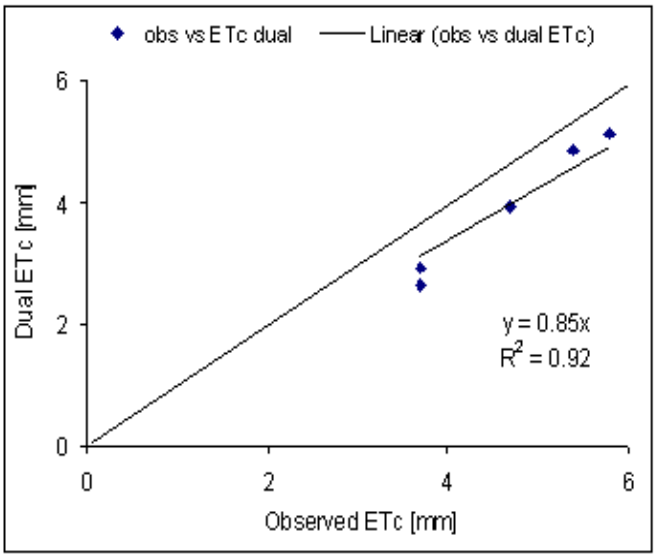

Figure 58 Scatter plot of measured versus simulated dual ET_c data for broccoli (Ventura, 1996).

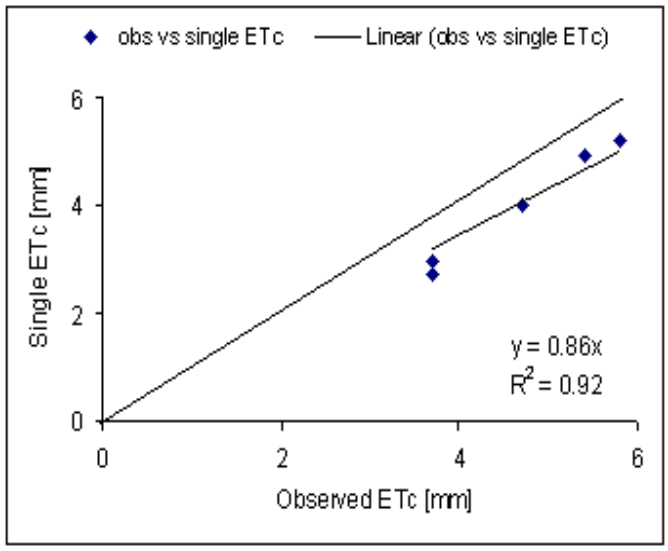

Figure 59 Scatter plot of measured versus simulated single ET_c data for broccoli (Ventura, 1996).

C) LETTUCE: After using the measured weather, $ET_{0,}$ soil and crop data as input, as described in M&M section, and running the KcMod program, simulated K_c, and ET_c values were tested against the observed ET_c values. Figure 60 shows the Kc curves of bare soil evaporation, FAO-56 table line, 'single' and 'dual' K_c simulated curves for Crisphead lettuce, grown in Imperial Valley research centre, California.

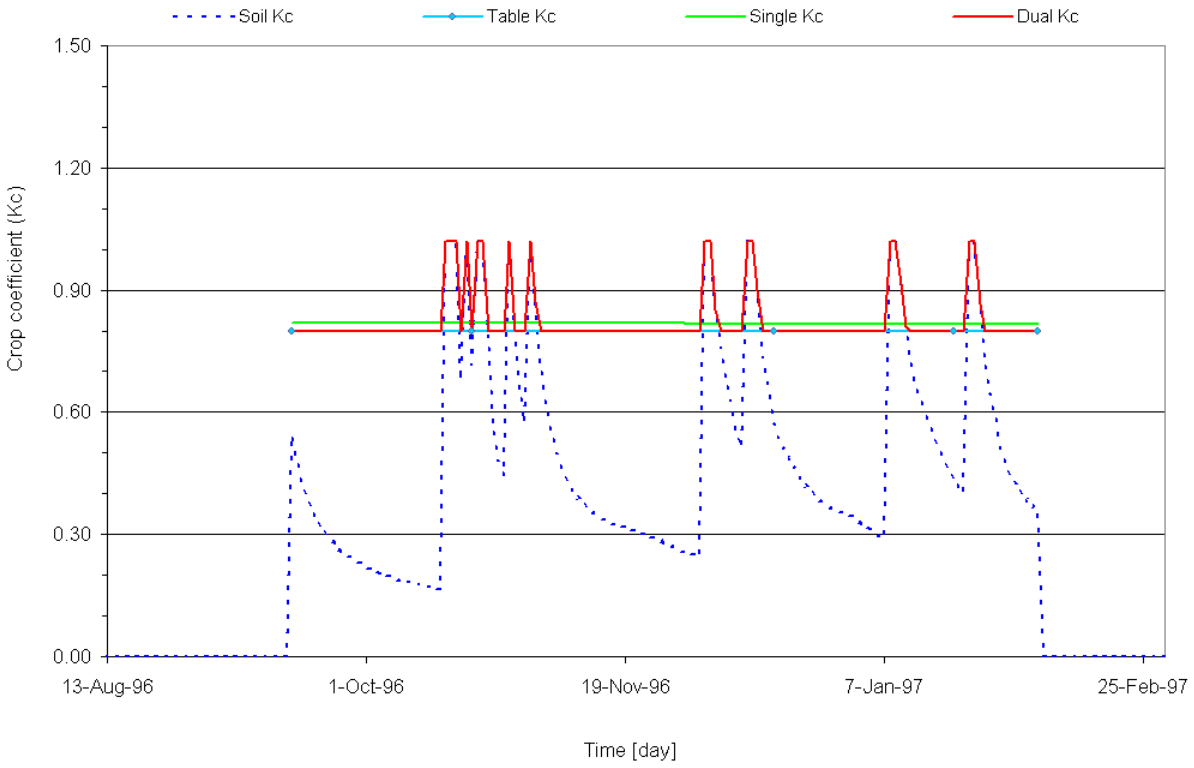

Figure 60 Simulated bare soil (blue dashed), FAO-56 Table K_c line (light blue), single K_c (green), and dual Kc (red) curves for Lettuce grown in Imperial Valley (California, 1996).

The average simulated K_c values are 0.83, 0.82 and 0.80, for the dual, single and the Table K_c respectively. Since the crop is harvest before the senescence stage, K_c value does not present any decrease in the last part of the growing period.

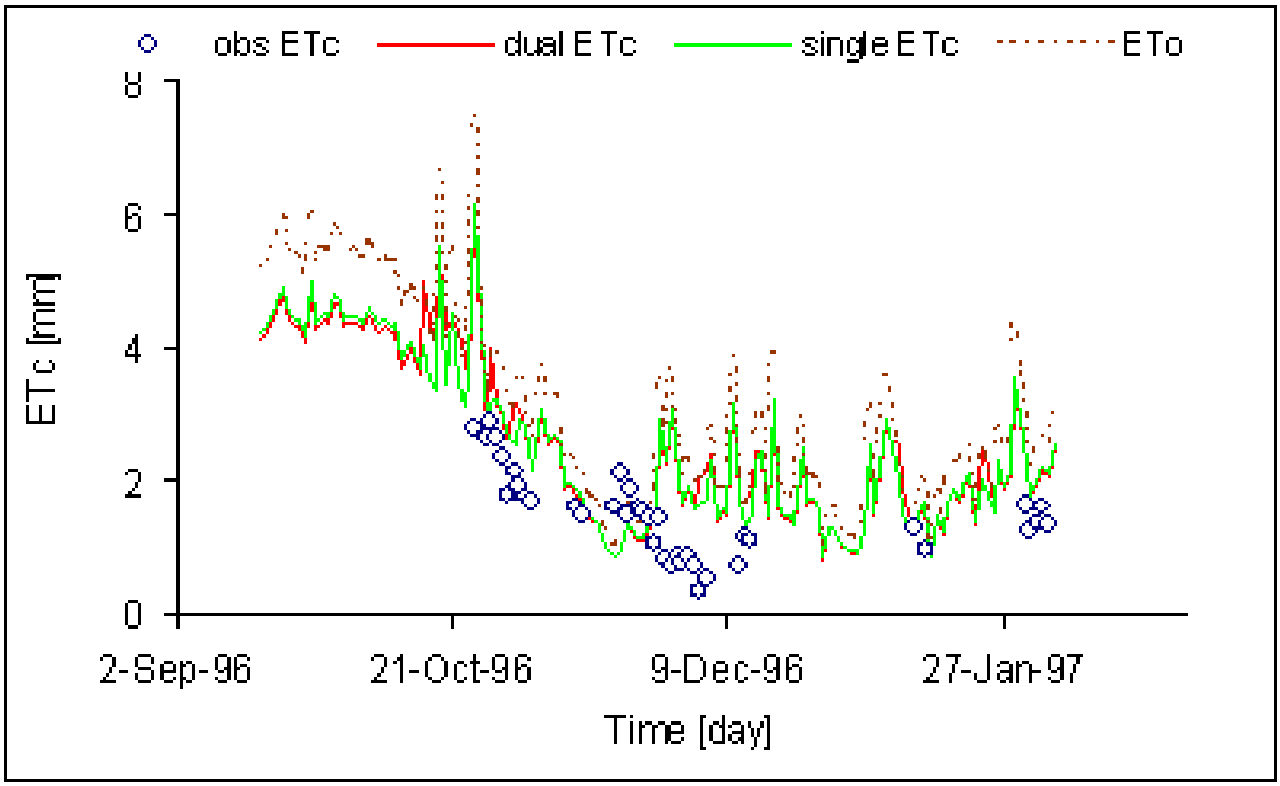

Figure 61 Temporal graph of measured versus simulated dual and single crop evapotranspiration temporal graph for Lettuce with ET_0, (California, 1996).

Figure 61 shows the temporal graphs for Lettuce, for the measured, 'dual' and 'single' simulated ET_c. The highest values occurs on October 25, and corresponds to an irrigation event (dual ET_c=6.00 mm d^{-1}, single ET_c=6.15 mm d^{-1} and measured ET_c=2.78 mm d^{-1}). In this case the model tends to overestimate the crop evapotranspiration, but, looking at the reference ET value on that day (ET_0), it is very high (ET_0=7.50 mm d^{-1}) and this could indicate or high temperature or high wind speed or an error during the weather data measurement or ET_0 calculation. Figure 62 represents the cumulative temporal graph for measured and simulated values for lettuce. Measured data are available only for a short period compared to the entire growing season. Nevertheless, the cumulative ET_c curves of measured and simulated data are comparable with good results. Cumulative ET_c for single and dual only differs for 3 mm (dual CET_c=371 mm, single CET_c=368 mm). The statistical tests confirm this partial congruence of measured and simulated data (Figures 63-64).

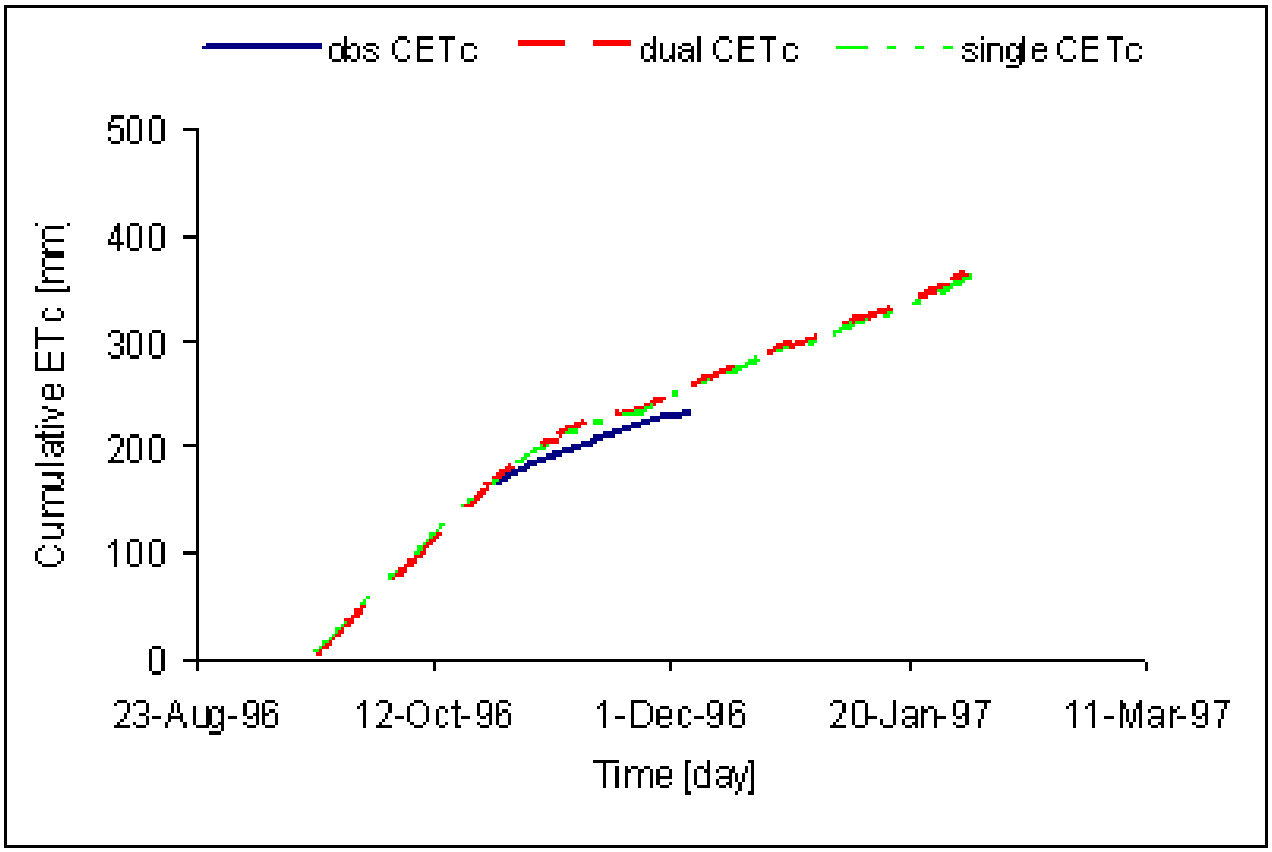

Figure 62 Temporal graph for measured, simulated dual and single cumulative ET_c for Lettuce (California, 1996).

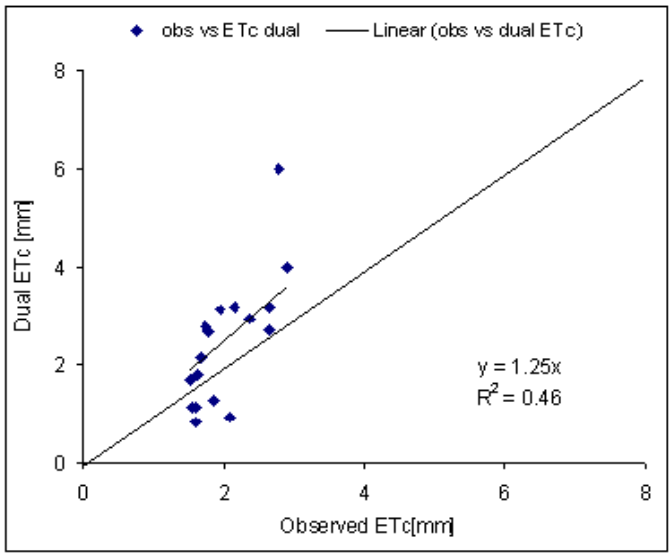

Figure 63 Scatter plot of measured versus simulated dual ET_c for lettuce (California, 1996).

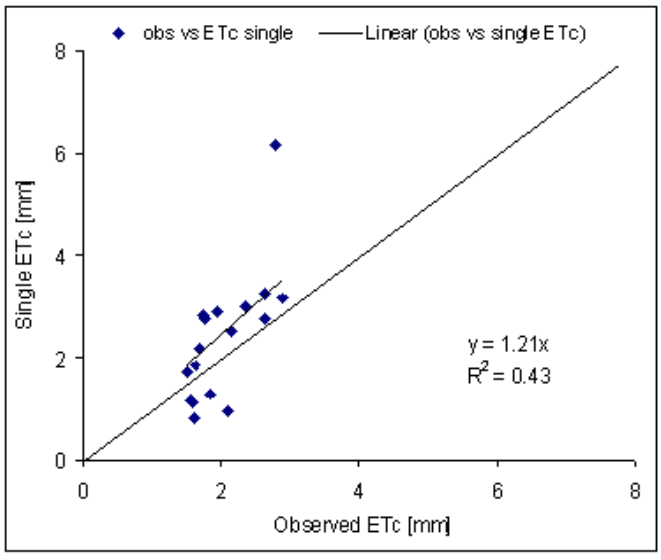

Figure 64 Scatter plot of measured versus simulated single ET_c for lettuce (California, 1996).

Figures 63-64 show the statistical results for measured against simulated 'dual' and 'single' ET_c values for lettuce. In this case the RMSE results were not good (dual ET_c=1.55 mm d^{-1}, single ET_c=1.53 mm d^{-1}). It is possible that the ET_0 estimate was in error on the date of the extreme values in Figure 61, which would explain the poor RMSE.

D) KIWIFRUIT

After having used the measured weather, $ET_{0,}$ soil and crop data as input, as described in Materials and Methods section, and run the KcMod program, simulated K_c, and ET_c values were tested against the measured ET_c values for kiwifruit orchard. Figure 65 shows the Kc curves of bare soil evaporation, FAO-56 table line, 'single' and 'dual' K_c simulated curves for Hayward kiwifruit, grown in Brisighella (Ravenna), Italy.

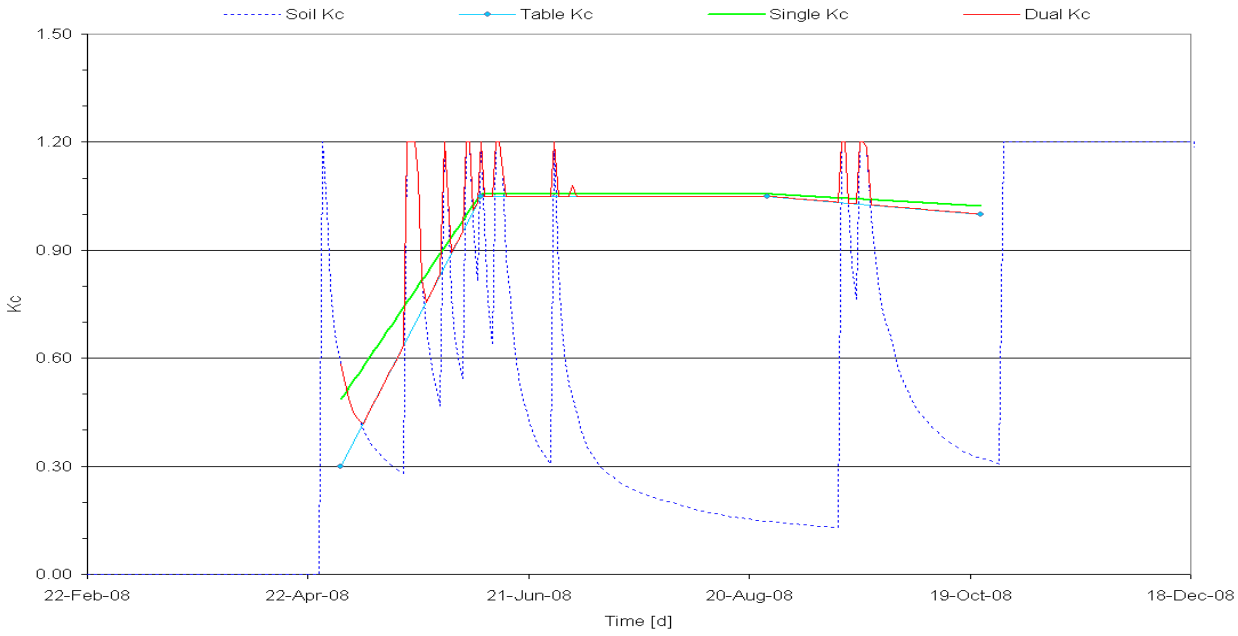

Figure 65 Simulated bare soil (blue dashed), FAO-56 Table Kc line (light blue), single Kc (green), and dual Kc (red) curves for kiwifruit, Brisighella (Italy, 2008).

The time period goes from end of April to end of October, 2008, because the rapid growth stage started after the gems breaking (end of March) and before the blooming (end of May), since kiwifruit is a type 3 deciduous crop, which means it loses leaves in the winter. The Table K_c range starts from 0.30 for the initial stage, it goes to 1.05 for the mid season and it equals 1.00 for the end season.

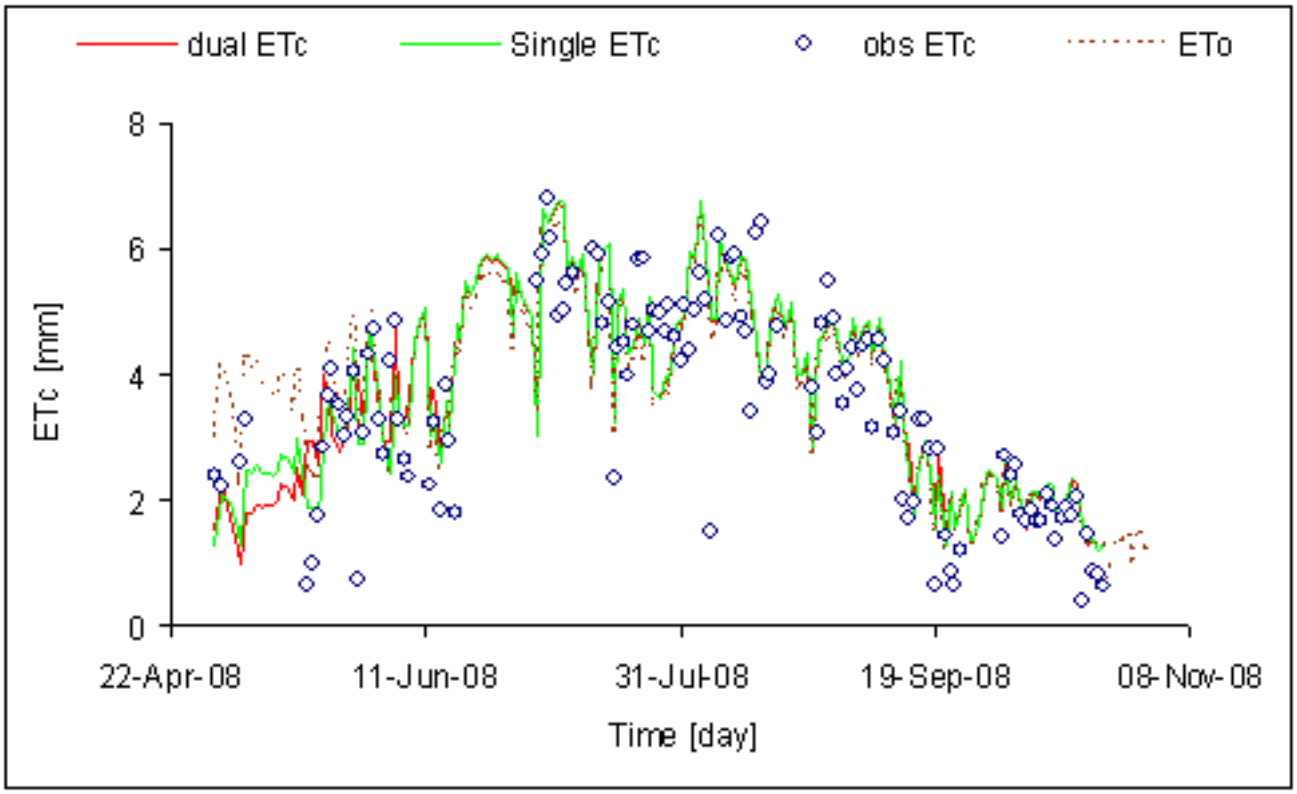

Figure 66 Temporal graph for ET_0 (brown) and ET_c graph for measured (blue), dual (red) and single (green) simulated values with ET_0 for Kiwifruit, (Italy, 2008).

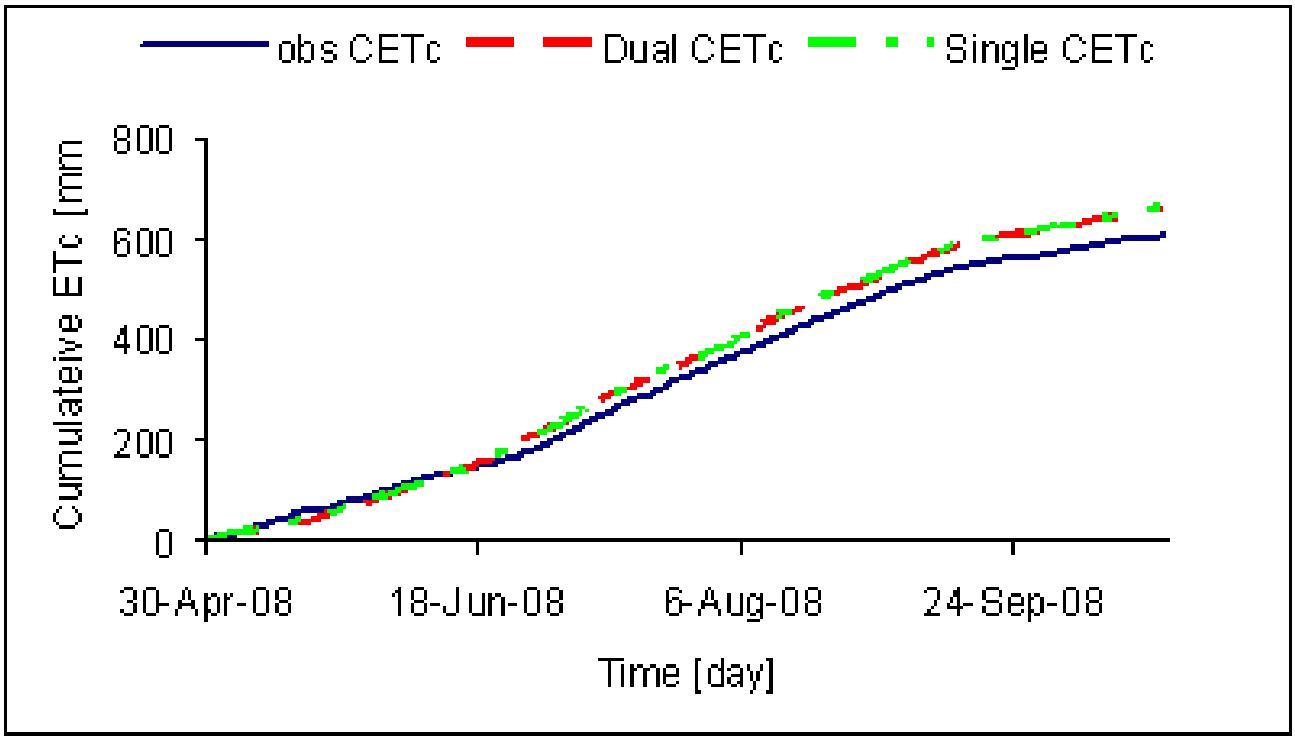

Figure 67 Temporal graph for measured, dual and single simulated cumulative ET_c for kiwifruit (Italy, 2008).

Figure 66 shows the temporal graphs for ET_c of kiwifruit, both for the measured, 'dual' and 'single' method. The two K_c curves are almost identical, except for the rapid growth period. The highest value occurred on July 5, and it corresponds to an irrigation event (dual ET_c=6.40 mm d^{-1}, single ET_c=6.44 mm d^{-1} and measured ET_c=6.81 mm d^{-1}). In general, there was good agreement between the models and the observed ET_c. Figure 67 shows the cumulative ET_c for kiwifruit. Between the simulated curves, dual and single methods are almost equivalent, with 3 mm d^{-1} of difference for the entire growing season (single CET_c=660 mm, dual CET_c=657 mm). The measured cumulative ET_c is comparable to simulated (measured CET_c=606 mm). The statistical tests confirm this good congruence of measured and simulated ET_c, in particular for single K_c method of calculation.

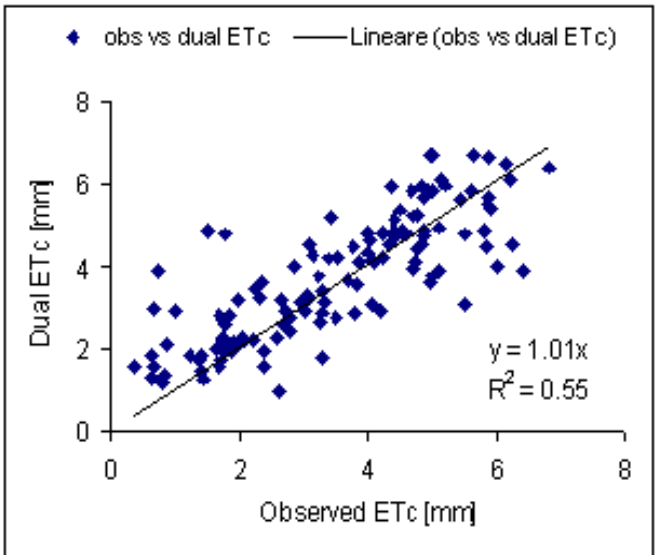

Figure 68 Scatter plot of measured versus simulated dual ET_c for kiwifruit (Italy, 2008).

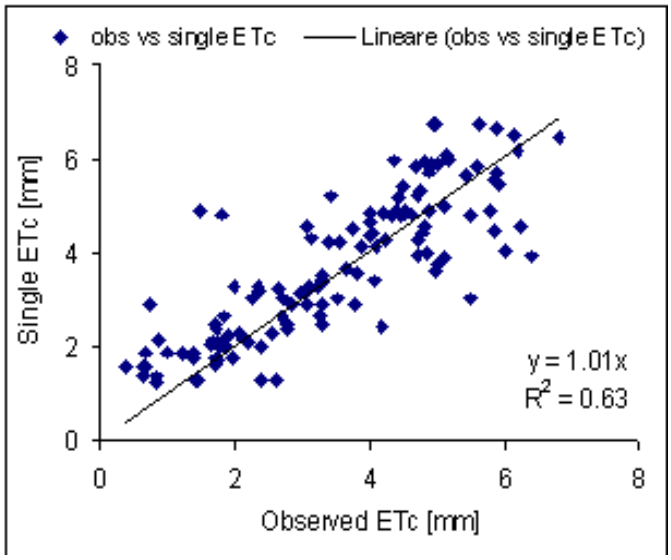

Figure 69 Scatter plot of measured versus simulated single ET_c for kiwifruit (Italy, 2008).

Figures 68-69 report the statistical results for measured against simulated 'dual' and 'single' ET_c values for kiwifruit. The RMSE test showed reasonably good agreement between the models and the observed ET_c (dual ET_c=1.00 mm d^{-1}, single ET_c=0.94 mm d^{-1}).

The statistical values resulting from the KcMod.xls validation are summerized in Table 13.

Table 13 Statistical values obtained from the KcMod validation for the different crops.

Figures	Location	Year	Crop	ET_C RMSE (mm d^{-1})	
				Dual	Single
38-39	Landriano, Italy	2006	maize	0.64	0.48
43-44	Landriano, Italy	2010	maize	1.25	1.80
48-49	Landriano, Italy	2011	maize	1.11	1.05
53-54	Livraga, Italy	2010	maize	0.57	1.27
58-59	Ventura, California	1995	broccoli	0.78	0.71
63-64	Imperial Vally, California	1996	lettuce	1.55	1.53
68-69	Brisighella, Italy	2008	kiwifruit	1.00	0.94
	Average RMSE			0.99	1.07

In general, the results were satisfying, because the RMSE were generally <1.0. In case of maize, grown in Landriano, Italy, in 2006, the single ET_c provided a results of RMSE<0.5. This indicates that the estimate of ET_c fells within 10% of the real value, which in term of evapotranspiration means an error less than 1 mm per day. Since the program was developed to simulate crop coefficients values and estimate crop evapotranspiration for very different climate and different types of crops, the results were good.

SUMMARY AND CONCLUSIONS

There is an increasing demand for research aimed at solving efficient water use issues at the farm and field level in order to advance practical solutions for wise use of irrigation water and to improve crop management in drought-prone regions. The crop coefficient (K_c) method is the most widespread approach to estimate crop evapotranspiration, but the K_c values in the literature vary dramatically depending on the location and climate characteristics.

Investigation of the FAO 56 K_{cmid} climate correction, which is based on wind speed, minimum relative humidity, and canopy height showed that the K_{cmid} increases when ET_0 increases even when the surface has the same canopy and aerodynamic resistance characteristics as the reference ET surface (i.e., $r_a=208/u_2$ and $r_c=70$). A surface with the same characteristics as the standardized reference surface should exhibit a $K_c=1.00$ regardless of the climate, so a new climate correction method is clearly needed. Using the same principle that was used to develop the standardized reference ET equation for tall canopies (Allen et al., 2005), a procedure was developed to adjust the midseason K_c values based on the ET_0 rate rather than on wind speed, minimum relative humidity, and canopy height. This method corrects for climate effects on K_c values, and canopies with the same characteristics as ET_0 will have K_c =1.00 regardless of the climate. A simple algorithm Eq. (49) was produced that relates all K_c corrections to the tabular crop coefficient (K_{ctab}) in a "base" climate with midseason ET_0=7.3 mm d^{-1}, which is typical for the climate where the Penman-Monteith equation was developed. Note that the correction applies only to crops with midseason during the summer. When Kcmid values are measured in a particular climate, Eq. (50) is used to convert from the experimentally observed midseason K_c values to tabular K_{ctab} values that are specific to a climate with ET_0=7.3 mm d^{-1}. Then, Eq. (49) will convert the tablular K_{ctab} values back to K_{cmid} values that apply in the climate where the experiment was conducted.

While the dual Kc method presented in FAO 56 provides a method to accurately determine crop coefficients, adoption and use of the method is minimal becaue of its complexity. On the other hand, the single Kc method presented in FAO 56 is simpler and widely adopted. The problem with the single Kc method is that it often does not account for local climate effects on ET_c, e.g., precipitation and irrigation frequency effects. Therefore, a new model "KcMod" for calculation of a single crop coefficient curve from a dual crop coefficient curve was developed to account for local climate and management while improving the accuracy by fitting the single K_c curve to the local calibrated dual K_c curve. Several crops were tested, and the cumulative ET_c curves from

the dual and single K_c methods were always similar and generally matched observations well. This should improve both the accuracy of ET_c estimation and farmer adoption. KcMod uses the root depth, soil water holding capacity, and the management allowable depletion to determine an irrigation schedule that is used to determine the dual Kc curve. Then, the single K_c curve is calculated from the dual crop coefficient curve using linear regression or cubic spline fitting.

KcMod was tested against measured data of different crop and different locations (Table 14). In general, the results were satisfying, because the average RMSE were 0.99 mm d^{-1} for the dual and 1.07 mm d^{-1} for the single method. In conclusion, the model provided good agreement between the dual and single K_c evapotranspiration estimates and measured data. In particular, the best results obtained for crops having mid season during summer were for maize (single method, ET_c RMSE=0.48 mm d^{-1}). Satisfying results were also obtained for the tree crop tested, which was kiwifruit (single method, ET_c RMSE=0.94 mm d^{-1}).

The use of the KcMod program permits more accurate irrigation scheduling by making single K_c curves better fit local climate conditions, which improves evapotranspiration estimates. This can improve water use efficiency without compromising yields and without wasting water resources. This method presents a new approach to increase the yield and stability of crops under drought conditions around the world. The method is likely to enhance food security in relation to climate change and increasing population.

A

Agrawal, M. K., Panda, S., N., Panigrahi, B., 2004. “Modeling water balance parameters for rainfed rice”. Journal of irrigation and drainage engineering ASCE /March /April, 2004. pp. 129-139.

Alcamo, J., Flörke, M. and Märker, M., 2007. “Future long-term changes in global water resources driven by socio-economic and climate changes”. Hydrol. Sci. J. 49(4), 549-562.

Allen, R. G., 2002. “Evapotranspiration: The FAO-56 Dual crop coefficient method and accuracy of predictions for project-wide evapotranspiration”. Paper presented at International meeting on Advances in Drip/Micro Irrigation, Tenerife.

Allen, R. G., and Pereira, L., S., 2009. “Estimating crop coefficients from fraction of ground cover and height”. Irrig Sci (28)17-34.

Allen, R.G., Pereira, L.S., Raes, D., and Smith, M., 1998. “Crop evapotranspiration. Guidelines for computing crop water requirements.” Irrig. & Drain. Paper No. 56, United Nations, FAO, Rome.

Allen, R. G., Pruitt, W. O., Raes, D., Smith, M., Pereira, L. S., 2005. „Estimating evaporation from bare soil and the crop coefficient fort he initial period using common soils information.“ Journal of irrigation and drainage engineering, ASCE/January/February, 14-23.

Allen, R.G., Walter, I.A., Elliott, R.L., Howell, T.A., Itenfisu, D., Jensen, M.E., and Snyder, R.L,. 2005. “The ASCE Standardized Reference Evapotranspiration Equation.” Amer. Soc. of Civil Eng., Reston, Virginia. 173 p.

Alshammary, S. F., Qian, S. J., Y. L., Wallner, S., J., 2004. “Growth response of four turfgrass species to salinity”. Agricultural Water Management (66) 97-111.

Amayreh, J., Al-Abed, N., 2005. “Developing crop coefficients for field-grown tomato (Lycopersicon esculentum Mill.) under drip irrigation with black plastic mulch”. Agricultural Water Management (73) 247-254

Anconelli, S., Mannini, P., Rossi, F., 2009. “Bilancio energetico e scambio di CO_2, i risultati di uno studio sul kiwi”. Water Scarcity and Desertification, ARPA Journal, May June 2009.

Ayars, J. E., Hutmacher, R. B., 1994. “Crop coefficients for irrigating cotton in the presence of groundwater”. Irrig Sci (15) 45-52.

B

Bandyopadhyay, P. K. and Mallik, S., 2003. “Actual evapotraspiration and crop coefficients of wheat (Triticum Aestivum) under varying moisture levels of humid tropical canal command area”. Agricultural Water management (59) 33-47

Bandyopadhyay, P. K., Mallik, S., Rana, S. K., 2003. “Actual evapotranspiration and crop coefficients of onion (Allium cepa L.) under varying soil moisture levels in the humid tropics of India”. Trop. Agric. (Trinidad) (80), April, pp. 83-90.

Barnett, J. and Adger, W. N., 2007. “Climate change, human security and violent conflict”.

Bazzaz, F.., Harvard University, Cambridge, MA, USA, and Sombroek, W., 1996. “Global climate change and agricultural production. Direct and indirect effects of changing hydrological, pedological and plant physiological processes”. FAO, Rome, Italy, and Wiley, J., & Sons Publisher

Bonciarelli, F., 1989. “Fondamenti di agronomia generale”, Edagricole, Bologna

Borrelli, J., Fedler, C, B., Gregory, J., M., 1998. “Mean Crop Consumptive Use and Free-Water Evaporation for Texas”. Texas Water Development Board Grant, February 1, 95-137

Brown, P. W., Mancino, C., F., Young, M., H., Thompson, T., L.., Wierenga, P. J., Kopec, D., 2001. “Penman Monteith Crop Coefficients for use with desert turf systems”. Crop Science (41) 1197-1206.

Bryla, D. R., Banuelos, G., S., Mitchell, J., P., USDA, ARS, 2003. “Water requirements of subsurface drip-irrigated faba bean in California”. Irrigation science. May, (22) p. 31-37

Buckman, H. O., and Brady, N. C., 1960.”The nature and property of soils – A challenge text of Edaphology (6^{th} ed.), New York: MacMillan, NY.

Burt, C. M., Mutziger, A.J., Allen, R. G., Howell, T. A., 2005. „Evaporation research: review and interpretation“. Journal of Irrigation and Drainage Engineering, ASCE, January/February 37-58.

C

Cahn, M., D.,Snyder, R., L., Hanson, B. R., 1999. “Estimating evapotranspiration in processing tomatoes”. Part 2. Proc. Workshop on Irrigation and Fertigation of Processing Tomato, Ed. B. J. Bièche, Acta Hort. 487, ISHS, pp. 493-497

Carr, M. K. V., 2001. “The water relations and irrigation requirements of coffee”. Expl Agric., (37), pp.1-36

Castellvì, F., Snyder, R., L., Baldocchi, D., D., 2008. “Surface energy-balance closure over rangeland grass using the eddy covariance method and surface renewal analysis”.Agricultural and Forest Meteorology (148) 1147-1160

Cayan, D. Luers, A. L., Hanemann, M. and Franco, G., 2006. “Scenarios of climate change in California: An overview”. California Energy Commission, CEC-500-2005-186-SF

CEC, European Commission, 2009. “Impact Assessment, Commission Staff Working Document accompanying the White Paper on Adapting to Climate Change: Towards a European Framework for Action” (147 final), SEC 387/2, Brussels

Chanzy, A., 2003. “Evaporation from soils”. Encyclopedia of waterscience, DOI: 10.1081/E-Ews 120010071.

Chaouche, K. Neppel, L., Dieulin, C., Pujol, N., Ladouche, B., Martin, E., Salas, D., Caballero, Y., 2010. “Analyses of precipitation, temperature, and evapotranspiration in a French Mediterranean region in the context of climate change”. Comptes Rendus Geoscience, 342, (3) 234-243

Chatzidaki, E., Ventura, F., 2010. “Adaptation to climate change and mitigation strategies in cultivated and natural environments. A review”. Italian Journal of Agrometeorology, 20(3) 21-38.

D

De Medeiros, G. A., Arruda, F., B., Sakai, E., Fujiwara, M., 2001. “The influence of crop canopy on evapotranspiration and crop coefficient of beans”. Agricultural Water management (49) 211-224

De Santa Olalla, F. M., Domínguez-Padilla, A., López, R., 2004. “Production and quality of the onion crop (Allium cepa L.) cultivated under controlled deficit irrigation conditions in a semi-arid climate”. Agricultural Water Management (68) 77-89

Duce, P., Spano, D., Snyder, R., L., and Pau U, K., T., 1997. “Surface renewal estimates of evapotranspiration”. Short canopies. Acta Hort. (449) 63-68

E

EEA, 2006. Vulnerability and adaptation to climate change in Europe. Technical report No 7. European Environmental Agency, pp. 84

EEA, 2008. Impacts of Europe’s changing climate – 2008 indicator based assessment. Report No. 4. European Environmental Agency, pp. 19

Entekhabi, D., Reichle, R. H., Koster, R. D., & Crow, W. T. (2010). Performance metrics for soil moisture retrievals and application requirements. Journal of Hydrometeorolgy, 11, 832–840.

F

Fabeiro, C., Martin De Santa Olalla, F. Lopez, R., Dominguez, A., 2003. “Production and quality of the sugar beet (Beta vulgaris L.) cultivated under controlled deficit irrigation conditions in a semi-arid climate”. Agricultural Water Management (62) 215-227

FAO, 2003. “Agriculture, food and water. A contribution to the World Water Development Report”. World water assessment Porgramme, UNESCO-WWAP

FAO, 2011. “The State of food insecurity in the World”.

Farquhar, G.D., Schulze, E.-D. and Küppers, M., 1980. “Responses to humidity by stomata of Nicotiana glauca L. and Corylus avellana L. are consistent with the optimization of carbon dioxide uptake with respect to water loss”. Austr. J. Plant Physiol. (7) 315-327

Fereres, E. and Soriano, M. A., 2006. “Integrated Approaches to Sustain and Improve Plant Production under Drought Stress.” Journal of Experimental Botany, (58)147–159, doi:10.1093/jxb/erl165 Advance Access publication 6 November

G

Gallardo, M., Snyder, R. L., Schulbach, Jackson, L., E., 1996, “Crop growth and water use model for lettuce”. Journal of Irrigation and Drainage engineering /November/ December, pp. 354-359

Gates, D., M., 1980. “Biophysical ecology”. Springler-verlag, New York Heidelberg Berlin

Gavin, H. and Agnew, C., A., 2004. “Modelling actual, reference and equilibrium evaporation from a temperature wet grassland”. Hydrol Process (18) 229-246. Published online in Wiley InterScience (www.interscience.wiley.com). DOI:10.1002/hyp.1372

GCOS (Global Climate Observing System, 2010. “Implementation plan for the global observing system for climate in support of the UNFCCC”. GOOS-184, GTOS-76, WMO-TD/No. 1523)

Giardini L., 2002. “Agronomia generale, ambientale ed aziendale”. V edizione, Patron, Bologna

Girona, J., Marsal, J., Mata., M., Del Campo, J., 2004. “Pear crop coefficients obtained in a large weighing lysimeter”. IVth IS on Irrigation of Hort. Crops, Ed. R. L. Snyder Acta Hort. 664, ISHS, pp. 277-281

Gleick, P.H. 1996. "Basic water requirements for human activities: Meeting basic needs." Water International Vol. 21, No. 2, pp. 83-92.

Goudriaan , J. and Unsworth, M.H., 1990. Implications of increasing carbon dioxide and climate change for agricultural productivity and water resources. Impact of Carbon Dioxide, Trace Gases, and Climate Change on Global Agriculture. ASA Spec. Pub No. 53. pp. 111-130

Grattan, S., R., Bowers, W., Dong, A., Snydder, R., L., Carrol, J., J., George, W., 1998. “New crop coefficients estimate water use of vegetables, row crops”, California Agriculture, (52), January-February, pp. 16-21

H

Haeblerli, W., Beniston, M., 1998. “Climate change and its impacts on glaciers and permafrost in the Alps”. Ambio,(27) 258-265.

Haileslassie, A., Blümmel, M., Clement, F., Descheemaeker, K., Amede, T., Samireddypalle, A., Acharya, N. S., Radha, V., Ishaq, S., Samad, M., Murty, M. V. R. and Khan, M. A. (2011). Assessment of the livestock-feed and water nexus across a mixed crop livestock systems intensification gradient: An example from the Indo-Ganga basin. Experimental Agriculture 47 (Suppl. 1): 113–1

Hanson , B., Putnam, D., Snyder, R., L., 2007. “Deficit irrigation of alfalfa as a strategy for providing water-short areas”. Agricultural Water Management (93) 73-80

Hanson, B., May, D., Voss, R., Cantwell, M., Rice, R., 2003. “Response of garlic to irrigation water”. Agricultural Water Management (58) 29-43

Higbie, R., 1935. “The rate of absorption of a pure gas into a still liquid during short periods of exposure”. Trans. Am. Inst. Chem. Eng. (31) 365-388

Hillel, D., 2003.“Introduction to Environmental Soil Physics”. Elsevier, Academic Press, University of Massachussetts.

Hollinger, D.Y., Kelliher, F.M., Schulze, E.-D. and Köstner, B.M.M.,1994. „Coupling of tree transpiration to atmospheric turbulence”. Nature (371) 60-62

Houser, P. R., De Lannoy, G., & Walker, J. P. (2010). Land surface data assimilation. In W. Lahoz, B. Khatattov, & R. Menard (Eds.), Data assimilation: Making sense of observations (pp. 549–598). The Netherlands: Springer.

Howell, T. A., Evett, S., R., Tolk, J., A., Schneider, A., D., 2004. “Evapotranspiration of Full-, Deficit-Irrigated, and Dryland Cotton on the Northern Texas High Plains”. Journal of Irrigation and Drainage Engineering ASCE/July/August, 277-285

Howell, T. A., Ziska, L. H., McCormick, R., L., Burtch, L., M., Fischer, B., B., 1987. “Response of sugar beet to irrigation frequency and cutoff on a clay loam soil”. Irrig Sci (8) 1-11

Hunsaker, D. J., 1999. “Basal crop coefficients and water use for early maturity cotton”. Transaction of the ASAE, American Society of Agricultural Engineers, July, Vol. (42) 927-936

Hunsaker, D. J., Pinter, P., J., Jr., Barnes, E., M., Kimball, B., A., 2003. “Estimating cotton evapotranspiration crop coefficients with a multispectral vegetation index”. Irrig Sci (22) 95-104 DOI 10.1007/s00271-003-0074-6

Hunsaker, D., J., Pinter, P., J., Jr., Cai, H., 2002. “Alfalfa Basal Crop Coefficients for FAO-56 Procedures in the Desert Regions of the SouthWestern U.S.”. Transaction of the ASAE, American Society of Agricultural Engineers ISSN 0001-2351, Vol. 45(6)1799-1815

I

Inman-Bamber, N. G., 2004. “Sugarcane water stress criteria for irrigation and drying off”. Field Crops research, (89)107-122, doi:10.1016/j.fcr. 01.018

Inman-Bamber, N. G., McGlinchey, M., G., 2003. “Crop coefficients and water-use estimates for sugarcane based on long-term Bowen ratio energy balance measurements”. Field Crops Research (83)125-138, DOI: 10.1016/S0378-4290(03)00069-8

Irmak, S., 2005. “Crop evapotranspiration and crop coefficients of Viburnum Odoratissimum (Ker.-Gawl)”. Applied Engineering in Agriculture, American Society of Agricultural Engineers ISSN 0883-8542, Vol. 21(3) 371-381

IPCC Expert Meeting Report - Towards New Scenarios for Analysis of Emissions, Climate Change, Impacts, and Response Strategies Noordwijkerhout, The Netherlands, 19-21 September 2007

J

Jacobs, C.M.J., 1994. “Direct Impact of Atmospheric CO2 Enrichment on Regional Transpiration”. Thesis. Wageningen Agricultural University. 179 pp

Jagtap, S. S., and Jones, J. W., 1989. “Stability of crop coefficients under different climate and irrigation management practices”. Irrigation Science, 10:231-244.

Jackson R.B., Sala, O. E., Field, C. B., Mooney, H. A., 1994. “CO2 alters water use, carbon gain, and yield for the dominant species in a natural grassland. Oecologia, Volume 98, Issue3-4, pp 257-262.

Jackson, RB, SR Carpenter, CN Dahm, DM McKnight, RJ Naiman, SL Postel, and SW Running. 2001. Water in a changing world. Ecological Applications 11:1027-1045

Jensen, J., R., 2007. “Remote sensing of the environment. An Earth resource perspective.” Prentice Hall Series in Geographic Information Science, II edition. Keith C. Clarke, Series Editor, 592 pp

Johnson, R. S., Ayars, J., Hsiao, T., 2004. “Improving a model for predicting peach tree evapotranspiration”. Acta Horticulture, (664) 341-346

K

Kadayifci, A., Tuylu, G., I., Ucar, Y., Cakmak, B., 2005. “Crop water use and water use of onion (Allium cepa L.) in Turkey”, Agricultural Water Manegement (72) 59-68

Kang, S., Gu, B., Du, T., Zhang, J., 2003. “Crop coefficient and ratio of transpiration to evapotranspiration of winter wheat and maize in a semi-humid region”. Agricultural Water management (59) 239-254

Kang, Y., Wang, F.-X. Liu, H.-J., Yuan, B.-Z., 2004. “Potato evapotranspiration and yield under different drip irrigation regimes”. irrigation Science, Springer-Verlag GmbH, ISSN: 0342 (Paper), 133-143

Kanton, R., A., L. and Dennett, M. D., 2004. “Water uptake and use by morphologically contrasting maize/pea cultivars in sole and intercrops in temperate conditions”. Expl Agric. (40) 201-214, Cambridge University Press. DOI: 10.1017/S0014479703001571

Kashyap, P. S. and Panda, R., K., 2003. “Effects of irrigation scheduling on potato crop parameters under water stressed conditions”. Agricultural Water Management (59) 49-66

Kashyap, P. S., and Panda, R., K., 2001. “Evaluation of evapotranspiration estimation methods and development of crop-coefficients for potato crop in a sub-humid region”. Agricultural Water Management (50) 9-25

Kerr, Y. H.,Waldteufel, P.,Wigneron, J. P., Delwart, S., Cabot, F., Boutin, J., Escorihuela,M. J., Font, J., Reul,N., Gruhier, C., Juglea, S. E., Drinkwater, M. R.,Hahne, A., Martín-Neira,M., & Mecklenburg, S., 2010. “The SMOSmission: New tool for monitoring key elements of the global water cycle”. Proceedings of the IEEE, 98(5), 666–687

Kimball, B.A., Mauney, J.R., Nakayama, F.S. and Idso, S.B. 1993. “Effects of increasing atmospheric CO2 on vegetation”. Vegetation (104/105) 65-75.

Kimball, B.A., Pinter, P.J. Jr., Garcia, R.L., LaMorte, R.L., Wall, G.W., Hunsaker, D.J., Wechsung, G., Wechsung, F. and Kartschall, Th., 1995. “Productivity and water use of wheat under free-air CO2 enrichment”. Global Change Biology 1 (6) 429-442.

Kipkorir, E. C. and Raes, D., 2002. “Transformation of yield response factor into Jensen's sensitivity index”. Irrigation and Drainage systems 16. Kluwer Academic Publishers, 47-52

Klenzendorf, B, 2008. “Effect of climate change on hydrologic cycle: the future of Lake Maend”. Final report

Kundzewicz, Z., W., 2001. “Water Problems of Central and Eastern Europe–A Region in Transition”. Hydrological Sciences Journal 46 (6) 896 - 909

Kuo, S. F., Ho, S.-S., Liu, C.-W., 2006. “Estimation irrigation water requirements with derived crop coefficients for upland and paddy crops in Chia Nan Irrigation Association, Taiwan”. Agricultural Water Management (82) 433-451

L

Lage, M., Bamouh, A., Karrou, M., El Mourid, M., 2003. “Estimation of rice evapotranspiration using microlysimeter technique and comparison with FAO Penman-Monteith and pan evaporation methods under maroccan conditions”. Agronomic (23) 625-631 INRA, EDP sciences, DOI: 10.1051/agro: 2003040

Lascano, R., J., et al., 2000. “A general system to measure and calculate daily crop water use”, Agronomy Journal, 92, pp. 821–832

Leuning, R., 1995. “A critical appraisal of a combined stomatal-photosynthetic model for C3 plants”. Plant Cell Environ. (18) 339-355

Long, S.P., Ainsworth, E.A., Rogers, A. and Ort, D.R., 2004. “Rising atmospheric carbon dioxide: plants FACE the future”. Ann. Rev. Plant Biol. (55) 591-628

Lopez-Urrea, R., F. Martın de Santa Olalla, A. Montoro, P. Lopez-Fuster, 2009. “Single and dual crop coefficients and water requirements for onion (Allium cepa L.) under semiarid conditions.” Agricultural Water Management (96) 1031–1036

Lourence, F.J. and Pruitt, W., O., 1971. “Energy balance and water use of rice grown in the Central Valley of California.” Agron. J., 827-832

Lovelli, S., Pizza, S., Caponio, T., Rivelli, A. R., Perniola, M., 2005. “Lysimetric determination of muskmelon crop coefficients cultivated under plastic mulches”. Agricultural Water Management (72) 147-159

M

Mao, Z., Dong, B., Pereira, L., S., 2004. “Assessement and water saving issues for Ningxia paddies, upper Yellow River Basin”. Paddy Water Environ (2) 99-110 DOI 10.1007/s10333-004-0048-1

Matzneller P., Ventura F., Gaspari N., Rossi Pisa P., 2010. “Analysis of trends in a long term agrometeorological data set in Bologna (Italy), Climatic change, 100 (3-4) 717-731

McKenney, M.S. and Rosenberg, N.J., 1993. “Sensitivity of some potential evapotranspiration estimation methods to climate change”. Agric. For. Meteorol. (64)81-110

McKenzie, R., H., Middleton, A., B., Flore, N., Bremer, E., 2004. “Evapotranspiration efficiency of pea in south and central Alberta”. Canadian Journal of Plant Science, 84(2) 473-476, 10.4141/P03-021

McNaughton , K.G., 1994. ”Effective stomatal and boundary-layer resistances of heterogeneous surfaces”. Plant Cell Environ. (17)1061-1068

McNaughton, K.G. and Jarvis, P.G., 1991. “Effects of spatial scale on stomatal control of transpiration”. Agric. For. Meteorol. (54) 279-301

Monteith, J. L., 1965. “Evaporation and Environment”. 19th Symposia of the Society for Experimental Biology, University Press, Cambridge (19) 205-234

Monteith, J., L. and Unsworth, M., H., 1990. “Principles of environmental Physics”. Second edition, Edward Arnold

Moore, J. L., King, J., P., Bawazir, A., S., Sammis, T., W., 2004. “A bibliography of evapotranspiration with special emphasis on riparian vegetation”. WRRI Miscellaneous Report No. M28, Account No. 01-4-23955

Morison, J,. I., L., and Gifford, R. M., 1983. “Stomatal sensitivity to carbon dioxide and humidity”. Plant Physiol. (71) 789 – 796

Morison, J., I., L., 1987. “Intercellular CO2 concentration and stomatal response to CO2”. In: Stomatal Function. E. Zeiger, G.D. Farquhar and I.R. Cowan (eds.). Stanford Univ. Press, California, 229-251

Mott, K.A. 1990. “Sensing of atmospheric CO2 by plants”. Plant, Cell Environ (13) 731-737

Mutziger, A. J., Burt, C. M., Howes, D. J., Allen, R. G., 2005. “Comparison of measured and FAO-56 modeled evaporation from bare soil“. Journal of Irrigation and Drainage Engineerig, DOI: 1061/(ASCE)0733-9437(2005)131:1(59)

N

Nelson, D., Adger, W. N. and Brown, K., 2007. “Adaptation to environmental change: contributions of a resilience framework. Annual Review of Environment and Resources. (32) 395–419

Nicolas, E., Torrecillas, A., Ortuño, M., F., Domingo, R., Alarcón, J., J., 2005, “Evaluation of transpiration in adult apricot trees from sap flow measurements”. Agricultural Water management (72) 131-145

O

Oke, T., R., 1978. “Boundary layer climates”. London, Methuen, XXI, 372

Olesen, J.E.; Carter, T.R.; Diaz-Ambrona, C.H.; Fronzek, S.; Heidmann, T.; Hickler, T.; Holt, T.; Minguez, M.I.; Morales, P.; Palutikof, J.; Quemada, M.; Ruiz-Ramos, M.; Rubk, G.; Sau, F.; Smith, B.; Sykes, M.: Uncertainties in projected impacts of climate change on European agriculture and terrestrial ecosystems based on scenarios from regional climate models.. Climatic Change, 81: 123-143

Onder, S., Caliskan, M., E., Onder, D., Caliskan, S., 2005. “Different irrigation methods and water stress effects on potato yield and yield components”. Agricultural Watr Menegament (73) 73-86

P

Parkes, M.,Jian, W., Knowles, R., 2005. “Peak crop coefficient values for Shaanxi, North-west China”. Agricultural Water management (73)149-168

Parry M. L., Arnell, N. W., Beniston, M., Berz, G., Bindi, M., Brander, K., Carter, T., Cramer, W. [et al.] 2000. “Assesment of potential effects and adaptations for climate change in Europe: the Europe ACACIA Project – summary and conclusions. Jackson Environment Insitute, University of East Anglia

Parry, M. L., C. Rosenzweig, A. Iglesias, G. Fischer, and M. Livermore. 1999. "Climate change and world food security: A new assessment," Global Environmental Change, Vol. (9)S51-S67 Suppl. 1, October

Parry, M., Keys, A.,J., Gutteridge, S., 1989. “Variation in the specificity factor of C3 higher plant Rubisco determined by the total consumption of ribulose-P-2”. Journal of Experimental Botany (40) 317–320.

Paw U, K., T., and Brunet, Y., 1991. “A surface renewal measure of sensible heat flux”. 52-53. In Preprints, 20th Conf. on Agricultural and Forest Meteorology, Salt Lake City, UT. Sept. 10-13, Am. Meteorol. Soc., Boston

Paw U, K., T., Qiu, J., Su, H., B., Watanabe, T., and Brunet, Y., 1995. “Surface renewal analysis: a new method to obtain scalar fluxes without velocity data.” Agric. For. Meteorol. (74) 119-137

Paw U, K.T., Snyder, R.L., Spano, D. and Su H.-B., 2005. “Surface renewal estimates of scalar exchange.” In: Hatfeld JL and Baker JM (eds.) Micrometeorology in Agricultural Systems. Agronomy Monograph. No. (47) 455-483.

Peacock, C. E:, and Hess, T. M., 2004. “Estimating evapotranspiration from a reed bed using the Bowen ratio energy balance method”. Hydrological processes, 18, 247-260.

Pelter, G. Q., Mittelstadt, R., Leib, B., G., Redulla, C., A., 2004. “Effects of water stress at specific growth stages on onion bulb yield and quality”, Agricultural Water Management (68) 107-115

Pereira L.S., Cordery I., Iacovisdes I. 2002. “Coping with water scarcity.UNESCO, IHP_VI, Technical Documents in Hidrology n.58, Paris

Pereira L.S., 2004. “Trends for Irrigated Agriculture in the Mediterranean Region: coping with water scarcity. European Water 7/8:47-64, E.W. Publications

Peters-Lidard, C., D., 1998. “The Effect of Soil Thermal Conductivity Parameterization on Surface Energy Fluxes and Temperatures”. 1 April American Meteorological Society, vol. (55)1209-1224

Prasanna, H. G., Chavez, J. L., Colaizzi, P. D., Evett, S. R., Howell, T. A., Tolk, J. A., 2008. “ET mapping for agricultural water management: present status challenges”. Irrig Sci, 26:223-237.

Prentice I, Farquhar G, Fasham M, Goulden M, Heinmann M., 2001. The carbon cycle and atmospheric carbon dioxide. In Climate Change 2001: The Scientific Basis. Contributions of Working Group I to the Third Assessment Report of the Intergovernmental Panel on Climate Change, ed. JT Houghton, Y Ding, DJ Griggs, M Noguer, PJ van der Linden, et al., 183–238. Cambridge, UK: Cambridge Univ. Press

Pruitt, W.O., Lourence, F., J., Von Oettingen, S., 1972. “Water used by crops as affected by climate and plant factors”. California Agriculture, October

R

Rana, G., 2001. “Evapotranspiration of sweet sorghum: A general model and multilocal validity in semiarid environmental conditions”. Resources, (32) 395-419

Roderick and Farquhar, 2002. “The cause of decreased pan evaporation over the past 50 years”. Science (298) 1410-1411.

Rotmans, J., Hulme, M., and Downing, T., E., 1994. “Climate change implications for Europe: an application of the ESCAPE model“. Global Env. Change (4) 97-124

S

Sammis, T. W., Mexal, J., G., Miller, D., 2004. “Evapotranspiration of flood-irrigated pecans”, Agricultural Water management (69)179-190

Sarr, B., Lecoeur, J., Clouvel, P., 2004. “Irrigation scheduling of confectionery groundnut (arachis hypogeaea L.) in Senegal using a simple water balance model”. Agricultural Water Management (67) 201-220

Scorer, R., S., 1997. “Dynamics of meteorology and climate”. Wiley-Praxis Series In Atmospheric Physics, 686

Shaha, S. B., Edling, R., L., Member, ASCE, 2000. “Daily evapotranspiration prediction from Louisiana flooded rice field”. Journal of Irrigation and Drainage Engineerig/January/February

Shapland T., “Improvements to the surface renewal method for vineyard evapotranspiration measurement”. Dissertation research proposal, unpublished.

Shapland T.M., McElrone, Paw U, K. T., Snyder; R.L., unpublished. “A turnkey data logger program for fiel-scale energy flux density measurments using Eddy Covariance and surface renewal”.

Shaw and Snyder, R. L., 2003. “Evaporation and eddy covariance”. In: Encyclopedia of Water Science. Stewart, B.A. and Howell, T. (Eds.). Marcel Dekker Inc., New York. Marcel Dekker Inc., New York. DOI: 10.1081/E-EWS 120010306

Shaw, D. A., Pittenger, D., R., 2003. “Performance of landscape ornamentals given irrigation treatments based on reference evapotranspiration”. ISHS Acta Horticulture 664: IV International Symposium on Irrigation of Horticultural Crops

Şimşek, M., Tonkaz, T., Kaçira, M., Çömlekçioğlu, N., Doğan, Z., 2005. “The effects of different irrigation regimes on cucumber yield and yield characteristics under open field conditions”, Agricultural Water Management (73)173-191

Sinclair, T., 2003. “Transpiration”, Encyclopedia of water science, DOI:10.1081/E-EWS 120010277”

Smeal, D., 2001. “Turfgrass ET and Kc at Farmington, New Mexico”, New Mexico State University, Agricultural Science Center at Farmington, ppt

Snyder, R. L., Bali, K., Ventura, F., Gomez-MacPherson, H., 2000. “Estimating evaporation from bare or nearly bare soil”. Journal of Irrigation and Drainage Engineerig/November/December/2000/399-403.

Snyder, R. L., Moratiel, R., Song, Z., Swelam, A., Jomaa, I., Shapland, T., 2011. “Evapotranspiration response to climate change”. Presented at the 28th International Horticulture Conference, Lisbon, Portugal, August 22-27, Acta Horticulturae Tetens, O. 1930. Uber einige meteorolgische. Begriffe, Zeitschrift fur Geophysik. (6) 297-309

Snyder, R., L., Spano, D., and Paw U, K., T., 1996. Surface renewal analysis for sensible and latent heat flux density. Bound.-Layer Meteorol. (77) 249-266

Snyder, R.L., and Pruitt, W.O., 1992. “Evapotranspiration Data Management in California”, Proc., Water Forum '92 - Irrig. & Drain. Session, ASCE, New York, N.Y.

Soppe, R.W. O., and Ayars, J., E., 2003. “Characterizing ground water use by safflower using weighing lysimeters”. Agricultural Water management (60) 59-71

Spano, D., Snyder, R., L., Duce, P., Paw U, K., T., 1997b. Surface renewal analysis for sensible heat flux density using structure functions. Agric. For. Meteorol. (86) 259-271

Spano, D., Snyder, R., L., Duce, P., Paw U., K., T., 2000. Estimating sensible and latent heat flux densities from grapevine canopies using surface renewal. Agric. Fores Meteorol. (104) 171-183

Stanghellini, C. and Bunce, J.A., 1994. “Response of photosynthesis and conductance to light, CO2, temperature and humidity in tomato plants acclimated to ambient and elevated CO2 “ Photosynthetica (29) 487-497

Steduto, P., Hsiao, T., 1998. “ Maize canopies under two soil water regimes II. Seasonal trends of evapotranspiration, carbon dioxide assimilation and canopy conductance, and as related to leaf area index. Agricultural and forest Meteorology (89) 185-200

Stull, R., B., 1984. “Transilient turbulence theory: 1. The concept of eddy-mixing across finite distances”. J. Atmos. Sci. (41) 3351-3367

Stull, R., B., 1988. “An introduction to boundary layer meteorology”. Kluwer Academic Publ., the Netherlands

Suleiman, A. A., C.M.T. Soler, and G. Hoogenboom, 2007. “Evaluation of FAO-56 crop coefficient procedures for deficit irrigation management of cotton in a humid climate”, Agric. Water Manage. (91) 33-42

Suyker, A. E. and Verma, S., B., 2009. “Evapotranspiration of irrigated and rainfed maize-soybean cropping systems”. Agricultural and Forest Meteorology (149) 443-452. ISSN: 01681923 DOI: 10.1016/j.agrformet.2008.09.010

T

Tennakoon, S. B.,Milroy, S., P., 2003. “Crop water use and water use efficiency on irrigated cotton farms in Australia”. Agricultural Water management (61) 179-194

Testi, L., Villalobos, F., J., Orgaz, F., 2000. “Transpiration in relation to aerodynamic and canopy conductance of a developing olive (Olea europea L.) orchard”. European Journal of Agronomy (13) 155-163

Testi, L., Villalobos, F., J., Orgaz, F., 2004. “Evapotranspiration of young irrigated olive orchard in southern Spain”. Agricultural and Forest Meteorology (121) 1-18

Tolk, J., A., Evett, S., R., Howell, T., A., 2006. “Advection Influences on Evapotranspiration of Alfalfa in a semiarid climate”. Agron. Journal (98) 1646-1654, Agroclimatology, doi: 10.2134/agronj2006.0031

Tolk, J.A., and Howell, T., A., 2001. “Measured and simulated evapotranspiration of grain sorghum grown with full and limited irrigation in three high plains soils”. Transaction of the ASAE, American Society of Agricultural engineers ISSN 0001-2351, 44(6)1553-1558

Towler, B. W., Cahoon, J. E., Stein, O. R, 2004. “Evapotranspiration crop coefficients for cattail and bulrush”. Journal of hydrologic engineering, DOY: 10.1061/(ASCE)1084-0699(2004)9:3(235).

Trout, T. J., and Gartung, G., 2004. “Irrigation water requirements of strawberries”. Ivth IS on Irrigation of Hort. Crops, Acta Hort. 664, ISHS

Tubiello, F. N., Soussana J-F., Howden S. M., and Easterling, W., 2007. “Crop and pasture response to climate change.” Proc. Natl. Acad. Sci., (104) 19686-19690, doi:10.1073/pnas.0701728104

Twine, T. E:, Kustas, W.P., Norman,J., M., Cook, D. R., Houser P. R., Meyers P R., Prueger J. H., Starks P. J., and Wesley M. L., 2000.”Correcting eddy-covariance flux underestimates over a grassland”. Agricultural and Forest Meteorology 103 (2000) 279–300

Tyagi, N. K., Sharma, D., K., Luthra, S., K., 2000. “Determination of evapotranspiration and crop coefficient of rice and sunflower with lysimeter”. Agricultural Water Management, (45) 41-54

Tyagi, N. K., Sharma, D., K., Luthra, S., K., 2003. “Determination of evapotranspiration for 0maize and berseem clover”. Irrig Sci (21)173-181. DOI: 10.1007/s00271-002-0061-3

Tyree, M. T. and Alexander, J. D., 1993. “Plant water relations and the effects of elevated CO2: a review and suggestions for future research”. Vegetatio (104/105) 47-62

U

Unlu, M., Kanber, R., Diker, K. and Staduto, P., 2001. “Comparing cotton Evapotranspirations Estimated by Micrometereological and Water Budget Methods”. Turk J Agric For 25 329-335

V

Van Atta, C., W., 1977. “Effect of coherent structures on structure functions of temperature in the atmospheric boundary layer.” Arch.Merch. (29)161-171

Ventura, F., Snyder, R. L., Bali, K. M., 2006. “Estimating evaporation from bare soil using soil moisture data”. Journal of Irrigation and Drainage Engineering DOI: 10.1061/(ASCE)0733-9437(2006)132:2(153)

Ventura, F., 2004. ”Il bilancio idrico”, University of Bologna, pdf document

Ventura, F., Faber, A. B., Bali, M. K., Snyder, R. L., Spano, D., Duce,P., Schulbach, K. F., 2001. “Model for estimating evaporation and transpiration from row crops”. Journal of Irrigation and Drainage Engineering / November / December, 339-345

Ventura F., Facini O., Piana S., Rossi Pisa P., 2010. “Soil moisture mesurements: a comparison of instrumentations performances.” Journal of Irrigation and Drainage Engineering, 136(2) 81-89

Villalobos, F.J. Testi, L., Moreno-Perez,, M., F., 2009. “Evaporation and canopy conductance of citrus orchard”. Agricultural Water management (96) 565-573

Villalobos, F.J., Testi, L., Rizzalli, R., Orgaz, F., 2004. “Evapotraspiration and crop coefficients of irrigated garlic in a semiarid-climate”. Agricultural Water management (64) 233-249

Villani, G., Tomei, F., Tomozeiu, R., Marletto, V., 2011.”Climatic scenarios and their impacts on irrigated agricolture in Emlia-Romagna, Italy”. Italian Journal of Agrometeorology -1/2011

Vlachos, E., James, L.D., 1993. Drought Impacts. In: V. Yevjevich, L. V. Cunha, E. Vlachos (Eds.) Coping With Droughts. Water Resources Publications, Littleton, CO, pp. 44-73.

Vörösmarty, C. J., Green, P., Salisbury,J., Lammers, R., B., “Global water resources: vulnerability from climate change and population growth”, Science (289) 5477.284

W

Watanabe, K., Yamamoto, T., Yamada, T., Sakuratani, T., Nawata, E., Noichana, C., Sributta, A. and Higuchi, H., 2004. “Changes in seasonal evapotranspiration, soil water content, and crop coefficients in sugarcane, cassava, and maize fields in Northeast Thailand”, Agric. Water Manage., (67) 133–143.

Wight, J. R., and Hanson, C. L., 1990. “Crop coefficients for rangeland”. Journal of range management 43(6), November

Wolfe, D.W. 1994. “Physiological and growth responses to atmospheric carbon dioxide concentration”. In: Handbook of Plant and Crop Physiology. M. Pessarakli (ed.). Marcel Dekker, New York, 223-242.

X

Xinmin, Z., Lin, H., X., B., Bingxiang, Z., Fahe, C., Xinzhang, S., 2007. “The most economical irrigation amount and evapotranspiration of the turfgrasses in Beijing city, China”. Agricultural Water management (89) 98-104

WEBSITES

http://w3.shorecrest.org/~Lisa_Peck/Physics/All_Projects/photojournal/tina/tina.html (20 October 2011)
http://www-naweb.iaea.org/nafa/news/water-management.html (20 October 2011)

http://edis-news.wp.ifas.ufl.edu/2011/08/22/net-irrigation-requirements-for-florida-turfgrass-lawns-part-2-reference-evapotranspiration-calculation-ae481ae481/ (20 October 2011)

http://www.biology.duke.edu/jackson/fig3.html (20 October 2011)

http://www.climatechange.ca.gov/publications/cat/2005-12-08_DRAFT_CAT_REPORT_TO_GOV+LEG.PDF (20 October 2011)

http://www.fao.org/docrep/X0490E/x0490e04.htm (20 October 2011)

http://www.fao.org/docrep/W5183E/w5183e07.htm (20 October 2011)

http://www.ecosearch.info/prodotti.php?prod_id=372 (1 November 2011)

http://cloudbase.phy.umist.ac.uk/people/dorsey/Edco.htm

http://www.ermesagricoltura.it/wcm/ermesagricoltura/consigli_tecnici/irrigazioni/sezione_irrigazioni.htm (3 March 2010)

http://it.encarta.msn.com/encnet/refpages/RefArticle.aspx?refid=761555207&pn=6 (15 April 2013)

http://www.dista.agrsci.unibo.it/Bollettino%20agrofenologico/ (15 April 2013)

http://www.fao.org/publications/sofi/en/ (15 April 2013)

http://www.arpa.emr.it/dettaglio_documento.asp?id=708&idlivello=64 (15 April 2013)
http://www.panda.org *(15 April 2013)*
[6]*http://www.unesco.org/water/ihp* (15 April 2013)

http://www.instrumentalia.com.ar/pdf/Invernadero.pdf (15 April 2013)

http://www.iac.ethz.ch/en/research/riet/instruments.html (15 April 2013)

biomet.ucdavis.edu (15 April 2013)

http://www.fao.org/docrep/006/Y4683E/y4683e07.htm (15 April 2013)
http://www.fao.org/docrep/X0490E/x0490e06.htm

ACKNOWLEDGEMENTS

I would like to thank anybody who directly and not directly helped me during these years of study, work and research. Thank to my advisors, Prof. Paola Rossi, Francesca Ventura and Rick Snyder, for having trusted me since the first day. Thank you to Marcela Doubkova, (ESA, Frascati), Celestina Pedras (Universidade Técnica de Lisboa), for their supporting my mention to Doc Europaeus. Thank to all the people, who collaborated to this work, sharing with me information, help and field data: Arianna Facchi, (Università di Milano), Luca Testi, (Instituto de Agricultura Sostenible, Cordoba), Pasquale Steduto, (FAO Rome), Stefano Anconelli, (CER, Bologna), Giulia Villani, Fausto Tomei, Gabriele Antolini, Vittorio Marletto (ARPA-SIMC Emilia Romagna). Thanks to all my colleagues, Fiorenzo Salvatorelli, Linda Pieri, Marco Vignudelli, Roberto Solone, Stefano Piana, Marco Bittelli and Nicola Gaspari. They made my experience here not only important from the educational and professional, but also from the human, point of view. I thank also all my family, that has always supported me in any possible way.

Appendix I Figure, and Table Index